Molecular Regulation of Inducible Nitric Oxide Synthase

Dissertation

Presented in Partial Fulfillment of the Requirements for the Degree Doctor of Philosophy in the Graduate School of The Ohio State University

By

Tingting Wang, B.S.

The Ohio State Biochemistry Program

The Ohio State University

2012

Dissertation Committee:

Yong Xia, Advisor

Terry S. Elton

Arthur R. Strauch

Mark D. Wewers

Qianben Wang

Copyright by

Tingting Wang

2012

ABSTRACT

Nitric oxide (NO) generated by inducible NO synthase (iNOS) plays critical roles in inflammation and host defense. While normally undetectable, iNOS is induced to express by inflammatory stimuli. Once expressed, iNOS exhibits constant activity. Hence NO production from iNOS has been thought to be primarily controlled via enzyme expression. In this study, we identify an array of novel mechanisms showing that iNOS is regulated at multiple levels including gene expression, protein aggregation, and protein degradation.

Calmodulin (CaM) has been long known as an iNOS cofactor facilitating intramolecular electron transfer amid NO syntheses. We now show that CaM is essential for iNOS induction. CaM inhibition or knockdown prevented iNOS expressions in macrophages stimulated by inflammatory mediators. Further studies revealed that CaM acted through Ca^{2+}/CaM-dependent kinase II (CaMKII), which functioned as a cardinal initiator in iNOS gene transactivation via both LPS-NF-κB and IFN-γ-STAT1 pathways. Our study also found that activating iNOS gene transcription required the elevations of cytosolic Ca^{2+}. CaM inhibitors or CaMKII blocker was found to prevent iNOS induction in endotoxemic mice and markedly improved survival rates. These studies extend the role of CaM from catalytic assistant to an essential modulator in iNOS gene transactivation.

Once expressed, biological iNOS output is determined by the levels of functional enzyme, which is influenced by protein stability. While previously thought as a soluble protein, iNOS was recently reported to form aggresomes inside cells. However, what causes iNOS aggresome formation is unknown. To explore iNOS protein stability, we first investigated iNOS aggregation under physiological conditions. Our studies revealed that iNOS aggresome formation is mediated by its own product NO. While initially existing as a soluble protein, iNOS progressively formed inactive protein aggregates. Treating the cells with NOS inhibitors blocked NO production and prevented iNOS aggregation inside cells. iNOS restored NO-generating activity and gradually formed aggregates upon NOS inhibitor removal. Furthermore, iNOS aggresome formation could be recaptured by adding exogenous NO to NOS-inhibited cells. The NO-mediated aggregation was found to be specific for iNOS as the other two NOS isoforms remained stable upon NO exposure. The finding that NO induces iNOS aggregation and inactivation suggests aggresome formation as a feedback inhibition mechanism in iNOS regulation.

After elucidating iNOS aggregation triggered by NO in physiological conditions, we then investigated iNOS protein stability under pathological circumstances upon heat shock protein 90 (Hsp90) or CaM inhibition. Hsp90 was previously reported to play an important role in iNOS function and gene expression. We now find that dissociation of Hsp90 from iNOS led to iNOS aggregation and deactivation. The mechanism underlying degradation of aggregated iNOS upon Hsp90 inhibition was also investigated. Our studies showed that iNOS aggregates were cleared by the ubiquitin-proteasome system

(UPS) inside cells. C-terminus of heat shock protein 70-interacting protein (CHIP), a previously reported E3 ligase of iNOS, was not responsible for aggregated iNOS turnover. Further studies revealed that the SPRY domain-containing SOCS box protein 2 (SPSB2), an E3 ligase-recruiting protein, was essential for the ubiquitination of iNOS aggregates under Hsp90 inhibition. SPSB2 knockdown or deleting the SPSB2-interacting domain on iNOS prevented the clearance of iNOS aggregates in Hsp90-inhibited cells. Thus our studies enhance the understanding on the roles of Hsp90 in iNOS regulation by revealing its iNOS protein stabilizing function. CaM inhibition also caused iNOS to form insoluble aggregates. Aggregated iNOS lost NO-generating activity. Our studies revealed that dissociation of CaM from iNOS resulted in the exposure of its hydrophobic CaM-binding domain, leading to iNOS aggregation. This study further extends the role of CaM to iNOS protein stabilizer beyond its previously discovered function in iNOS gene transactivation.

Previous studies demonstrate that iNOS is degraded through the UPS pathway. However, the ubiquitination site of iNOS remains to be elucidated. In this study we identified four amino acid (AA) residues among the N-terminal region of iNOS crucial for its proteasomal degradation. The N-terminal 1-100 AAs were found to be responsible for iNOS degradation by the construction of a series of truncated iNOS mutants. Substitution of all lysines with arginines among the N-terminal 1-100 AAs failed to prevent iNOS degradation. Further mutation of 2 cysteines to alanines decelerated iNOS turnover. Additional alanine replacements of serines (S) and threonines (T) revealed four AA residues (T31, S37, T39 and S46) essential for proteasomal degradation of iNOS.

These results reveal that unlike the conventionally thought lysine residue, cysteines, serines, and threonines appear to mediate proteasomal degradation of iNOS.

In summary, our investigations change the notion that iNOS biology is largely dependent on the levels of its gene expression. The knowledge gained from this work provided a comprehensive understanding of iNOS regulation via three interrelated aspects including protein induction, stability and degradation.

Dedication

Dedicated to my family

ACKNOWLEDGEMENTS

There are many people that I would like to acknowledge for their support and assistance during these years. First of all, my deepest gratitude is to my advisor, Dr. Yong Xia, for his continuous support, encouragement, help and patience in my graduate study. From him, I learned not only various laboratory skills, but also how to discover interesting phenomena, analyze the experiment results, design the next step of study, and solve the problems encountered with great courage and fortitude. I have been amazingly fortunate to be supervised by Dr. Xia.

I would also like to thank my committee Dr. Terry S. Elton, Authur R. Strauch, Mark D. Wewers, and Qianben Wang for their time, advice and help for my project development.

To my previous and present lab mates, Honghua Qin, Juan Chen, Deqin Lu, Suxin Luo, Li Lin, Zhihong Xiao, Chao Huang, Xiaomei Yuan, Lijun Zhang and Guanming Yang, I owe my sincere thanks for your encouragement and assistance over the years. I had a wonderful time working with you. Among them, I would especially give my gratitude to our lab manager, Honghua Qin. Thank you for the training, support and help during my entire study.

I thank Dr. Jill A. Rafael-Fortney and Dr. Ross E. Dalbey for their support and guidance during my study in the OSBP program.

I also thank my parents and boy friend for their endless love and unconditional support throughout the years.

VITA

1984……Born – Changzhou, China

2006……B.S., Biotechnology
Nanjing University, China

2006 - Present……..Graduate Research Associate
The Ohio State University

PUBLICATIONS

1. **Wang T**; Xia Y. Inducible nitric oxide synthase aggresome formation is mediated by nitric oxide. Biochem Biophys Res Commun. 2012

2. Xiao Z, **Wang T**, Qin H, Huang C; Feng Y; Xia Y. Endoplasmic reticulum Ca^{2+} release modulates endothelial nitric-oxide synthase via extracellular signal-regulated kinase (ERK) 1/2-mediated serine 635 phosphorylation. J Biol Chem. 2011; 286(22):20100-8.

3. Luo S, **Wang T**, Qin H, Lei H, Xia Y. Obligatory role of heat shock protein 90 in iNOS induction. Am J Physiol Cell Physiol. 2011; 301(1):C227-33.

4. Xiao Z, **Wang T**, Qin H, Huang C; Feng Y; Xia Y. Endoplasmic Reticulum Ca^{2+} Release Triggers Endothelial NO Synthase Serine 635 Phosphorylation and Activity through ERK1/2. Circulation. 2010; 122: A16962.

5. Luo S, **Wang T**, Chen L, and Xia Y. Abstract 5144: The Obligatory Role of Heat Shock Protein 90 in iNOS Induction in Postischemic Hearts. Circulation. 2009; 120: S1060.

FIELDS OF STUDY

Major Field: Biochemistry

TABLE OF CONTENTS

LIST OF FIGURES

LIST OF ABBREVIATION

A	alanine
AA	amino acid
BH_4	(6R)-5, 6, 7, 8-tetrahydrobiopterin
C	cysteine
CaM	calmodulin
CaMKII	calcium/calmodulin-dependent protein kinase II
CHIP	C-terminus of heat shock protein 70-interacting protein
CLP	cecal ligation and puncture
E. coli	*Escherichia coli*
EDTA	ethylenediaminetetraacetic acid
eNOS	endothelial nitric oxide synthase
FAD	flavin adenine dinucleotide
FMN	flavin mononucleotide
GA	geldanamycin
GAS	gamma activated sequence
h	hour
heam	iron protoporphyrin IX
Hsp90	Heat shock protein 90
IFN-γ	Interferon-γ

iNOS	Inducible nitric oxide synthase
K	lysine
LPS	lipopolysaccharide
min	minute
NADPH	reduced nicotinamide adenine dinucleotide phosphate
nNOS	neuronal nitric oxide synthase
NO	nitric oxide
NOS	nitric oxide synthase
p	phospho
R	arginine
S	serine
SPSB2	SPRY domain–containing SOCS (suppressor of cytokine signaling) box protein 2
T	threonine
TFP	trifluoperazine
U	unit
UPS	ubiquitin-proteasome system
WT	wild-type

CHAPTER 1

1 Introduction

1.1 Nitric oxide and nitric oxide synthase

1.1.1 Function of NO

Nitric oxide (NO) is a fundamental signaling molecule and effector involving in a variety of biological processes (1-3). In cardiovascular system, NO modulates vascular tone and cardiac contractility (4). NO also functions as a neurotransmitter participating in neuronal signal transmission in both central and peripheral nerve systems (5, 6). Unlike conventional signaling molecules, NO is a gaseous free radical. While physiological levels of NO convey cell signals, high levels of NO damage cells and tissues. In fact, the immune system employs the toxic effect of NO to fight against microbe infection and eliminate tumor cells (7, 8). Because of the widespread function and the unique nature that can exert both beneficial and detrimental actions, NO production must be precisely controlled. Abnormalities of NO production cause diseases (9). For example, insufficient NO formation occurs in hypertension and atherosclerosis. Excessive NO production, on the other hand, has been demonstrated to contribute to septic shock and heart failure (10-13).

1.1.2 NOS structure

In biological system, NO is mainly produced by a family of NO synthases (NOS) (14). So far, three mammalian NOS isoforms have be identified as: neuronal NOS (nNOS, type I), inducible NOS (iNOS, type II), and endothelial NOS (eNOS, type III) (15). nNOS and eNOS constitutively exist in cells. In contrast, iNOS is not detectable in quiescent cells under physiological condition.

Three NOS isoforms exhibit a similar bidomain structure. The N-terminal oxygenase domain contains the binding site of L-arginine, iron protoporphyrin IX (heme), and (6R)-5, 6, 7, 8-tetrahydrobiopterin (BH_4). The C-terminal reductase domain of NOS contains the binding site of flavin mononucleotide (FMN), flavin adenine dinucleotide (FAD) and reduced nicotinamide adenine dinucleotide phosphate (NADPH) (16). These two domains are linked by a region containing a Calmodulin (CaM)-binding sequence (Figure 1.1) (17, 18). All active NOS are dimeric enzymes containing two identical monomers. The two NOS monomers interact with each other via the interface generated by two segments of the oxygenase domain shown in the primary structure of NOS (Figure 1.1). The interface of the dimeric NOS includes the binding site for BH_4 and helps to construct the active-site where the heme and L-arginine binding sites locate (19). Thus BH_4, heme and L-arginine all promote and stabilize the dimerization of NOS proteins.

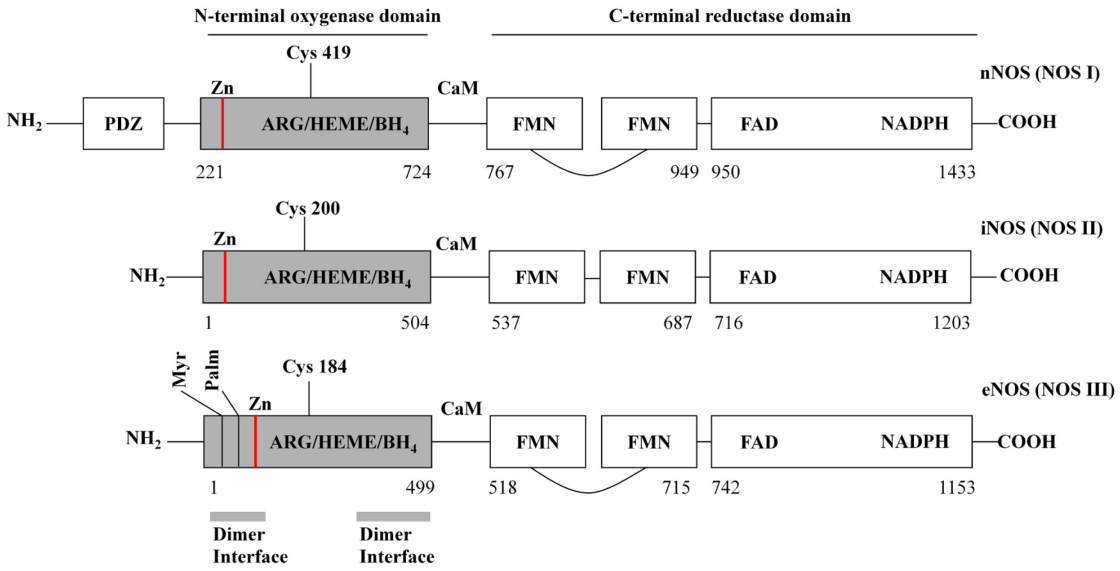

Figure 1.1 Schematic view of human nNOS, iNOS and eNOS.

Although all three NOS enzymes possess similar structure, there are some differences among them in terms of their activities and cellular locations. Only nNOS contains an N-terminal PDZ protein interaction domain to organize signaling pathways by increasing the efficiency and specificity of signal transduction (20, 21). Since nNOS and eNOS are constitutively expressed in cells, the autoinhibitory loop within the FMN regions of the two NOS enzymes is critical to control their activity (22, 23). Among three NOS isoforms, eNOS could either exist in cytosol or be anchored on membrane depending on its acylation status. eNOS is co-translationally and irreversibly myristoylated at the N-terminal glycine residue, while palmitoylation occurs post-translationally and reversibly at cysteine residues (24, 25). Palmitoylation of eNOS is dynamically regulated by intracellular Ca^{2+} levels, and can efficiently localize eNOS to the cell membrane (26).

1.1.3 NO synthesis by NOS

Three NOS isoforms are all cytochrome P-450 reductase-like hemoproteins, which use L-arginine, oxygen, and NADPH as co-substrates to synthesize NO and L-citrulline (15). Their catalytic activities require the same cofactors: CaM, BH_4, FAD, FMN and heme (18). Spectroscopic studies showed that NOS activity is controlled through a CaM-promoted electron transfer from NADPH to the heme (27). As shown in Figure 1.2, electrons are donated by NADPH in the reductase domain and proceed via FAD and FMN redox carriers at the oxygenase domain, where the electrons interact with the heme iron and BH_4 to catalyse the reaction in which O_2 and L-arginine are substrates and NO and L-citrulline are products (28). In brief, the reaction takes place in two discrete steps with N-hydroxy-L-arginine being formed as the intermediate. Three electrons are consumed to produce one molecule of L-citrulline. Apparently, CaM binding induces an enzyme conformational change, which enables electron transfer from the NOS reductase domain to oxygenase domain (29).

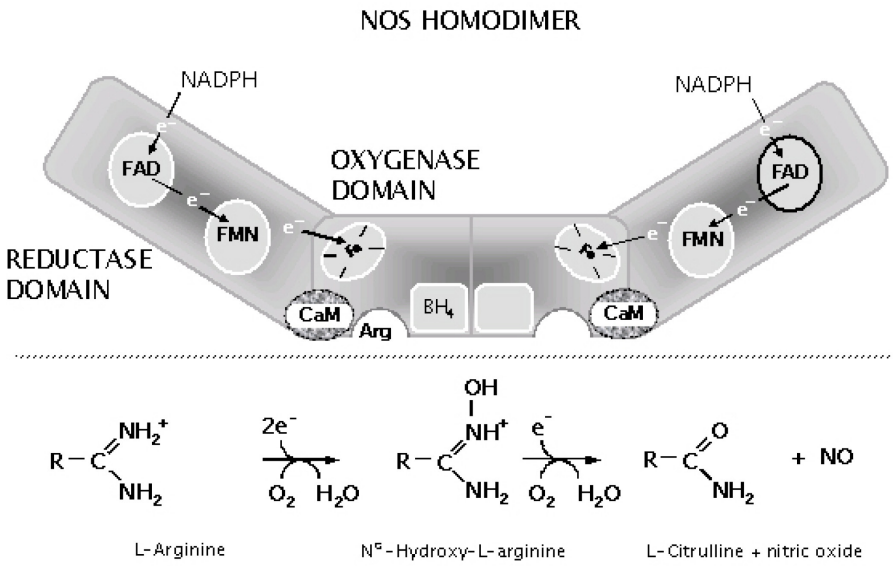

Figure 1.2 Schematic view of NO synthesis by NOS.

1.2 Regulation of iNOS

1.2.1 Function of iNOS

Under physiological circumstances, relatively low levels of NO produced by nNOS and eNOS participate in neuronal transmission and cardiovascular function. In activated immune cells, iNOS generates much higher amounts of NO compared to other NOS isoforms. iNOS-derived NO can be either beneficial or detrimental. On one hand, NO is crucial in host defense against microbe infection; on the other hand, excessive NO is associated with cell injury. In addition, NO also reacts with superoxide radical to form peroxynitrite (30), a potent cytotoxic oxidant known to cause severe cell injury and tissue damage (31). Due to its harmful activity, iNOS-generated NO has been reported to be implicated in various diseases, including Alzheimer's disease, asthma, stroke, arthritis,

and septic shock (32-34). Under such circumstances, selective inhibition of iNOS activity is potentially beneficial.

Sepsis is a severe medical condition usually caused by the failure of initial host response to certain infection. Sepsis is characterized by a systemic inflammatory response and consequent failure of multiple organs. High levels of iNOS expression are observed in septic tissues (10, 11, 35, 36). In sepsis, overproductions of NO by iNOS result in hypotension, cardiodepression, and vascular hyporeactivity. So far sepsis remains a lethal disease with few specific therapeutic options. Studies performed by different groups showed that inhibition of NO synthesis prevented hypotension, attenuated metabolic derangement and improved survival in several animal models of septic shock (36-41). However, the efficacy of iNOS inhibition is discrepant in treating septic patients (42). It remains uncertain whether iNOS inhibitor therapy benefits human. Since blocking iNOS yields inconsistent results in the clinical therapy, an alternative approach is to target on iNOS induction process (43). Such an approach demands a comprehensive understanding on the molecular mechanism of iNOS gene expression. In this study, based on the detailed study of the effects of CaM on iNOS induction, we explored whether blocking iNOS expression via the inhibitors of CaM or upstream kinase can be a new approach to treat this disease (Chapter 2).

Two most commonly used animal models for the study of sepsis are endotoxemia model and cecal ligation and puncture (CLP) model. The endotoxemia model can be simply established by a bolus injection of LPS (44). However, recent studies have reported significant differences between this model and true sepsis (45). In CLP model,

sepsis originates from a polymicrobial infection initiated from abdominal cavity and then into the blood compartment. The CLP model is considered as the gold standard due to the advantages of high consistency and controllable severity grades with different rates and degrees of mortality (46).

1.2.2 Induction of iNOS expression

Unlike constitutively expressed eNOS and nNOS, iNOS does not exist in quiescent cells. The expression of iNOS is mainly induced by inflammatory substances, such as microbial endotoxin lipopolysaccharide (LPS) and cytokines. Studies showed that LPS activates iNOS gene transcription through the IKK-NF-κB signaling pathway (47, 48). Cytokines, such as interferon-γ (IFN-γ), induce iNOS expression via the JAK-STAT1 cascade (49-51). In diseases where multiple inflammatory stimuli are present, iNOS induction is likely involved in both IKK-NF-κB and JAK-STAT1 pathways (Figure 1.3).

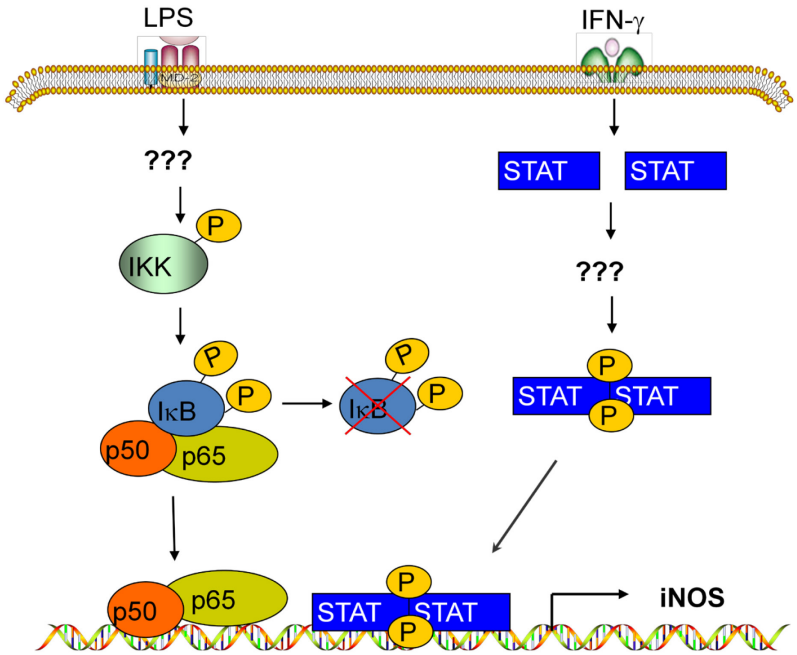

Figure 1.3 Schematic view of iNOS induction by IKK-NF-κB and IFN-γ-STAT1 pathways.

iNOS induction by IKK-NF-κB pathway

In resting cells, transcription factor NF-κB couples with the inhibitory IκB protein and stays dormant in cytosol. LPS binds with CD14 on the cell surface and activates the associated Toll-like receptors. Through a yet to determined mechanism, Toll-like receptor activation leads to IKK phosphorylation. This in turn activates IKK. Activated IKK phosphorylates IκB and phosphorylated IκB undergoes ubiquitination and subsequent degradation by proteasome. NF-κB is then released and activated. The activated NF-κB enters the nucleus and initiates iNOS gene transcription.

iNOS induction by IFN-γ-STAT1 pathway

IFN-γ binds with the IFN-γ receptor, leading to the activation and autophosphorylation of the associated Janus kinases (JAK1 and JAK2). The activated JAK subsequently phosphorylates the cytoplasmic domain of the IFN-γ receptor, creating a docking site for two latent STAT1 molecules. STAT1 molecules are then recruited to the receptor and undergo phosphorylation on tyrosine residues. Following tyrosine phosphorylation, STAT1 proteins are released into cytosol as active STAT1 homodimers. STAT1 is also phosphorylated on serine residues and this augments transcriptional activity of STAT1. Activated STAT1 is translocated into nucleus and binds to respective promoter region (GAS, the gamma activated sequence), initiating iNOS gene transcription.

The IKK-NF-κB and JAK-STAT1 are two common signaling pathways employed by various inflammatory stimuli and environmental stress. The specific action of one particular stimulus is achieved via the distinctive upstream mechanisms controlling the IKK-NF-κB and JAK-STAT1 cascades. Although the roles of NF-κB and STAT1 are well established in iNOS induction, the upstream mechanisms leading to NF-κB and STAT1 activation are not fully understood. Our preliminary studies showed that CaM is required for both LPS- and IFN-γ-stimulated iNOS expression. These data suggest that a CaM-dependent mechanism may govern both NF-κB and STAT1 pathways in iNOS expression. We therefore used a combination of molecular and cellular approaches to identify such a master controlling mechanism in iNOS induction in this study.

1.2.3 iNOS aggregation

In cells, newly synthesized proteins must undergo proper folding processes to become functional molecules. But protein misfolding occurs as an inevitable consequence of genetic mutations, protein overexpression, or environmental insults such as oxidative stress. Cells normally adopt a refined quality-control mechanism to eliminate aberrant proteins. The misfolded proteins can be refolded and stabilized by a variety of chaperones. Misfolded proteins that cannot be restored are destined to be degraded through the ubiquitin-proteasome pathway. When the chaperone and proteasome systems are impaired or overloaded, misfolded proteins are resolved by forming cytoplasmic aggregates (52). Aggregated proteins are recognized and transported to specialized holding stations called aggresomes. Aggresomes not only act to sequester potentially harmful aggregated proteins, but also concentrate aggregated proteins to facilitate their degradation by autophagy (53). The failure in elimination of aggregated proteins can cause cell toxicity leading to diseases such as neurodegenerative disorders. Understanding the molecular processes responsible for formation and clearance of aggregated proteins is critical for developing new therapies for the diseases caused by protein aggregation.

Largely due to its hallmark feature as a highly inducible protein, iNOS research has been largely focused on the mechanism of enzyme expression. Little is known about how iNOS protein stability is maintained. Whether or not iNOS aggregates and how it may affect the biological function of iNOS are largely unclear. Nevertheless, a recent study by Kolodziejska et al reported that iNOS is expressed initially as a cytosolic protein

but is eventually targeted to a perinuclear location, revealing a possible role of iNOS aggregation in iNOS regulation (54, 55). But the process and control mechanism underlying iNOS aggregation remain unknown. Key questions remain regarding what factors determine whether iNOS aggregates or not. In this study, we investigated the role of CaM, self-derived NO as well as heat shock protein 90 (Hsp90) in regulating iNOS protein stability (Chapter 3-5).

1.2.4 iNOS degradation

The fate of a protein is dynamically regulated by both protein expression and degradation. In particular, misfolded proteins or protein aggregates must be promptly removed to avoid cytotoxicity. The two major routes responsible for protein elimination in eukaryotic cells are the ubiquitin-proteasome system (UPS) and autophagy-lysosome pathway (56-58). In UPS route, substrate proteins targeted for degradation are covalently linked to multiple ubiquitins, a polypeptide consisting of 76 amino acids. The attachment of ubiquitins to the substrate protein is mediated by a series of sequential reactions involving three enzymes. First, ubiquitin is activated by an ubiquitin-activating enzyme (E1), and then the activated ubiquitin is transferred to an ubiquitin-conjugating enzyme (E2), which transiently carries ubiquitin via a thiol-ester bound. Finally an ubiquitin-protein ligase (E3) binds to the substrate and facilitates the transfer of the activated ubiquitin from E2 enzyme to the substrate usually through a covalent linkage to the lysine residues in the substrate. E3 enzymes specifically recognize certain substrate for final ubiquitin molecule conjugation, thus confer specificity to ubiquitination. The preceding ubiquitin serves as a substrate for further ubiquitination, resulting in the attachment of a

polyubiquitin chain linked by lysine-48 residue of ubiquitin molecules. The polyubiquitin chain constitutes a signal recognized by 26S proteasome for degradation (Figure 1.4) (59, 60). Previous studies conducted by Eissa group reported that UPS route is the major pathway responsible for iNOS turnover (61, 62). Moreover, recent investigations suggested that two E3 ligases, C-terminus of heat shock protein 70-interacting protein (CHIP) and SPRY domain–containing SOCS (suppressor of cytokine signaling) box protein 2 (SPSB2), may be involved in iNOS ubiquitination (63-65).

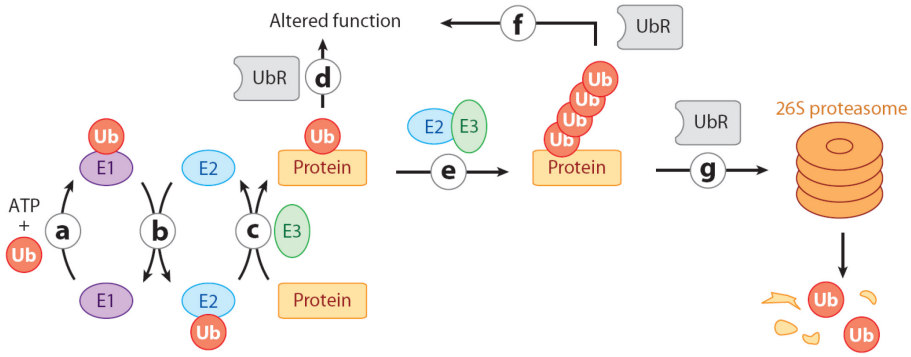

Figure 1.4 Degradation of protein through ubiquitin-proteasome system.

CHIP is a highly conserved protein containing an N-terminal tetratricopeptide repeat (TPR) domain and a U-box domain at its carboxy terminus (66). CHIP interacts with the molecular chaperones Hsp70 and Hsp90 through its TPR domain, and its U-box domain renders E3 ubiquitin ligase activity (67, 68). Thus CHIP acts as an E3 ligase responsible for the ubiquitination of client proteins recruited by chaperones bound to the

CHIP TPR domain. Recent studies conducted by Sha et al and Chen et al respectively reported that CHIP interacted with iNOS and promoted its ubiquitination and degradation by the proteasome (30, 63).

The SPSB2 protein, also known as SSB-2, is characterized by a SPRY domain and a C-terminal SOCS box motif. The SOCS box motif is about 40 residues in length and contains a BC box and a Cul5 box, which binds Elongin B/C and Cullin5, respectively (69, 70). The SPRY domain is essential for determining the substrate for ubiquitination (71, 72). Taken together, the presence of the SOCS box and SPRY domain suggests the possible function of SPSB2 as part of the E3 ubiquitin ligase complex. Recent studies by Kuang et al and Nishiya et al reported that SPSB2 participates in iNOS ubiquitination and turnover under normal conditions (64, 65). Kuang et al suggested that SPSB2 interacts with the DINNN sequence at the N-terminal of iNOS via the SPSB2 SPRY domain and recruits Elongin B/C, Cullin5 and Rbx2 via its SOCS box to form an active E3 ubiquitin ligase complex that ubquitinates iNOS and targets it for proteasomal degradation.

The autophagy-lysosome pathway is involved in bulk degradation of macromolecules such as aggregated proteins and organelles (73). Lysosome, a spherical organelle enveloped by double-membrane, contains acid hydrolases that only work at the pH 4.5 in lysosomal interior. Different from the complicated degradation process mediated by UPS system, lysosome primarily fuses with the vacuole containing target substrate and dispenses lysosomal enzymes into the vacuoles to decompose the content (Figure 1.5) (74). Recent progresses showed that ubquitination has important roles in

protein recognition and targeting in the route of autophagy-lysosome pathway (75). Thus autophagy-lysosome pathway may also play a role in the elimination of iNOS aggregates.

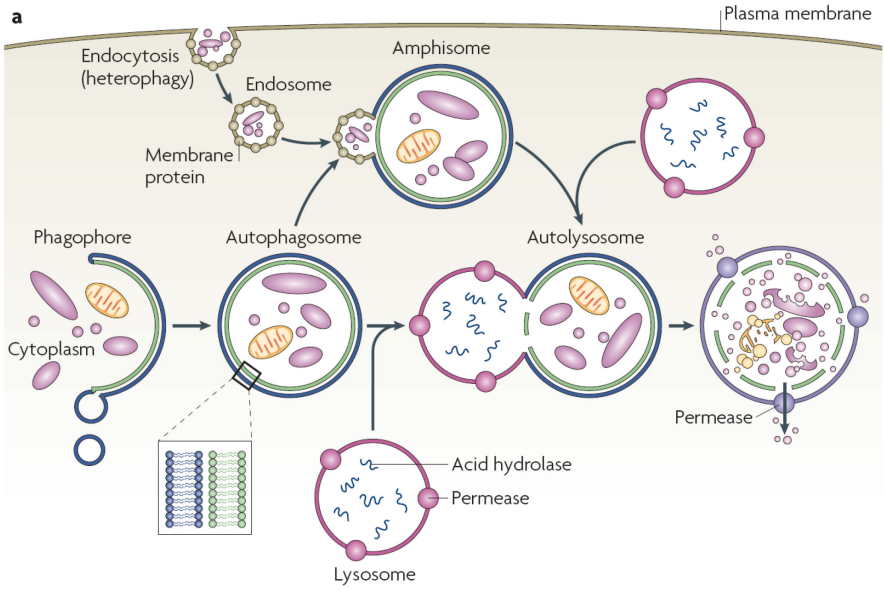

Figure 1.5 Protein turnover via autophagy-lysosome pathway.

Although degradation of normal iNOS was reported to be mediated by UPS, the ubiquitination sites on iNOS have not been identified. Important questions remain regarding if iNOS is ubiquitinated at the conventional lysine residues or the other possible residues such as cysteines or serines/threonines. Furthermore, whether or not aggregated iNOS will also be cleared by UPS pathway is unknown. Moreover, CHIP and SPSB2 are two E3 ligases reported to be involved in the ubiquitination of normal iNOS, but whether they are responsible for the ubiquitination of aggregated iNOS remains unclear. Therefore, in this study, the degradation mechanisms of both aggregated and normal iNOS were investigated, respectively (Chapter 5 and Chapter 6). The roles of

CHIP and SPSB2 in the elimination of aggregated iNOS under pathological circumstances were elucidated (Chapter 5).

1.3 Calmodulin

1.3.1 Structure of CaM

Studies have found that CaM binding is essential to the activities of all three NOS isoforms (76-78). CaM is a small Ca^{2+} binding protein found in all eukaryotic cells. It is composed of 148 amino acids and its sequence is highly conservative in all organisms. CaM contains four Ca^{2+} binding sites, two at each globular end of the molecule, termed EF-hand motif. The conformation of the EF-hand motif changes upon binding Ca^{2+} (79). Each EF-hand motif contains two α-helices connected by a 12-residue loop. The Ca^{2+} binds to the loop region and changes the relative positions of the α-helices. In the absence of Ca^{2+}, the α-helices in the EF-hand motif of CaM are positioned almost parallel to each other, known as the closed conformation (Figure 1.6A) (80). Upon binding Ca^{2+}, CaM undergoes large conformational change. The crystal structure of Ca^{2+}-loaded CaM exhibits a dumbbell shape (Figure 1.6B). Both X-ray and NMR studies show that the α-helices of the EF-hand motif change their positions relative to each other, forming an almost perpendicular conformation, which is known as the open conformation (81). This radical change exposes the hydrophobic pocket, which is the key recognition site of CaM target enzymes. Therefore Ca^{2+} binding allows CaM to increase its binding affinity for a number of target proteins. CaM is active only when all four Ca^{2+} binding sites are filled.

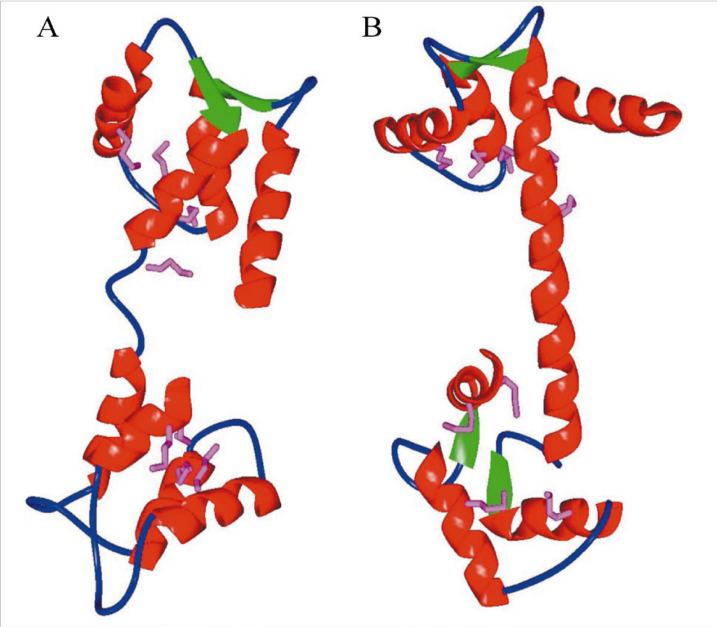

Figure 1.6 Conformations of CaM in the absence or presence of Ca^{2+}.
(A) CaM in the form without Ca^{2+}. (B) Ca^{2+}-loaded CaM.

1.3.2 CaM inhibitors

W-7 and trifluoperazine are two different CaM inhibitors that are widely used for the inhibition of CaM (Figure 1.7). W-7 and trifluoperazine inhibit CaM function via different mechanisms according to their different chemical structures (82, 83).

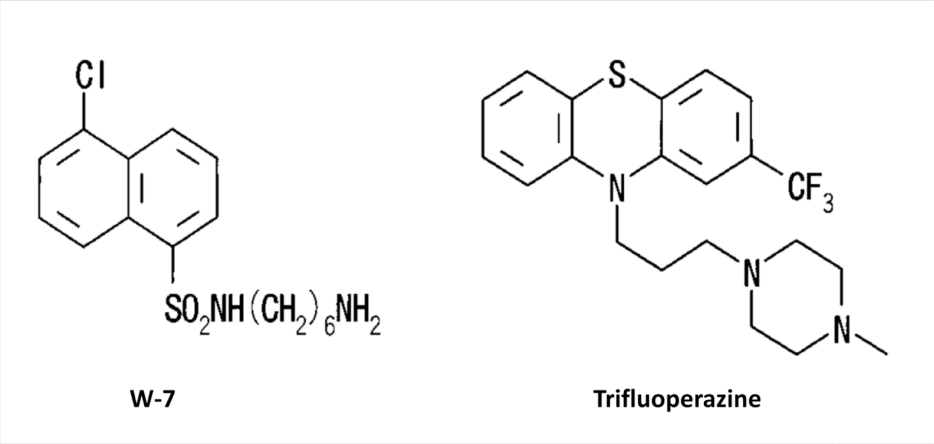

Figure 1.7 Chemical structures of CaM inhibitors, W-7 and trifluoperazine.

Two W-7 molecules bind to each of the two globular domains of CaM (84). In each binding site, the W-7 chloronaphthalene ring interacts with four methionine methyl groups and other aliphatic or aromatic side-chains in a deep hydrophobic pocket, where CaM binds to CaM-dependent enzymes such as CaM kinase II (CaMKII). The competitive binding at the same site between W-7 and CaM-dependent proteins suggests the mechanism by which W-7 inhibits CaM to inactivate its client enzymes.

Binding of trifluoperazine to Ca^{2+}-CaM renders a major conformational movement of the Ca^{2+}-CaM (83, 85). The tertiary structure of Ca^{2+}-CaM changes from an elongated dumbbell to a compact globular form. Accompanied with this structural change, the hydrophobic binding pockets of CaM for its client proteins binding disappear and CaM loses the ability to interact with its target enzymes. Thus inactivation of CaM is ascribed to trifluoperazine association that initiates and stabilizes tertiary-structural

alteration of Ca^{2+}-CaM, which is similar to the conformational change caused by target enzyme binding.

1.3.3 CaM and NOS

CaM is indispensable for the activity of all three NOS enzymes. Upon CaM binding, NOS enzyme undergoes a conformational change that enables electron transfer from the NOS reductase domain to oxygenase domain, which is essential for NO synthesis (18, 78).

nNOS and eNOS are constitutively expressed in cells and the binding of CaM requires an elevation of intracellular Ca^{2+} concentration. Thus nNOS and eNOS are characterized as Ca^{2+}/CaM-dependent enzymes (29). Compared to nNOS and eNOS, iNOS possesses a distinctively high binding affinity with CaM (86). In fact, CaM is an intrinsic component of iNOS structure once the enzyme is expressed in cells. Therefore, iNOS is constantly active even at basal Ca^{2+} levels and has been described as Ca^{2+}-independent (87). Structural studies suggested that several hydrophobic residues, which are only present in iNOS, render such a unique feature to iNOS (Figure 1.8) (88). So far, CaM has been viewed as a cofactor for NOS catalysis. Whether or not CaM may have functions beyond assisting enzymatic reaction has not yet been explored in NOS biochemistry.

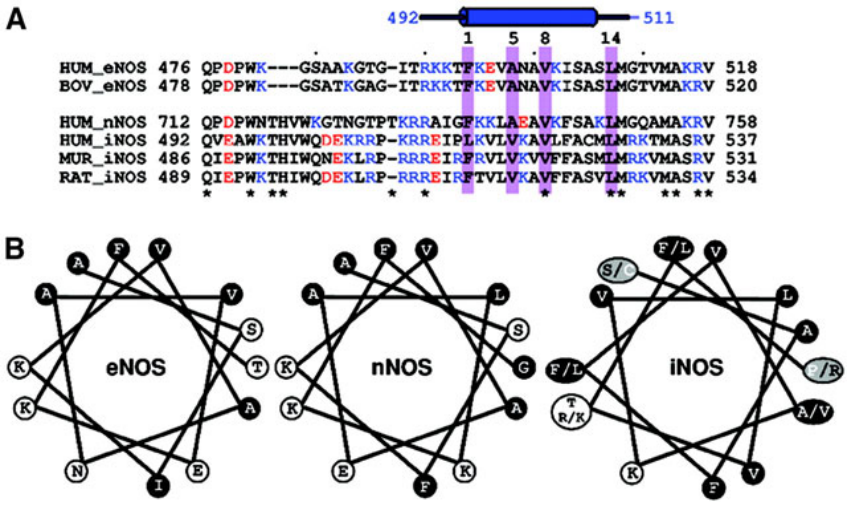

Figure 1.8 Sequence comparisons of CaM-binding domains from the three NOS isozymes.
(A) Sequence alignment of the CaM recognition sites of NOS isozymes from different species. Acidic residues are shown in red, and basic residues in blue. Four key hydrophobic residues involved in CaM binding are highlighted in purple. (B) Helical wheel represents the α-helical portion and residues from NOS. eNOS and nNOS have similar distribution patterns of charged or polar residues (open circles) and hydrophobic or non-polar residues (filled circles). Hydrophobic residues in iNOS replace some charged residues in eNOS and nNOS.

1.3.4 CaMKII

The CaM-dependent kinases (CaMKs) are a family of kinases whose activity depends on the Ca^{2+}/CaM (29, 89). CaMK possesses the catalytic and the adjacent regulatory domains. The regulatory domain includes an autoinhibitory and a CaM-binding domain. The autoinhibitory domain contains a pseudosubstrate site that associates with the catalytic site to block its kinase activity. With an elevated intracellular Ca^{2+} level, Ca^{2+} binds to CaM and consequently induces a conformational alteration of CaM, which activates Ca^{2+}/CaM. Activated Ca^{2+}/CaM binds to the CaM-binding domain in the regulatory domain of CaMK. As a result, the Ca^{2+}/CaM-CaMK interaction releases

the previously sequestered catalytic domain from the autoinhibitory domain and CaMK becomes active.

CaMKII, one family of multifunctional kinases among the large CaMK family, is a category of serine/threonine kinases involved in various cellular processes. The CaMKII enzymes form a polymer comprised of 8-12 holoenzymes through its C-terminal self-association domain (90). Upon Ca^{2+}/CaM binding, CaMKII not only phosphorylates its substrates, but also autophosphorylates a threonine residue in its autoinhibitory domain, preventing the autoinhibitory domain from interacting with the catalytic domain (91). Therefore, this phosphorylation abolishes autoinhibition and renders CaMKII permanently active and independent of Ca^{2+}/CaM. The inactivation of CaMKII is regulated by the CaMK-dedicated phosphatase which removes the phosphate on the threonine residue.

Previous study has reported that CaMKII can be activated by cytokine (92). CaMKII has been identified as a mediator of the IKK activation in the IKK-NF-κB signaling pathway, and a kinase involved in the JAK-STAT1 signaling cascade (92-94). Whether CaMKII is a target protein of CaM and an upstream kinase of both IKK-NF-κB and JAK-STAT1pathways in iNOS induction were explored in this study (Chapter 2).

1.4 Heat shock protein 90 and NOS

1.4.1 Hsp90 function

The 90-kDa heat shock protein (Hsp 90) belongs to a group of highly conserved proteins known as molecular chaperone. As one of the most abundant cytosol proteins in

eukaryotes, Hsp90 functions under both heat-stressed and non-stressed conditions. Hsp90 constitutively exists in cells and its expression can be induced by stress such as heat. Hsp90 not only functions as a chaperone involved in various cellular processes including assisting protein folding, maintaining protein stability, and mediating protein turnover, but also facilitates intracellular signal transduction (95-97).

The primary function of Hsp90 is to assist protein folding and maintain protein conformation (98). Hsp90 not only interacts with nascent proteins for their maturation but also associates with misfolded proteins to assist their refolding. With its protective chaperone function, Hsp90 has been shown to prevent the aggregation of a large number of its substrate proteins.

Studies have also identified the role of Hsp90 in protein degradation via the ubiquitin-proteasome pathway. Misfolded or damaged proteins failed to refold into their normal structures are targeted by polyubiquitination and eliminated by the 26S proteasome, whose conformation stabilization requires functional Hsp90. In addition, Hsp90 is also crucial for the ATPase activity of the proteasome.

Hsp90 is also known to maintain the state and assist the translocation of certain steroid receptors (99). Furturemore, it is reported that Hsp90 help to stabilize proteins including some growth factor receptors, signaling molecules and mutant proteins.

1.4.2 Hsp90 inhibitors

Geldanamycin and radicicol are two widely used Hsp90-specific inhibitors (100). Both inhibitors have been demonstrated to bind with the N-terminal ATP/ADP-binding

site of Hsp90 with high affinity, resulting in the inhibition of the ATPase activity of Hsp90 and loss of Hsp90 function.

Given Hsp90 is important for stabilizing its client proteins, Hsp90 inhibition has been proved to destabilize its associated proteins by promoting their ubiquitination and subsequent proteasome degradation. Since some client proteins such as c-Raf and p53 mutants were found to be involved in cancer, Hsp90 antagonists sometimes can be used as antitumor drugs (101, 102).

1.4.3 Hsp90 regulation of eNOS and nNOS

eNOS and nNOS constitutively exist in cells and their function is initially thought to be regulated by Ca^{2+}/CaM coupling. Recent studies showed that eNOS and nNOS activity was also mediated by posttranslational protein-protein interactions and protein phosphorylation. A large group of proteins have been identified to interact with eNOS and nNOS to mediate their catalytic activity. Among them, Hsp90 was reported to be an important allosteric enhancer of eNOS and nNOS.

Hsp90 was first found to bind with eNOS in resting endothelial cells and this association was enhanced by shear stress, estrogen, and vascular endothelial growth factor (103, 104). Structure studies showed that Hsp90 interacts with the N-terminal domain of eNOS and its association increases eNOS activity (105). The raised eNOS activity by the interaction with Hsp90 is due to the enhanced CaM association affinity to eNOS (106). In endothelial cells, eNOS is localized in caveolae via coupling with caveolin-1, resulting in the blockade of eNOS activity. Enhanced association between

CaM and eNOS by Hsp90 binding was also found to facilitate the dissociation between eNOS and caveolin-1, leading to elevated eNOS activity (107).

Further studies revealed another crucial role of Hsp90 in the maintenance of eNOS serine 1179/1177 (bovine/human) phosphorylation (108, 109). Hsp90 was demonstrated to not only serve as a module to scaffold Akt to phosphorylate eNOS, but also stabilize 3-phosphoinositide-dependent kinase 1 (PDK1), the upstream kinase of Akt (110). In summary, Hsp90 not only serves as an allosteric protein of eNOS, but also acts on both Akt and PDK1 to maintain eNOS serine 1179 phosphorylation.

Subsequent study showed that Hsp90 also interacts with nNOS and this interaction increases NO production (111). It has been proved that Hsp90 directly augments nNOS activity, which is partially mediated by the enhancement of CaM binding affinity (112, 113). Further study discovered that inhibition of $O_2^{-\cdot}$ generation from nNOS by Hsp90 also contributes to the enhanced NO synthesis from nNOS (114). In summary, Hsp90 serves as a positive modulator of both eNOS and nNOS via enhanced CaM coupling with the two enzymes.

1.4.4 Hsp90 and iNOS

Unlike eNOS and nNOS, whose activities are regulated by Ca^{2+}/CaM coupling, protein-protein interaction and phosphorylation status, iNOS is constantly active once expressed with an intrinsically bound CaM. Thus the NO synthesis from iNOS is thought to be mainly regulated by iNOS gene transactivation and protein expression rather than posttranslational modulation. However, our study identified Hsp90 as an iNOS enhancer

through its direct interaction with iNOS (115). Our study also revealed that functional Hsp90 played important role in the cytotoxic action of iNOS. Furthermore, our recent study revealed that inhibition of Hsp90 abolished iNOS gene transactivaiton (116). Therefore, in addition to its regulation of iNOS function via a posttranslational manner, Hsp90 is also indispensable in the induction of iNOS expression.

The levels of active iNOS are also regulated by protein stability and turnover besides protein expression. Whether or not Hsp90 also plays a role in controlling iNOS protein stability has not been identified. Furthermore, the question of how cells deal with changed iNOS stability remains to be answered in the study of Hsp 90 regulation of iNOS.

CHAPTER 2

2 Role of CaM in induction of iNOS expression

2.1 Introduction

NO is an important signaling moledule and effector in biological system. NO has been discovered to play critical roles in cardiovascular system, neuronal signal transmission, and host defense. In biological system, NO is produced by a family of NOS enzymes including eNOS, iNOS and nNOS.

The activity of all three NOS enzymes in mammals requires CaM (86, 117-119). CaM coupling with NOS facilitates the electron transfer from the reductase domain to the oxygenase domain of the enzyme, leading to NO production (27, 88). nNOS and eNOS constitutively exist in cells and their activities are initiated by elevated intracellular Ca^{2+} concentration and subsequent CaM binding. Unlike the two isoforms, iNOS is undetectable in resting cells. iNOS expression could be induced by bacterial product lipopolysaccharide (LPS) and cytokines, such as interferon-γ (IFN-γ), via NF-κB and STAT1 signaling pathways, respevtively (87). Once iNOS is expressed, it is tightly bound with CaM even at basal Ca^{2+} level and thus exhibits constant activity in cells (86, 117). Therefore, nNOS and eNOS are categorized as Ca^{2+}/CaM-dependent enzymes, whereas iNOS is referred to as Ca^{2+}-independent NOS.

Compared with the other two NOS isoforms, iNOS exhibits higher NO-generating potency (18). The constant and potent NO-producting capacity has been thought to fulfill the host defense function of iNOS (8). On the other hand, massive NO productions from iNOS also causes cell injury and this has been implicated in various diseases such as endotoxemia. Endotoxin shock is a fatal disorder commonly found in the intensive care unit but the effective therapy is scarce (35, 43). In endotoxemia, endotoxin together with pro-inflammatory cytokines triggers abundant iNOS expressions, and the massive amounts of NO produced by iNOS play a causative role in organ failure and shock.

Since NO production from iNOS is primarily determined by enzyme protein levels, understanding the mechanism of iNOS induction has been the central issue of iNOS research. CaM has always been viewed as an enzymatic cofactor and is thought as an intrinsic component of iNOS structure due to its high binding affinity to iNOS. Whether or not CaM may have functions beyond assisting enzymatic reaction has not yet been explored in iNOS biochemistry. iNOS has long been known as a Ca^{2+}-independent enzyme as its catalytic activity does not require cytosolic Ca^{2+} increases. However, whether or not the initiation of iNOS expression requires Ca^{2+} flux remains unknown. Our prior study discovered that coexpression of iNOS and CaM in *E. coli* is essential for the purification of iNOS from bacteria, raising the question of how CaM affects iNOS expression. Here we show that CaM is indispensable for iNOS induction. The present study revealed that CaM inhibition or knockdown prevented iNOS expression in macrophages induced by LPS or IFN-γ. Further experiment demonstrated that CaM governs iNOS expression by regulating the signal transduction via both LPS-NF-κB and

IFN-γ-STAT1 pathways. Furthermore, CaMKII was identified as an upstream kinase governing the activation of both NF-κB and STAT1 pathways. Moreover, our study demonstrated that the rise of intracellular Ca^{2+} is essential for iNOS gene transactivation. In addition to cell biology studies, we have proved that CaM or CaMKII inhibition also markedly attenuated iNOS induction in mouse endotoxemia model. In response to decreased iNOS expression levels, the animal survival rates were remarkably raised. These studies revealed a novel role of CaM in iNOS gene expression and rendered CaM and CaMKII as novel therapeutic targets to intervene iNOS in endotoxin shock.

2.2 Materials and methods

2.2.1 Materials

Cell culture materials and Greiss reagent kit were purchased from Invitrogen (Carlsbad, CA). Anti-iNOS antibody was obtained from BD Transduction Laboratories (Franklin Lakes, NJ). Lipopolysaccharide (LPS, *E. coli* serotype O26:B6), recombinant mouse interferon-γ (IFN-γ), Trifluoperazine dihydrochloride, anti-GAPDH antibody were products of Sigma (St. Louis, MO). W-7, Trifluoperazine Dimaleate, Autocamtide-2 Related Inhibitory Peptide II (AIPII), KN-93 and KN-92 were purchased from Calbiochem (San Diego, CA). Antibodies against phospho-IKK, IKKα, IκBα, phospho-STAT1 (Ser727), phospho-STAT1 (Tyr701), STAT1, CAMKII and phospho-CAMKII (Thr286) were obtained from Cell Signaling Technology (Beverly, MA). Antibody against β-tubulin was product of Santa Cruz Biotechnology (Santa Cruz, CA). Anti-CaM antibody was purchased from Upstate Biotechnology (Lake Placid, NY). The protease

inhibitor tablet was the product of Roche Applied Science (Indianapolis, IN). Unless otherwise indicated, all other chemicals used in this study were purchased from Sigma.

2.2.2 Cell culture

Mouse macrophage cells (RAW264.7, ATCC) were grown in Dulbecco's modified Eagle's medium with 10% fetal calf serum (Invitrogen) in a 37˚C humidified atmosphere of 95% air and 5% CO_2. Expressions of iNOS in RAW264.7 cells were induced by LPS (2 μg/ml, serotype 026:B6) and IFN-γ (100 units/ml) (120). Adenoviruses, encoding for dominant negative CaMKII and constitutively active CaMKII mutants, were directly added to the cell culture medium and incubated for 24 hours before further treatments.

2.2.3 Western blot analysis

Cells were harvested and lysed on ice for 30 min in a lysis buffer (50 mM Tris-HCl, pH 7.4, 150 mM NaCl, 1% Nonidet P-40, 0.25% sodium deoxycholate, 50 mM NaF, 1 mM Na_3VO_4, 5 mM sodium pyrophosphate, and protease inhibitor tablet). Cell lysates were centrifuged at 14,000 × g for 15 min, and the supernatant were recovered. The protein concentrations were determined using the detergent compatible protein assay kit (Bio-Rad). After 5 min boiling in 1×SDS/PAGE sample buffer (62.5 mm Tris-HCl, pH 6.8, 2% SDS, 40 mm dithiothreitol, 10% glycerol, and 0.01% bromophenol blue), the proteins were separated by SDS/PAGE, transferred to nitrocellulose membranes, and probed with the appropriate primary antibodies. Membrane-bound primary antibodies were detected using secondary antibodies conjugated with horseradish peroxidase.

Immunoblots were developed on films using the enhanced chemiluminescence technique (SuperSignal West Pico, Pierce).

2.2.4 RT-PCR

Total RNA was extracted using Trizol Reagent (Invitrogen) according to the manufacturer's instructions. Reverse transcription was carried out using High Capacity cDNA Reverse Transcription Kit (Applied Biosystems). PCR was performed with Taq DNA polymerase. The following primers were used for iNOS: 5'-GGGATGGCTTGCCCCTGG-3' and 5'-CGGAGGCAGCACATCAAAG-3'. Primers 5'-GGTGAAGGTCGGAGTCAACG-3' and 5'-CAAAGTTGTCATGGATGACC-3' were used for GAPDH.

2.2.5 siRNA

The siRNA oligonucleotides corresponding to mouse calmodulin (5'-GCUAACAGAUGAAGAAGUAUU-3') were purchased from Dharmacon. siRNA oligonucleotides (100 nM) were transfected into cells using Lipofectamine 2000 reagent (Invitrogen). After 48 h of transfection, Western blottings were carried out to examine the knockdown of targeted proteins.

2.2.6 Nitrite assay

Total nitrite released in cell culture medium was measured with a Griess reagent kit (Invitrogen). The reaction consisted of 20 μl of Griess Reagent, 150 μl of medium, and 130 μl of deionized water. After incubation of the mixture for 30 min at room temperature, nitrite levels were measured at 548 nm using a spectrophotometric

microplate reader (Molecular Devices). Nitrite levels in serum were similarly measured after passing the whole blood samples through the Microcon YM-3 filters (Millipore).

2.2.7 Endotoxin shock and mouse survival studies

C57BCL/6 mice were purchased from Charles River Laboratories. Mice were maintained in a pathogen free environment and experiments on mice were conducted according to the protocols approved by the animal ethical committee. Mice were injected intraperitoneally with LPS at a dose of 40 mg/kg. Mice received saline injections were used as control in the sham group. For protection study, W-7 (40 mg/kg), trifluoperazine (25 mg/kg), or KN-93 (5 mg/kg) was administered intraperitoneally one hour before LPS injection. The survival of injected mice was assessed every two hours. Animal tissues were collected at indicated times after LPS injection from a designated group.

2.2.8 Cecal ligation and puncture model and mouse survival studies

Cecal ligation and puncture (CLP) model will be performed through the following procedures. Mice will be anesthetized prior to a shave at abdomen. After skin midline incision, the cecum will be located, exteriorized, ligated and punctured. Animal will then be sutured and resuscitated by injecting prewarmed normal saline (50 ml/kg). For protection study, trifluoperazine (25 mg/kg) was administered intraperitoneally or orally one hour after the surgical procedure. The survival of animals was assessed 4 times daily.

2.2.9 Statistical analysis

The data are expressed as the Means ± SE. Comparisons among treatment groups were made using a two-tailed Student's *t* test. The Kaplan-Meier method was used to analyze mortality. Differences were considered statistically significant at $P < 0.05$.

2.3 Results

2.3.1 Role of CaM in iNOS expressions in macrophages by combined LPS and IFN-γ stimuli

To determine the role of CaM in iNOS expression, mouse macrophage cells (RAW264.7) were exposed to LPS (2 μg/ml) and IFN-γ (100 units/ml). As expected, LPS/IFN-γ stimulated iNOS expressions in a time-dependent manner (Figure 2.1A, B). Pretreating the cells with the CaM inhibitor W-7 (100 μM) abolished LPS/IFN-γ-induced iNOS expressions. To substantiate that the blockade of iNOS induction was due to CaM inhibition rather than a particular action of W-7, we examined the effect of trifluoperazine, another CaM inhibitor that structurally differs from W-7. Trifluoperazine (50 μM) also prevented the iNOS induction by LPS/IFN-γ (Figure 2.1C, D). Consistent with the loss of iNOS expressions, NO productions from the LPS/IFN-γ-stimulated cells were abrogated by W-7 and trifluoperazine (Figure 2.1E).

To further corroborate these results obtained by pharmacological inhibitors, we used siRNA to knock down intracellular CaM. Consistent with the action of chemical antagonists, CaM knockdown markedly diminished iNOS expressions in cells stimulated by a combination of LPS and IFN-γ (Figure 2.2).

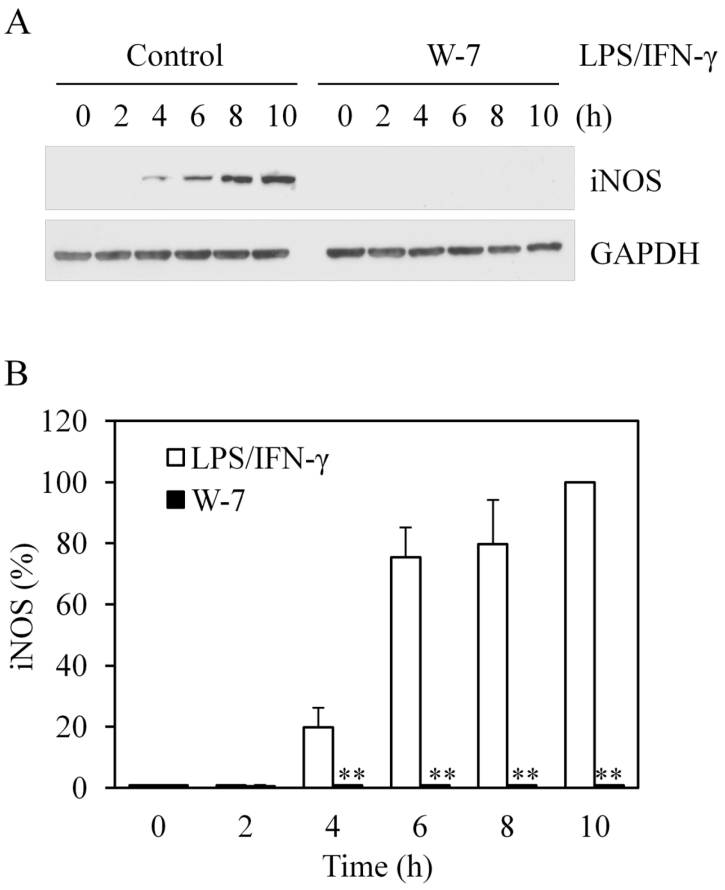

Continued

Figure 2.1 Role of CaM in iNOS expression in cells induced by lipopolysaccharide (LPS)/interferon-γ (IFN-γ).

(A) CaM-specific inhibitor W-7 (100 μM) prevented iNOS expression in cells stimulated by LPS/IFN-γ. Representative blots are shown from at least three independent experiments. (B) Quantitative analyses of the effects of W-7 on iNOS expression. Data are means ±SE. ** $P < 0.01$ vs. control, n = 3-5. (C) Trifluoperazine (50 μM), another CaM inhibitor that structurally differed from W-7, also blocked iNOS expression in stimulated cells. (D) Quantitative analyses of the effects of trifluoperazine on iNOS expression (n = 3-5). (E) Corresponding to the loss of iNOS expression, NO production in LPS/IFN-γ-stimulated cells was also blunted by CaM inhibition (n = 3-5).

Figure 2.1 continued

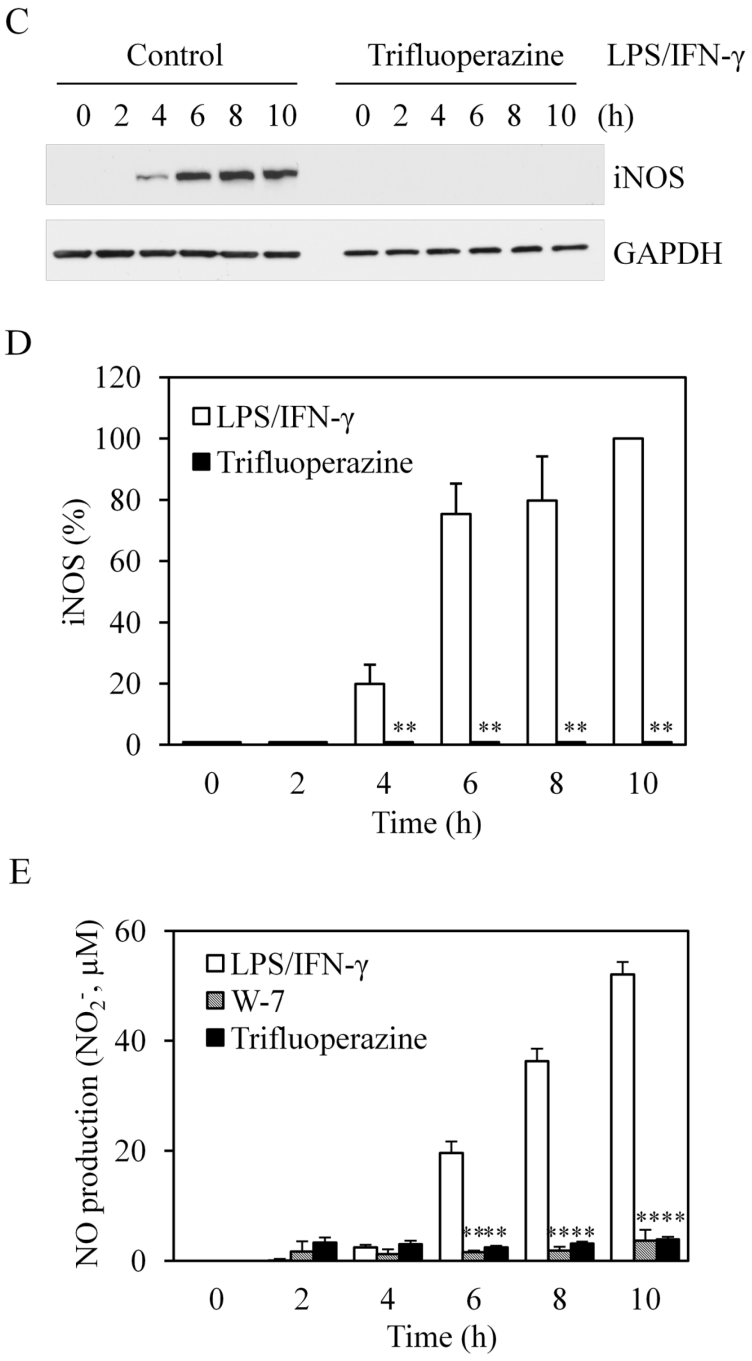

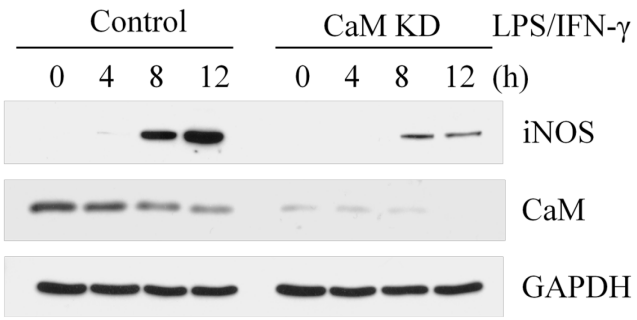

Figure 2.2 Effect of CaM knockdown on iNOS expression in LPS/IFN-γ-stimulated cells.

Representative data were shown from triplicate experiments.

2.3.2 An obligatory role of CaM in LPS- or IFN-γ-induced iNOS expressions

LPS or IFN-γ alone can stimulate iNOS expression in macrophage cells. We therefore explored if CaM was necessary in iNOS induction in cells stimulated by LPS or IFN-γ alone. As shown in Figure 2.3A, LPS induced iNOS expression as a function of time. Preincubating cells with either W-7 or trifluoperazine remarkably blocked iNOS protein expressions. NO productions were also ablated in CaM-inhibited cells (Figure 2.3B).

In IFN-γ-treated cells, CaM inhibition with W-7 and trifluoperazine also abolished iNOS protein expressions (Figure 2.4A), similar to the effects on LPS-induced iNOS expressions. Corresponding to the blockade of iNOS protein productions, NO syntheses in cells were also halted (Figure 2.4B). Thus, CaM was required in both LPS- and IFN-γ-initiated iNOS protein expressions.

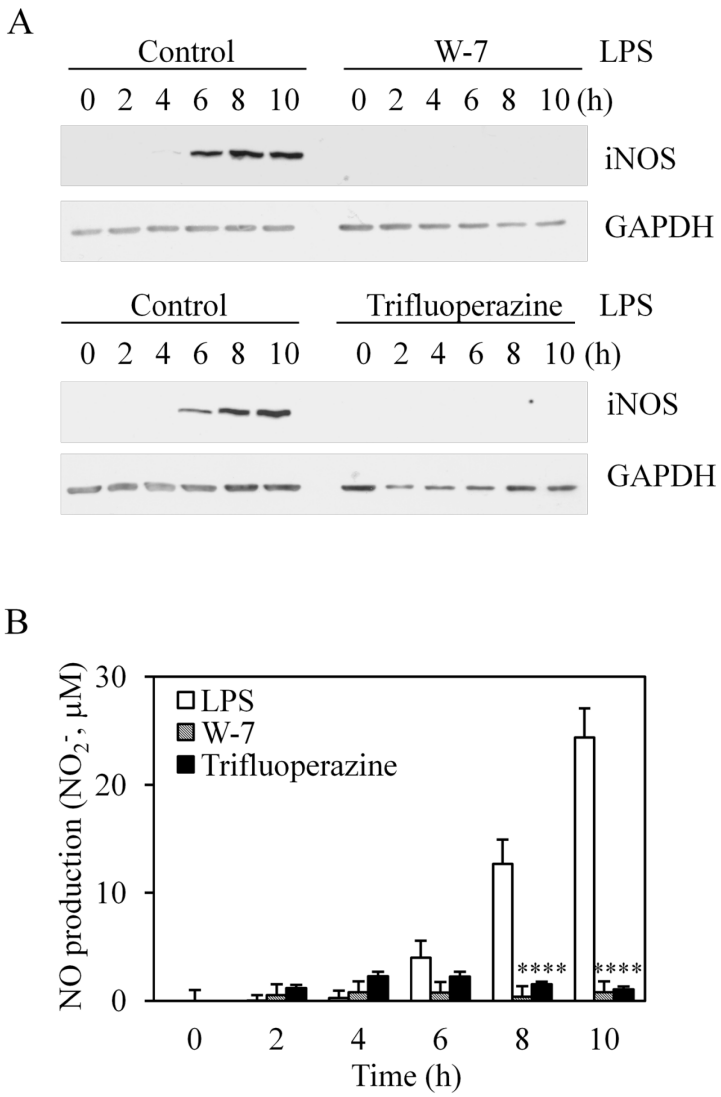

Figure 2.3 An obligatory role of CaM in iNOS expressions induced by LPS.
(A) CaM inhibition abolished iNOS protein expressions in LPS-stimulated cells. (B) CaM inhibition prevented NO productions in LPS-treated cells. Data were shown as Mean ± SE. ** $P < 0.01$ vs. control, n = 5.

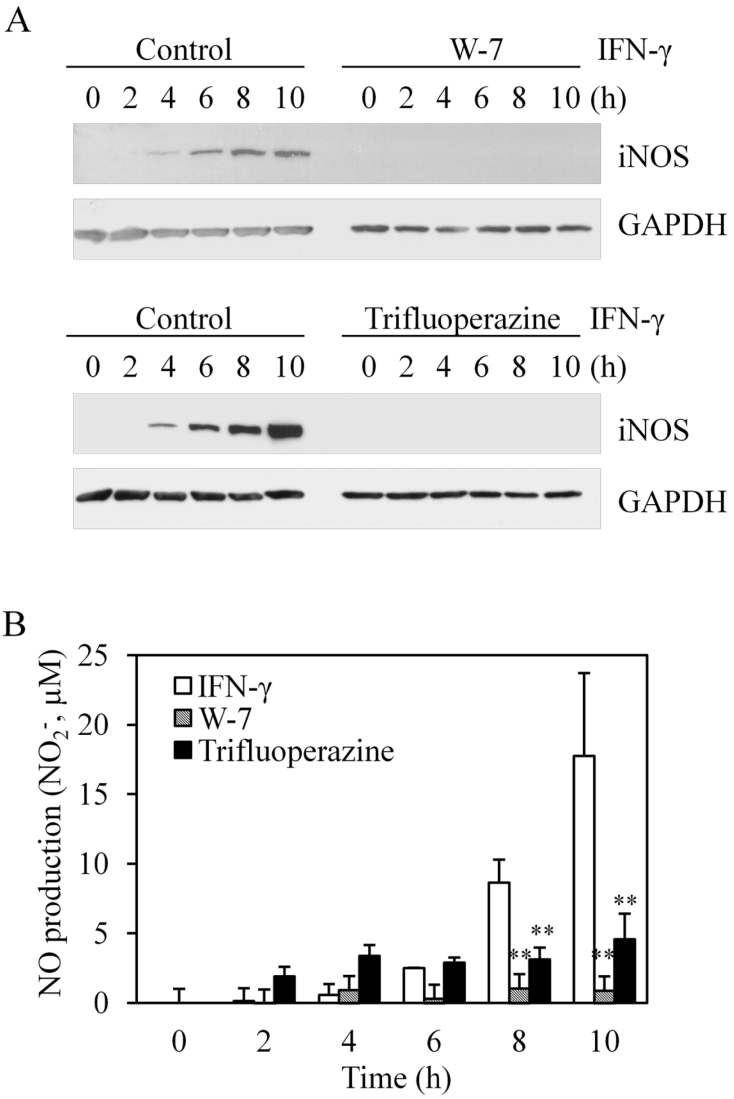

Figure 2.4 An essential role of CaM in IFN-γ-induced iNOS expressions.
(A) Effects of CaM inhibitors on iNOS expression in cells exposed to IFN-γ. (B) CaM inhibition prevented NO productions in IFN-γ-treated cells. Data were shown as Mean ± SE. ** $P < 0.01$ vs. control, n = 5.

2.3.3 Effects of CaM inhibition on iNOS mRNA formation in macrophages stimulated by LPS or IFN-γ alone or in combination

The absence of iNOS proteins in CaM-inhibited cells could be a result of the failure of iNOS gene transcription, or deficiency of iNOS protein translation. To elucidate how CaM affects iNOS induction, iNOS mRNA levels were monitored in LPS/IFN-γ-stimulated cells in the absence and presence of CaM inhibitors. As shown in Figure 2.5A, LPS/IFN-γ stimulated the synthesis of iNOS mRNA in a time-dependent manner, whereas CaM inhibition with either W-7 or trifluoperazine abolished iNOS mRNA formation. These results indicated that CaM was indispensable for iNOS gene transcription in macrophages induced by endotoxin and cytokines, such as IFN-γ.

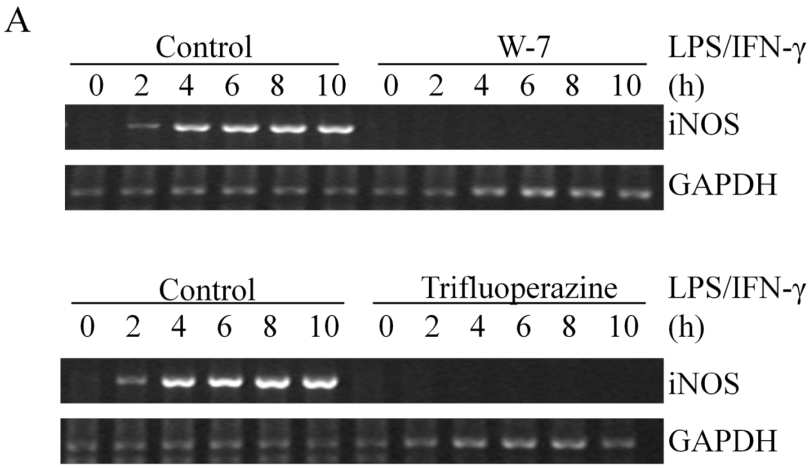

Continued

Figure 2.5 CaM inhibition abolished iNOS mRNA formation induced in mouse macrophages.
(A) Effects of CaM inhibitor W-7 (100 μM) and trifluoperazine (50 μM) on iNOS mRNA transcription in mouse macrophages stimulated with LPS/IFN-γ. (B) CaM inhibition prevented iNOS mRNA formation in LPS-treated cells. (C) CaM inhibition abolished iNOS mRNA expression in IFN-γ-treated cells. Representative data were shown from five independent experiments.

Figure 2.5 continued

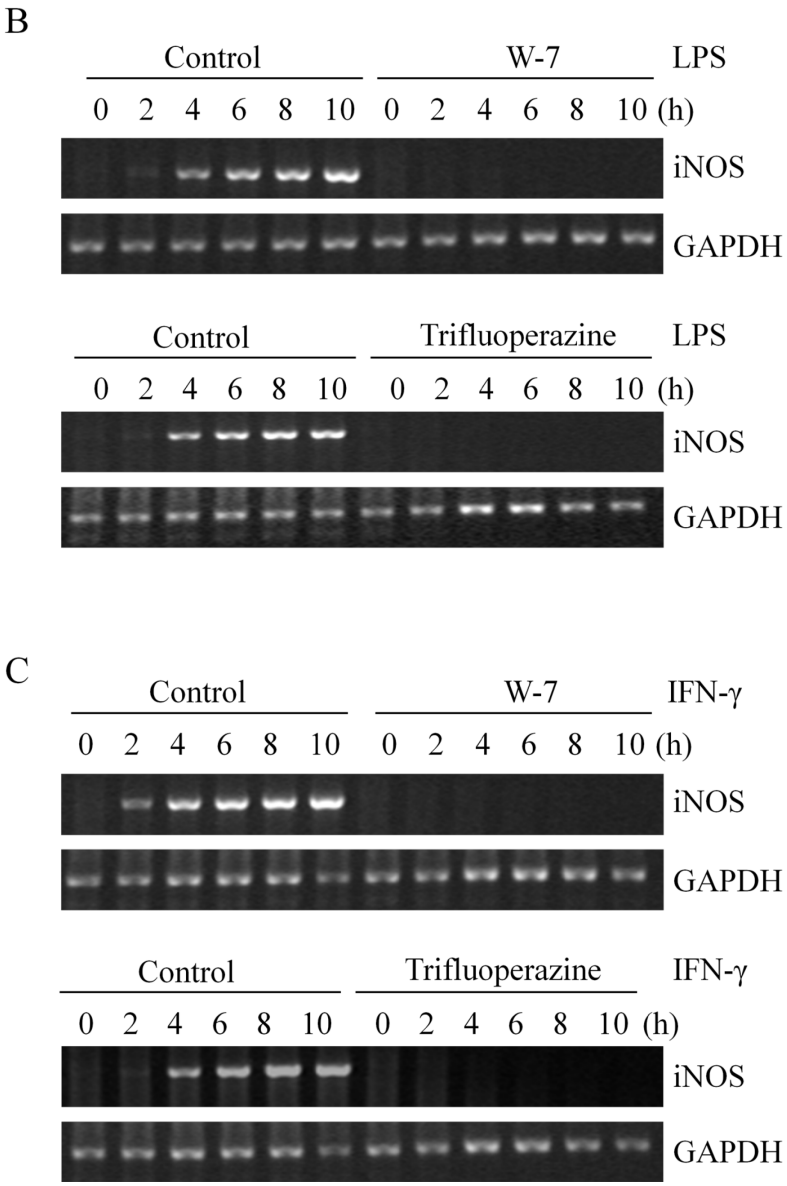

LPS or IFN-γ alone can activate iNOS gene transcription. RT-PCR experiments showed that iNOS mRNA formation was blocked by CaM inhibition in LPS-stimulated cells (Figure 2.5B). iNOS mRNA formation in cells treated with IFN-γ alone were also investigated. Similar to the effects on iNOS gene transcription initiated by LPS, the presence of CaM inhibitors abolished iNOS mRNA formation in IFN-γ-treated cells (Figure 2.5C). These data demonstrated that CaM function was required for iNOS gene transcription stimulated by both LPS and IFN-γ.

2.3.4 Effects of CaM inhibition on signal transducers and activators of LPS-IKK-NF-κB and IFN-γ-STAT1 pathways amid iNOS induction

LPS and IFN-γ activate iNOS expressions through distinctive signaling pathways and transcriptional factors. LPS induces iNOS gene transcription via the IKK-NF-κB pathway, whereas IFN-γ induces iNOS expression primarily through the JAK-STAT1 cascade. To explore the mechanism underlying the action of CaM inhibition on iNOS gene transactivation, we measured the effects of CaM inhibitors on the activation of IKK-NF-κB pathway. As shown in Figure 2.6, CaM inhibition prevented LPS-induced IKK activation. Consequently, the degradation of IκB in LPS-treated cells was blunted, indicating that the NF-κB activation was blocked. These results suggested that CaM was required for the activation of IKK-NF-κB pathway.

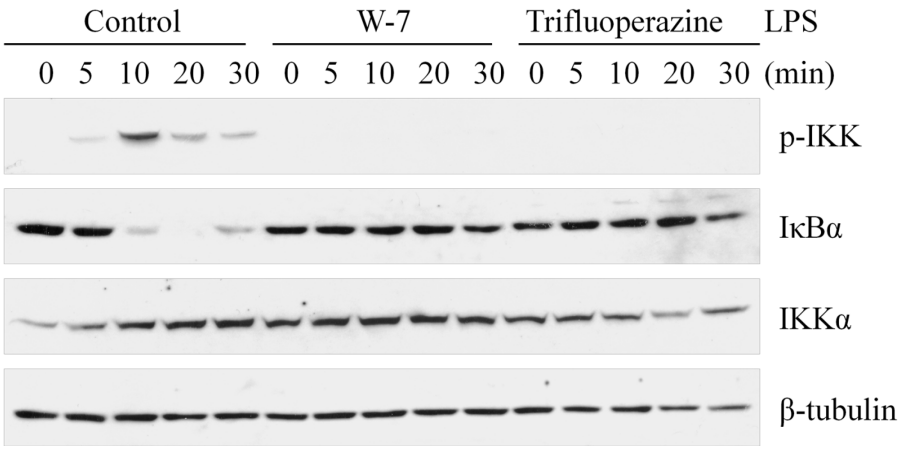

Figure 2.6 CaM inhibition prevented LPS from activating IKK-NF-κB pathway. As shown, LPS-elicited IKK phosphorylation and IκB degradation were all abrogated in CaM-inhibited cells. Representative blots are shown from three independent experiments.

We also studied the effect of CaM antagonists on the STAT1 signaling pathway in the process of iNOS expression in IFN-γ-stimulated cells. As expected, in the absence of CaM inhibitors, IFN-γ activated STAT1 by initiating the phosphorylation of its Tyr701 and Ser 727 residues. Similar to the effect on NF-κB, CaM inhibition also abolished STAT1 activation in IFN-γ-treated cells (Figure 2.7), indicating CaM function is indispensable for signal transduction via STAT1 pathway. Therefore, CaM function was essential for NF-κB and STAT1 activation in the process of iNOS induction.

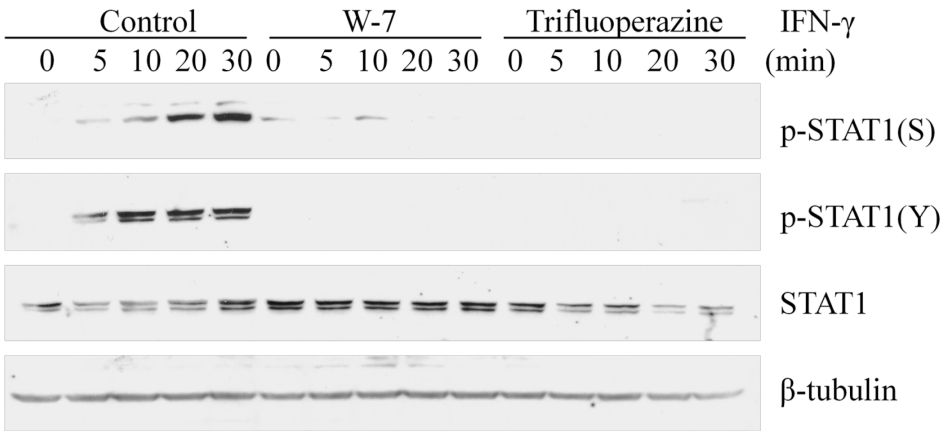

Figure 2.7 CaM inhibition abolished STAT-1 activation in IFN-γ-treated cells. Representative blots are shown from three independent experiments.

2.3.5 CaMKII mediates the signal transduction in iNOS induction

We then sought to identify the target that CaM acted upon in iNOS expressions. Previous studies reported that CaMKII was activated by cytokine and involved in NF-κB cascade (93, 121), we thus examined if CaMKII was a target of CaM in its action during iNOS induction. Indeed, CaMKII activation was seen in LPS/IFN-γ-stimulated macrophages and this was sensitive to W-7 (Figure 2.8). To probe if CaMKII was requested for iNOS expressions, we treated the cells with the CaMKII blocker KN-93 (50 μM). Equal amounts of KN-92, an inactive compound structurally resembling KN-93, were used as control. As shown in Figure 2.9A, KN-93 but not KN-92 blocked iNOS expressions in LPS/IFN-γ-treated cells. NO productions from the stimulated cells were also eradicated by CaMKII blockade (Figure 2.9B). To reconfirm these findings gained by chemical blockers, we investigated the effect of AIPII, a cell-permeable peptide inhibitor specifically targeting CaMKII, on iNOS induction. As expected, AIPII (20 μM)

markedly reduced iNOS expressions in cells exposed to LPS or IFN-γ (Figure 2.9C). Similar to the effect of CaM inhibition, blocking CaMKII with KN-93 or AIPII also largely prevented iNOS mRNA formations in stimulated cells (Figure 2.10A, B). These findings indicated that CaM targeted CaMKII, and the activation of CaMKII was necessary to iNOS gene transcription.

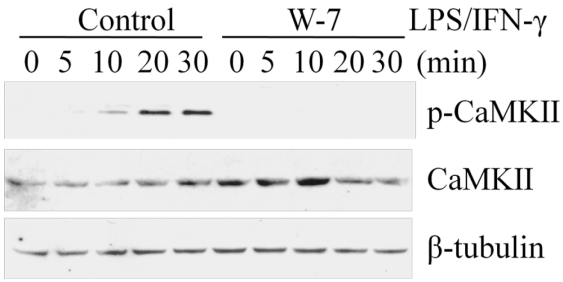

Figure 2.8 CaMKII was activated in LPS/IFN-γ-stimulated cells and this activation was prevented by CaM inhibition.
Representative blots are shown from three independent experiments.

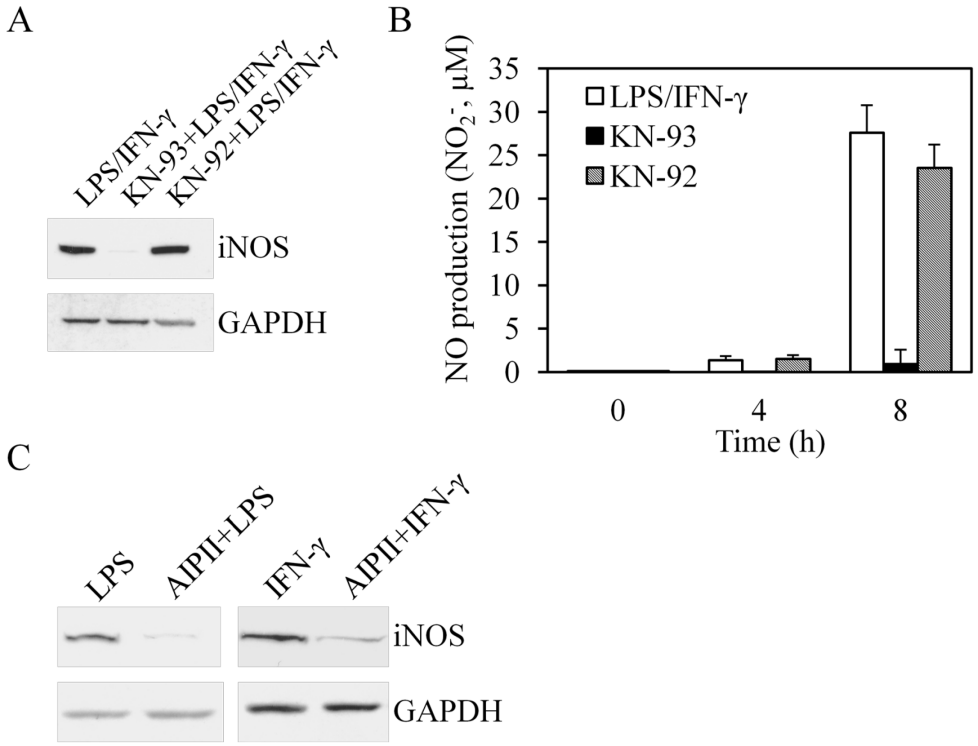

Figure 2.9 CaMKII inhibition blocked iNOS expression.
(A) Effects of CaMKII inhibitor KN-93 (50 μM) and KN-92 (50 μM), a negative control of KN-93, on iNOS protein expression in LPS/IFN-γ-stimulated cells. (B) CaMKII inhibition abolished NO productions in cells stimulated by LPS/ IFN-γ. (C) AIPII, another CaMKII-specific peptide inhibitor, also attenuated iNOS expression in LPS- or IFN-γ-stimulated cells. Representative blots are shown from three independent experiments.

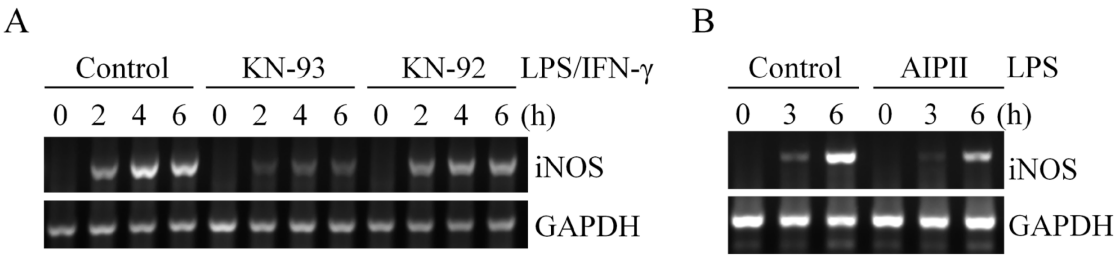

Figure 2.10 CaMKII blockade attenuated LPS/IFN-γ-induced iNOS mRNA transcriptions.
(A) KN-93 reduced iNOS mRNA formation in LPS/IFN-γ-stimulated cells. (B) AIPII also blocked iNOS mRNA transcriptions in LPS-stimulated cells. Representative blots are shown from three independent experiments.

2.3.6 CaMKII acts as an upstream kinase governing the activation of both NF-κB and STAT1 pathways

Experiments were also performed to establish CaMKII as an upstream kinase that signaled both NF-κB and STAT1 activation in iNOS induction. As shown in Figure 2.11A, CaMKII blockade with AIPII prevented LPS-induced IKK activation and IκB degradation. In IFN-γ-stimulated cells, STAT1 activation was also abolished by CaMKII blockade (Figure 2.11B). There data suggested CaMKII as an upstream kinase that governed both LPS-NF-κB and IFN-γ-STAT1 pathways in iNOS induction. This notion was further supported by the findings that dominant negative CaMKII (dn-CaMKII) mutant markedly decreased LPS/IFN-γ-induced iNOS expressions (Figure 2.12A). Moreover, forced CaMKII activity by expressing the constitutively active CaMKII (ca-CaMKII) mutant into cells was sufficient to induce iNOS expressions in the absence of LPS/IFN-γ (Figure 2.12B). The fact that activating CaMKII bypassed LPS or IFN-γ stimulation and directly triggered iNOS expressions underscored the key role of CaMKII in governing iNOS gene transcription.

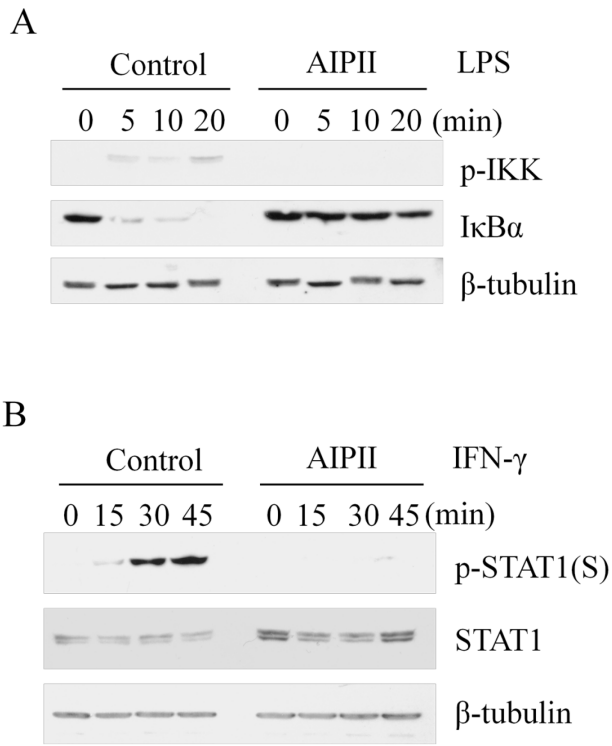

Figure 2.11 CaMKII signaled both NF-κB and STAT1 activation in iNOS induction. (A) CaMKII inhibition prevented the activation of IKK-NF-κB cascade by LPS. (B) CaMKII blockade abolished STAT-1 activation in IFN-γ-stimulated cells. Representative blots are shown from three independent experiments.

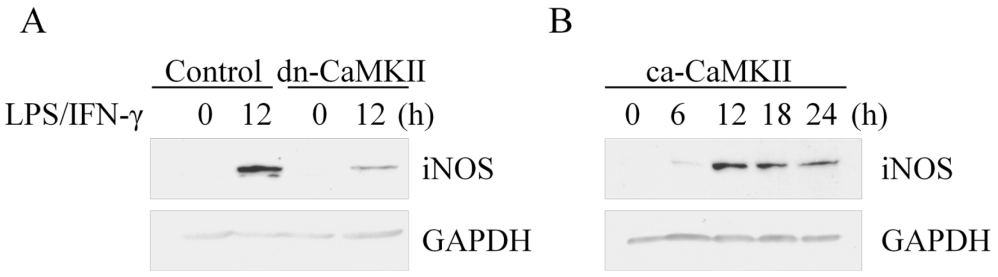

Figure 2.12 CaMKII acted as an upstream kinase that governed both LPS-NF-κB and IFN-γ-STAT1 pathways in iNOS induction.
(A) Expressions of dominant negative CaMKII (dn-CaMKII) reduced iNOS expressions in LPS/IFN-γ-treated cells. (B) Expressions of constitutively active CaMKII (ca-CaMKII) induced iNOS expression in mouse macrophages in the absence of LPS/IFN-γ. Representative blots are shown from three independent experiments.

2.3.7 Transient Ca^{2+} elevations is indispensable in iNOS induction

CaMKII is primarily activated by the elevations of cytosolic Ca^{2+} concentrations. While both LPS and IFN-γ have been reported to cause transient Ca^{2+} increases in cytosol (92, 122), iNOS has been categorized as "Ca^{2+}-independent" as its catalytic activity doesn't require elevated intracellular Ca^{2+} concentrations (86, 117). However, we argued that iNOS gene transactivation might be "Ca^{2+}-dependent". To examine this hypothesis, we loaded the cells with the intracellular Ca^{2+} chelator BAPTA-AM prior to LPS/IFN-γ exposure. Remarkably, preventing the elevations of Ca^{2+} in cytosol with BAPTA-AM (100 μM) abolished iNOS mRNA and protein expressions in LPS/IFN-γ-treated cells (Figure 2.13A, B). Consistent with the suppressed expression of iNOS mRNA and protein, NO productions from cells were also completely blocked by BAPTA-AM (Figure 2.13C). Furthermore, quenching the rise of intracellular Ca^{2+} prevented CaMKII activation in LPS/IFN-γ-stimulated cells (Figure 2.14). NF-κB and STAT1 activation were accordingly abrogated (Figure 2.14). Thus, in contrast to its enzymatic function, iNOS gene transactivation depended on the rise of cytosolic Ca^{2+}. LPS and IFN-γ caused transient intracellular Ca^{2+} elevations, which subsequently activated CaMKII, leading to the initiation of iNOS gene transcription.

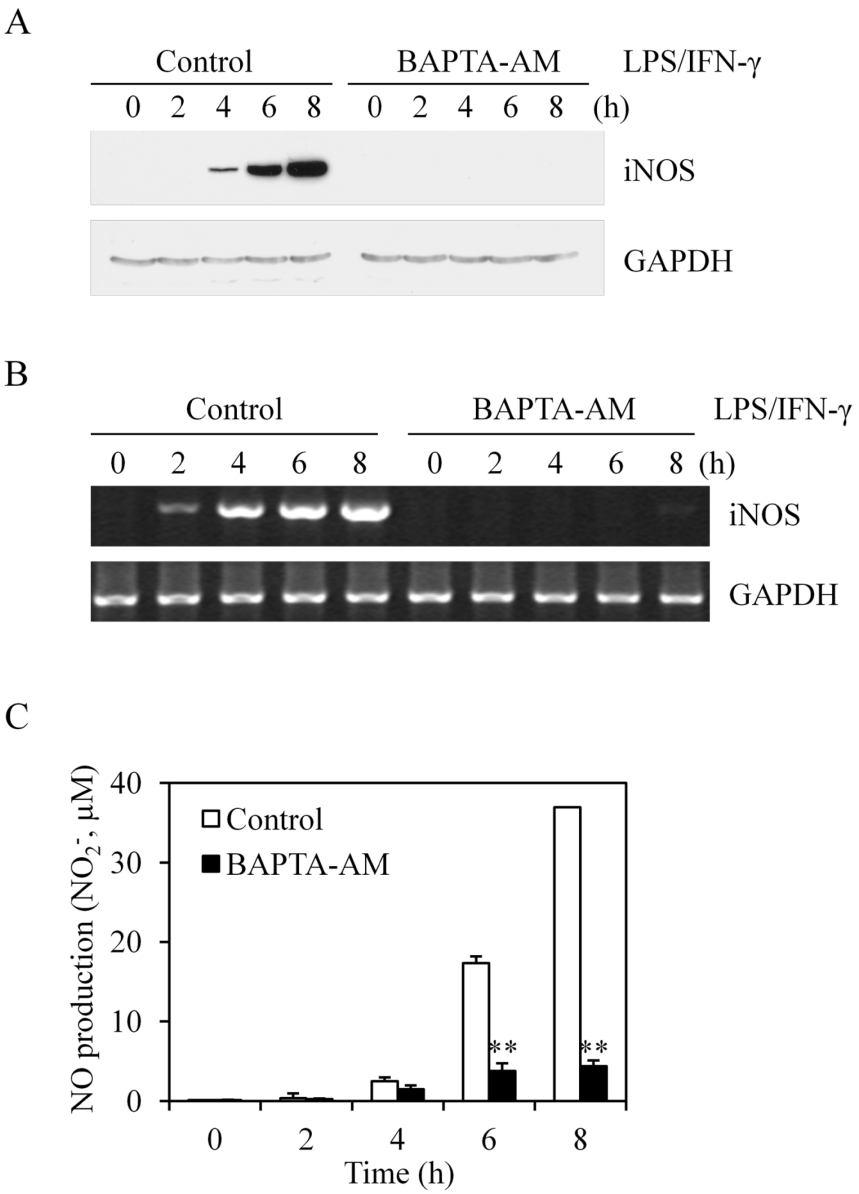

Figure 2.13 Transient Ca^{2+} elevations were required in iNOS induction.
(A) Intracellular Ca^{2+} chelating with BAPTA-AM prevented iNOS expressions in LPS/IFN-γ-induced cells. (B) Abolishing intracellular Ca^{2+} elevations prevented iNOS mRNA transcription. (C) Abolishing intracellular Ca^{2+} elevations prevented NO formation in LPS/IFN-γ-treated cells. Data were shown as Mean ± SE. ** $P < 0.01$ vs. control, n = 5.

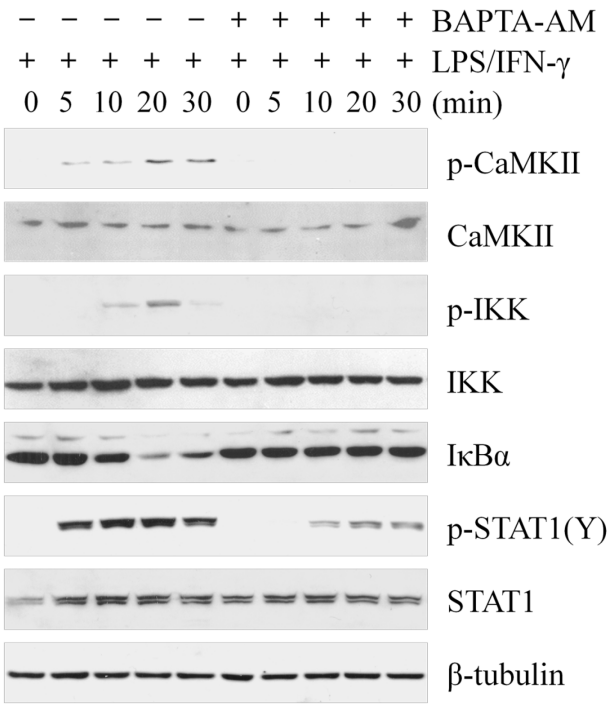

Figure 2.14 Activation of IKK-NF-κB and STAT-1 pathways amid iNOS induction was dependent on the elevations of intracellular Ca^{2+}.

2.3.8 Roles of CaM or CaMKII in iNOS expression *in vivo*

The above studies demonstrated the important role of CaM in iNOS induction in cultured cells exposed to inflammatory substances such as LPS. To investigate whether these cell biology findings occurred *in vivo*, we monitored the effect of CaM on iNOS expression in endotoxemic mice. Mice were injected with LPS (40 mg/kg, i.p.) to induce endotoxin shock. While iNOS was undetectable in the tissues of the sham animals injected with saline, massive iNOS proteins were seen in all vital organs of the mice injected with LPS (Figure 2.15). Corresponding to protein expression, iNOS mRNAs were also detected in the organic samples of LPS-injected mice (Figure 2.16). Dramatic elevations of NO metabolites were measured in the serum of the mice in endotoxin shock

(Figure 2.17). CaM inhibitor W-7 (40 mg/kg/day, i.p.) blocked the iNOS expressions in LPS-injected mice, and therefore the increases of NO productions in serum were inhibited (Figure 2.15, 2.16 and 2.17). Trifluoperazine (TFP, 25 mg/kg/day, i.p.) also efficiently prevented iNOS induction and NO generations in mice suffering endotoxin shock (Figure 2.15, 2.16 and 2.17). These data demonstrated that CaM inhibition prevented iNOS expressions in endotoxin shock.

Our studies identified CaMKII as the target of CaM in iNOS induction. We then assessed whether direct blockade of CaMKII had effect on iNOS expression in endotoxemic mice. Consistent with the results obtained from cell culture studies, CaMKII inhibition with KN-93 (5 mg/kg/day, i.p.) blocked iNOS expressions in endotoxemic mice (Figure 2.18A). The NO metabolites in the serum were also blunted by pretreating LPS-injected mice with KN-93 (Figure 2.18B).

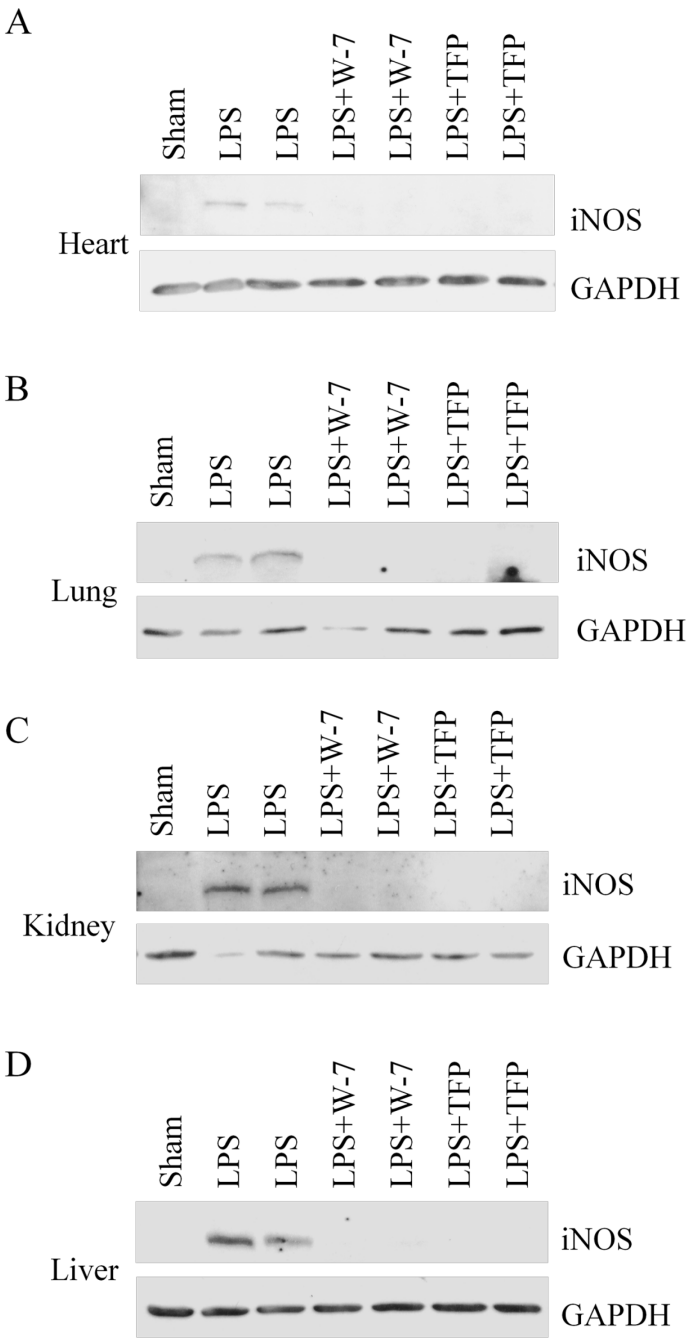

Figure 2.15 CaM inhibition prevented iNOS expressions in vital organs of mice injected with lethal doses of LPS.
(A-D) CaM inhibitors abolished iNOS expression in heart, lung, kidney and liver of LPS-injected mice, respectively.

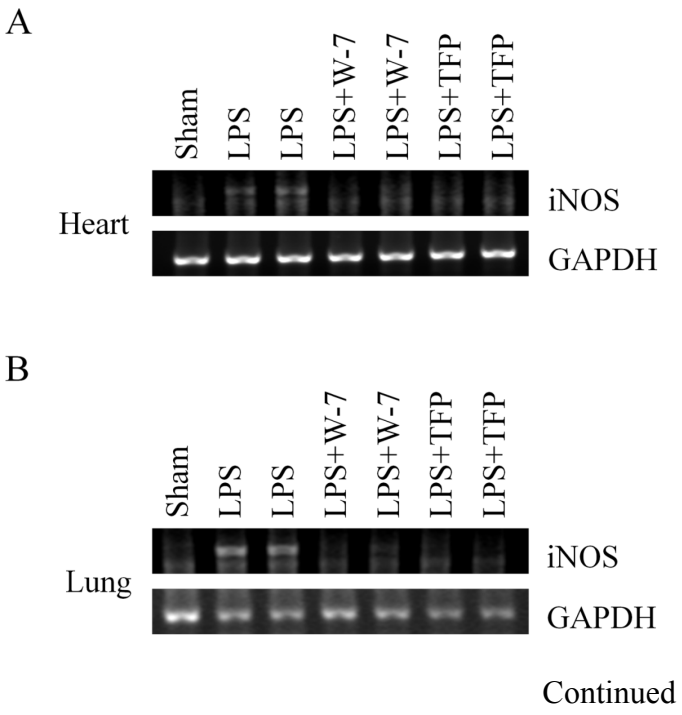

Continued

Figure 2.16 CaM inhibition prevented iNOS mRNA transcription in vital organs of LPS-injected mice.
(A-E) iNOS mRNA formation in heart, lung, kidney, liver and aorta from endotoxemic mice were blocked by CaM inhibition, respectively.

Figure 2.16 continued

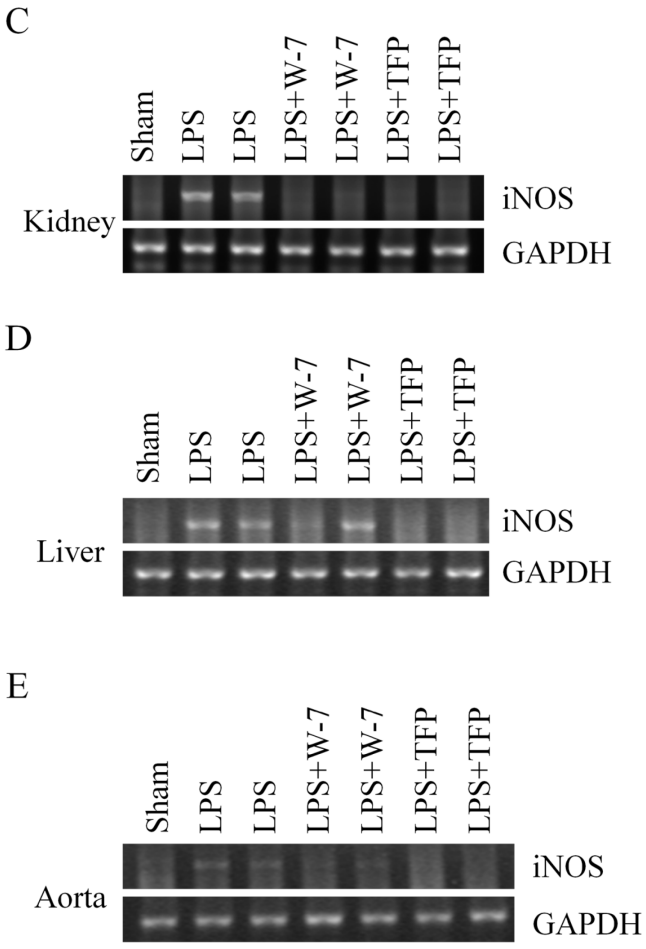

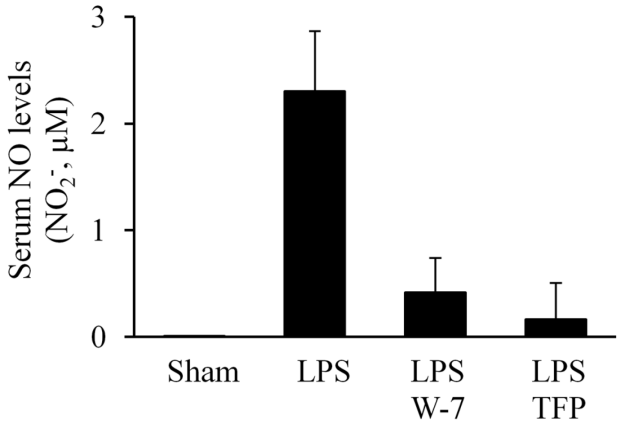

Figure 2.17 CaM inhibition abolished the increases of NO productions in the serum of endotoxemic mice.

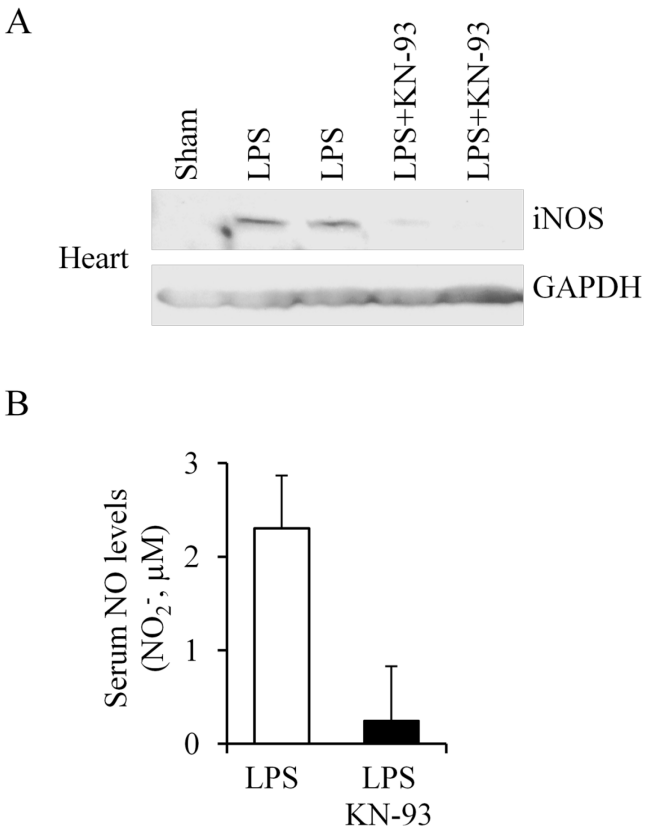

Figure 2.18 CaMKII blockade with KN-93 prevented iNOS expressions and NO productions in LPS-injected mice.
Data shown were (A) the levels of iNOS expressions in heart and (B) NO productions in serum of endotoxemic mice.

2.3.9 CaM or CaMKII blockade enhances mouse survival in endotoxemia model

Lethal doses of LPS (40 mg/kg, i.p.) were injected into mice to establish the endotoxemia model. In endotoxemic mice, massive iNOS proteins were induced and the large amount of NO generated by iNOS had been reported to cause hypotension and vascular hyporeactivity in previous studies. It had also been proved that the great amount of iNOS-derived NO contributed to the high mortality rate of endotoxin shock. Our

studies showed that blockade of CaM markedly inhibited iNOS and NO expressions in LPS-treated mice. Thus we explored if blocking iNOS expressions by CaM inhibition could protect mice against endotoxin shock. By pretreating mice with CaM antagonists prior to LPS injection, we monitored the effects of CaM inhibitors on animal survival rates. In the absence of CaM inhibitors, mice injected with lethal doses of LPS (40 mg/kg, i.p.) died within 30 h. As shown in Figure 2.19, the presence of W-7 markedly improved the survival rate of the mice injected with LPS. The protective effect of trifluoperazine on LPS-treated mice against endotoxin shock appeared to be more potent than that of W-7, resulting in a remarkably retarded mortality curve (Figure 2.20). These results demonstrated that blockage of iNOS expressions by CaM inhibition led to the enhancement of mouse survival in endotoxin shock.

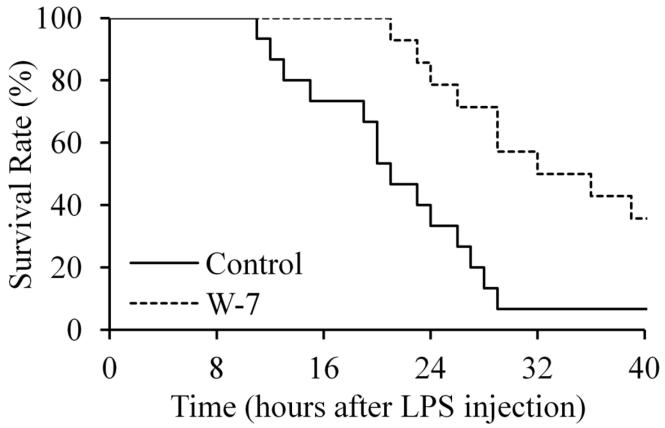

Figure 2.19 CaM inhibition with W-7 improved the survival rate of endotoxemic mice.

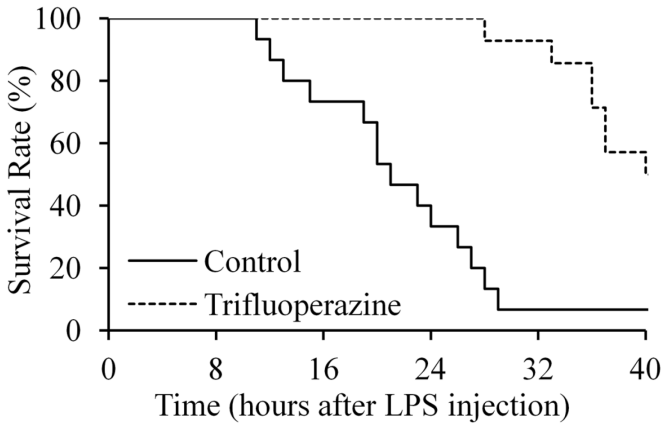

Figure 2.20 CaM inhibition with TFP markedly protected mice against endotoxin shock.

Our studies have demonstrated that CaMKII inhibition also resulted in blunted iNOS and NO expressions in LPS-treated mice. Thus CaMKII was also a possible target for regulating the amounts of iNOS and NO in mice suffering endotoxin shock to improve the survival rate. The protective effect of CaMKII inhibitor on endotoxemic mice was also assessed. Indeed, KN-93 (5 mg/kg/day, i.p.) significantly reduced the mortality rate of LPS-injected mice (Figure 2.21). These results indicated that protection against endotoxin shock could be achieved by directly targeting CaMKII.

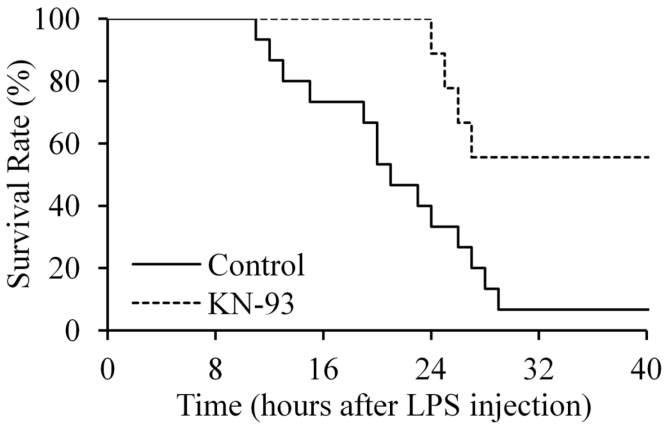

Figure 2.21 CaMKII blockade enhanced the survival of mice suffering endotoxin shock.

2.3.10 CaM inhibition has no protective effect on mouse survival rates in cecal ligation and puncture (CLP) model

Recent studies have indicated some limitations of the endotoxemia model. Cecal ligation and puncture (CLP) model, with high consistency and controllability, has been suggested as an improved model for sepsis study. It was believed that CLP model possessed more similarity with actual sepsis condition and was considered as gold standard. We thus investigate the effects of CaM inhibitor against septic shock in CLP model. Unfortunately, either intraperitoneally or orally administered trifluoperazine (25 mg/kg/day) failed to protect mice against death. The mortality rates of mice in CLP models appeared to be similar regardless of the presence or absence of trifluoperazine treatment (Fiugre 2.22).

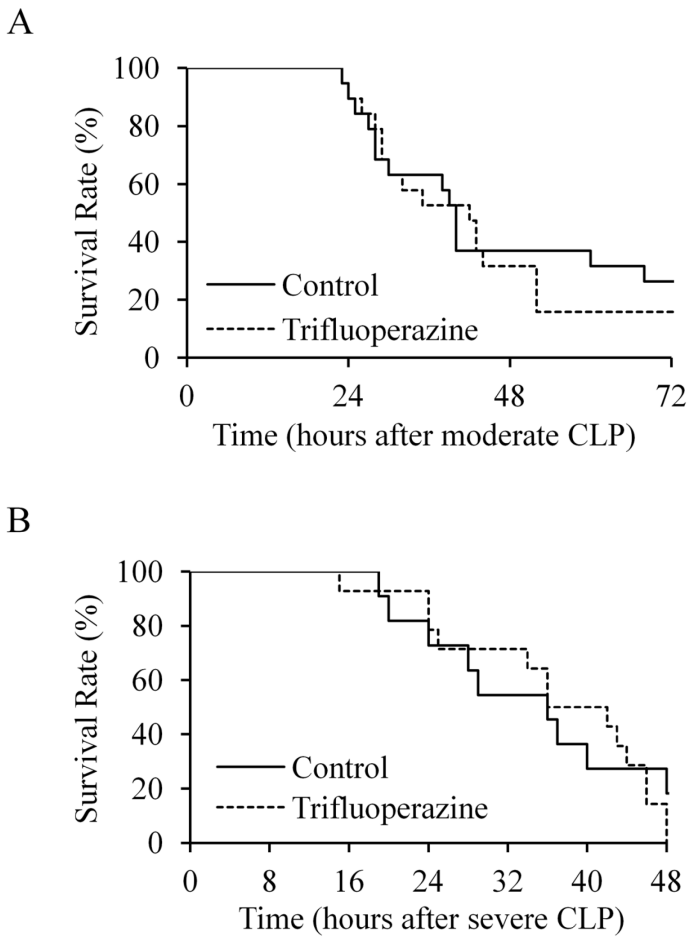

Figure 2.22 CaM inhibition had no protective effect on survival rates of mice in CLP model.
The mortality curves of mice in (A) moderate and (B) severe CLP models, respectively.

2.4 Discussion

The key finding of this study is that CaM is essential for iNOS gene transcription. CaM has been known as a ubiquitous cofactor for the catalysis of all NOS isoforms for years. CaM binds with a consensus region between the NOS reductase domain and oxygenase domain. Enzymatic and structural studies showed that CaM binding induces NOS conformational changes, which enable electrons transfer from the reductase domain

to the oxygenase domain to initiate NO syntheses. The findings in current study extended the role of CaM from an enzyme cofactor to an obligatory component in the initiation of iNOS gene transcription. We further identified that CaM targets CaMKII, which functions as an upstream kinase of both NF-κB and STAT1 pathways in iNOS gene transactivation. Since NF-κB binding sites also exist in nNOS and eNOS promoter, CaM and CaMKII may regulate NOS gene transcription in general.

The finding on the role of Ca^{2+} in iNOS induction is unexpected. Unlike nNOS and eNOS whose bindings with CaM require the elevations of intracellular Ca^{2+}, iNOS binds with CaM at basal Ca^{2+} levels in quiescent cells. This unique feature renders iNOS constantly active once expressed. The present study shows that although iNOS catalytic function does not require the elevations of cytosolic Ca^{2+}, transient Ca^{2+} increases are essential for CaMKII activation and subsequent initiation of iNOS gene transcription. Thus, targeting transient Ca^{2+} may be a new approach to intervene iNOS expression in inflammation.

Sepsis causes 300,000–500,000 deaths in North America each year (35, 43). While sepsis is a prominent cause of death in the United States, no treatment strategy has been proved to be promising for the routine management of patients with sepsis. As infections evolve into sepsis, endotoxemia plays primary role in triggering the excessive productions of pro-inflammatory cytokines and chemokines. These hyperactive inflammatory responses are the central mechanism of tissue damage and organ failure in sepsis. iNOS is highly expressed in septic tissues. Massive NO generated by iNOS not only result in hypotension but also render septic vasculatures inert to vasoconstrictor

therapy (18, 43, 87). The present study demonstrated that CaM or CaMKII inhibition prevented iNOS expressions and enhanced the survival of the mice in endotoxemia model. It is noteworthy that CaMKII activation was shown to promote apoptosis and CaMKII blockade was reported to improve the function of failing hearts (123-125). The protection against endotoxin shock by CaMKII inhibition hence may involve other mechanisms beyond iNOS.

Although CaM or CaMKII inhibitors effectively improved the survival of LPS-injected mice, CaM blockade appeared to have little protective effects on CLP-treated mice. The inconsistency of the results obtained from two different models of sepsis may be ascribed to the differences between the two models. Endotoxemia model is formed by a bolus injection of bacterial product LPS, whereas CLP model is performed by the leakage of mixed population of enteric bacteria to abdominal cavity. It has also been reported that the CLP procedure resulted in a substantial amount of devitalized tissue which in turn caused abscess formation. Thus CLP initiates responses more complex than those resulting from LPS injection. This may explain why CaM inhibition protected LPS-treated mice against endotoxin shock, but failed to decrease the mortality rate of animal in CLP model. Several recent studies have suggested that synergistic antibiotics combined with certain treatment showed improved efficacy in treating sepsis. Therefore, the effectiveness of CaM inhibition in treating CLP-performed mice should be reexamined with simultaneous antibiotic administration in future study, as the combined treatment of trifluoperazine with antibiotics may lead to a different therapeutic result. Regardless, our findings suggest CaM and CaMKII as potential targets for septic therapy.

It is worth noting that trifluoperazine is a clinically used and orally available medicine. Given the positive results seen in endotoxemic mice, the effectiveness of TFP in treating sepsis is readily examinable on patients.

In summary, our studies identified a novel role of CaM in the induction of iNOS. Thus the role of CaM is extended from an enzyme cofactor to an obligatory component in the initiation of iNOS gene transactivation. Further studies not only identified CaMKII as the target of CaM, but also demonstrated it as the upstream kinase governing both NF-κB and STAT1 signaling cascades. Transient intracellular Ca^{2+} increase was found to be crucial for iNOS gene transactivation. Animal studies showed that CaM or CaMKII inhibition attenuated iNOS expression levels and improved the survival rates of endotoxemic mouse. Taken together, these studies suggested CaM as a potential modulator for iNOS expression in diseases related with excessive NO production from iNOS such as endotoxin shock.

CHAPTER 3

3 Role of CaM in controlling iNOS stability

3.1 Introduction

NO is an important signaling molecule involved in a variety of biological processes. Based on its concentration, NO plays different roles in cells. While physiological levels of NO convey cell signals, high levels of NO damage cells and tissues (1). In mammals, NO is produced by a family of NOS proteins. NO synthesized by nNOS and eNOS primarily participates in neuronal signal transmission and cardiovascular regulation, respectively (4, 25, 126, 127). Unlike the other two isoforms, iNOS mainly involves in inflammation and host defense (8). Compared to eNOS and nNOS, iNOS possesses higher NO-generating potency and thus massive iNOS-derived NO is employed by the immune system against microbe infection and tumor cells.

Unlike constitutively expressed eNOS and nNOS, iNOS is not detectable in quiescent cells. Inflammatory mediators such as bacterial endotoxin and cytokines induce robust iNOS expression. LPS and IFN-γ are potent inducers commonly used for iNOS expression. Once expressed, iNOS associates with its catalytic cofactor CaM with high binding affinity and exhibits constant activity (128). Due to the constantly active feature of iNOS, NO production from iNOS is mainly determined by the level of iNOS proteins. Besides gene expression, the levels of a functional protein are also affected by its protein

stability. iNOS was recognized as a soluble and stable protein in cytosol once expressed in cells. However, recent studies reported that iNOS formed aggresomes and aggregated iNOS down-regulated NO production from iNOS (54, 55). Although our prior studies identified CaM as an essential modulator in iNOS induction, its role in controlling iNOS protein stability remains unexplored. It is unknown whether CaM inhibition also affects iNOS protein stability. Here we show that loss of interaction with CaM causes iNOS to form insoluble aggregates. Such aggregation markedly attenuates NO-generating activity of iNOS. Further studies revealed that deleting CaM-binding domain on iNOS significantly prevented the aggregation of iNOS in the presence of CaM inhibitors. These observations suggest that CaM also plays an essential role in maintaining iNOS protein stability in addition to assisting enzyme catalysis and regulating iNOS gene transactivation. Taken together, our studies extend the function of CaM from an enzyme cofactor to a crucial regulator of protein induction and stability in iNOS biochemisty.

3.2 Materials and methods

3.2.1 Materials

Cell culture materials and Greiss reagent kit were purchased from Invitrogen (Carlsbad, CA). Anti-iNOS antibody was obtained from BD Transduction Laboratories (Franklin Lakes, NJ). Lipopolysaccharide (LPS, *E. coli* serotype O26:B6), recombinant mouse interferon (IFN)-γ, Trifluoperazine dihydrochloride, anti-GAPDH antibody were products of Sigma (St. Louis, MO). W-7 was purchased from Calbiochem (San Diego, CA). Anti-CaM antibody was obtained from Upstate Biotechnology (Lake Placid, NY).

2', 5'-ADP-Sepharose 4B was the product of Amersham Bio-sciences (Sunnyvale, CA). Unless otherwise indicated, all other chemicals used in this study were purchased from Sigma.

3.2.2 Cell culture

Mouse macrophage (RAW264.7, ATCC) and human embryonic kidney 293 (HEK293) cells were grown in Dulbecco's modified Eagle's medium with 10% fetal calf serum in a 37°C humidified atmosphere of 95% air and 5% CO_2. Expression of iNOS in RAW264.7 cells was induced by LPS (2 μg/ml, serotype 026:B6) and IFN-γ (100 U/ml).

3.2.3 Cell fractionation

iNOS-induced macrophages were lysed on ice for 30 min in a high-detergent lysis buffer (50 mM Tris-HCl, pH 7.4, 150 mM NaCl, 1% Nonidet P-40, 0.25% sodium deoxycholate, 50 mM NaF, 1 mM Na_3VO_4, 5 mM sodium pyrophosphate, 1% SDS, 1 mM EDTA and protease inhibitor tablet). The cell lysates were then passed through 30G needles and centrifuged at 14,000 × g for 15 min at 4°C. The supernatants were recovered as SDS-soluble fractions. The insoluble pellets were washed by PBS, and boiled in 1.5×SDS/PAGE sample buffer (90 mM Tris-HCl, pH 6.8, 3% SDS, 15% glycerol, 0.01% bromophenol blue and 62.5 mM dithiothreitol) for 7 min, making the SDS-insoluble fractions.

HEK293 cells expressing iNOS proteins were lysed in lysis buffer containing moderate detergent (50 mM Tris-HCl, pH 7.4, 150 mM NaCl, 1% Nonidet P-40, 0.25% sodium deoxycholate, 50 mM NaF, 1 mM Na_3VO_4, 5 mM sodium pyrophosphate, 0.2%

SDS, 1 mM EDTA and protease inhibitor tablet). After 30 min incubation on ice, cell lysates were fractionated as soluble fractions (supernatants) and insoluble fractions (pellet) by 15-min centrifugation at 14,000 × g at 4°C.

3.2.4 Western blot analysis

Protein concentrations of the SDS-soluble fractions were determined by using the detergent-compatible protein assay kit (Bio-Rad). After 5 min boiling in 1×SDS/PAGE sample buffer, the proteins were separated by SDS-PAGE, transferred to nitrocellulose membranes, and probed with the appropriate primary antibodies. Membrane-bound primary antibodies were detected with secondary antibodies conjugated with horseradish peroxidase. Immunoblots were developed on films using the enhanced chemiluminescence technique (SuperSignal West Pico, Pierce).

3.2.5 Nitrite assay

Total nitrite released in cell culture medium was measured with a Griess reagent kit (Invitrogen). The reaction consisted of 20 μl of Griess Reagent, 150 μl of medium, and 130 μl of deionized water. After incubation of the mixture for 30 min at room temperature, nitrite levels were measured at 548 nm using a spectrophotometric microplate reader (Molecular Devices).

3.2.6 CaM-iNOS dissociation assay

Recombinant murine iNOS was purified from an *E. coli* expression system as previously reported. To obtain ΔCaM-iNOS mutants, ΔCaM-iNOS vector was transfected to HEK293 cells by Lipofectamine 2000 reagent (Invitrogen) according to the

manufacturer's instructions. After 24 h of plasmid expression, cells were lysed on ice in lysis buffer (50 mM Tris-HCl, pH 7.4, 150 mM NaCl, 1% Nonidet P-40, 0.25% sodium deoxycholate, 50 mM NaF, 1 mM Na_3VO_4, 5 mM sodium pyrophosphate and protease inhibitor tablet). Cell lysates were centrifuged at 14,000 × g for 15 min, and the supernatants containing ΔCaM-iNOS were recovered. Either purified murine iNOS or cell lysates involving ΔCaM-iNOS proteins were incubated with trifluoperazine (80 μM) in pull down buffer (20 mM NaH_2PO_4, pH 7.4, 150 mM NaCl, 5 mM β-mercaptoethanol and 0.75 mM $CaCl_2$) for designated time. After the incubation with trifluoperazine, iNOS proteins were pulled down with 2', 5'-ADP-Sepharose 4B resins by 1 h rotation at 4°C. The reisins were washed twice with high salt buffer (20 mM NaH_2PO_4, pH 7.4, 500 mM NaCl, 5 mM β-mercaptoethanol and 0.75 mM $CaCl_2$), followed by one time pull down buffer wash. Resin-harvested iNOS was then eluted by 5-min boiling of the beads in SDS/PAGE sample buffer. The supernatants of the pull down solution were also collected and concentrated by the Microcon YM-3 centrifugal filters (Millipore) at 14,000 × g for 1 hour. Both supernatants and eluted samples were characterized by Western blot with appropriate antibodies.

3.2.7 Plasmid construction

The cDNA encoding murine iNOS gene was subcloned into pCMV-Tag2B and pEGFP-C3 vectors (Stratagene), respectively. The resulting pCMV-Tag2B/iNOS plasmids generate flag-tagged iNOS and the pEGFP-C3/iNOS plasmids express GFP-iNOS fusion proteins in cells transfected with corresponding plasmids.

3.2.8 Site-directed mutagenesis

CaM-binding site on iNOS was deleted by using the QuikChange Site-directed Mutagenesis Kit (Stratagene) according to the manufacturer's protocol. The following pair of primers 5'- GCA GAA TGA GAA GCT GAG GCC CCG AAA GGT CAT GGC TTC ACG and 5'- CGT GAA GCC ATG ACC TTT CGG GGC CTC AGC TTC TCA TTC TGC without CaM interacting sequence (AA 503-523 of iNOS) was used, forming ΔCaM-iNOS. The deletion of CaM-binding domain on ΔCaM-iNOS cDNA was verified by DNA sequencing.

3.2.9 Fluorescence imaging

HEK293 cells were plated in 35 mm cell culture dishes (USA Scientific) one night before transfection and grown to 70–80% confluence. Previously constructed pEGFP-C3/iNOS and pEGFP-C3/ΔCaM-iNOS vectors encoding GFP-WTiNOS and GFP-ΔCaM-iNOS fusion proteins were introduced into HEK293 cells by Lipofectamine 2000 reagent (Invitrogen) according to the manufacturer's instructions. One day (20-24 h) after transfection, cells were incubated with W-7 (60 μM) for another 16 h at 37°C. Following the incubation, cells were then imaged with a Zeiss Axioskop 40 Microscope equipped with a Nikon DS-Qi1 Monochrome Digital Camera.

3.3 Results

3.3.1 CaM regulation of iNOS stability in mouse macrophages

To determine the effect of CaM on iNOS protein stability, mouse macrophage RAW264.7 cells were exposed to LPS/IFN-γ. After 12-hour iNOS induction, LPS/IFN-γ was removed. Cells were then rinsed with PBS for three times and cultured in fresh

medium in the absence or presence of CaM inhibitors. At designated time point, cells were harvested and fractioned into supernatant (soluble) and pellet (insoluble) fractions in a high-detergent lysis buffer (1% SDS). As shown in Figure 3.1, under normal condition iNOS was expressed as a SDS-soluble protein and was almost undetectable in the pellet fractions. The incubation of iNOS with W-7 (100 μM), a specific CaM inhibitor, led to time-dependent decreases of soluble iNOS levels and corresponding increases of SDS-insoluble iNOS in the pellet fractions (Figure 3.1A). This finding suggested that CaM inhibition converted iNOS from soluble protein to insoluble aggregates. To corroborate the result obtained with W-7, the above experiment was repeated with trifluoperazine (80 μM), another CaM inhibitor with different structure than that of W-7. Consistent with the effect of W-7 on iNOS protein stability, 2 hours after CaM inhibition with trifluoperazine, soluble iNOS level was remarkably reduced. At the same time insoluble iNOS accumulated in the pellet fractions in a time-dependent manner (Figure 3.1B). These results revealed a novel role of CaM in maintaining iNOS protein stability.

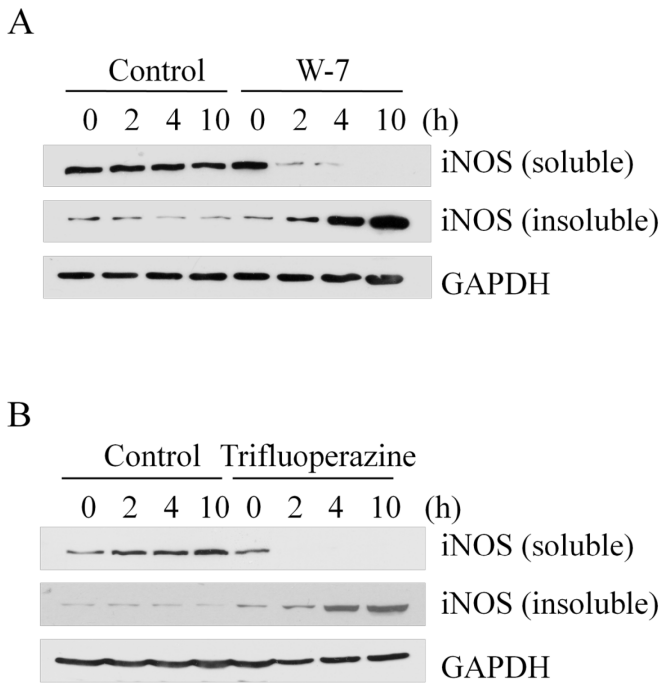

Figure 3.1 CaM inhibition led to iNOS aggregation in macrophages.
(A) CaM inhibition with W-7 (100 μM) caused iNOS aggregation. (B) Trifluoperazine (80 μM), another CaM inhibitor that structurally differed from W-7, also triggered iNOS aggregation.

3.3.2 Aggregation deactivates iNOS

Aggregation usually causes proteins to lose their functions. To determine the effect of protein aggregation on iNOS function, we compared the NO productions from iNOS in macrophages in the absence and presence of CaM inhibitors. Without CaM inhibitor, iNOS-derived NO accumulated in cell culture medium as a function of time, whereas blockage of CaM function with either W-7 or trifluoperazine markedly decreased NO productions in iNOS-induced macrophages (Figure 3.2). These results suggested that iNOS aggregation upon CaM inhibition led to the loss of its NO-generating activity.

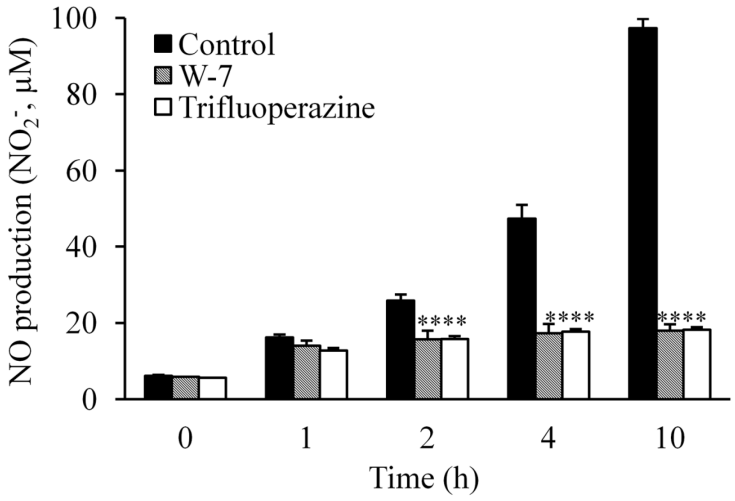

Figure 3.2 NO production from iNOS expressed in RAW264.7 cells in the absence and presence of CaM inhibitors.
Data are means ± SE. ** $P < 0.01$ vs. control, n = 3.

3.3.3 Effect of CaM blockade on the protein stability of iNOS expressed in HEK293 cells

Our previous studies were performed on native iNOS proteins induced in LPS/IFN-γ-stimulated mouse macrophages. To ascertain whether CaM inhibition also caused exogenous iNOS aggregation, we constructed a pCMV-Tag2B/iNOS plasmid encoding murine iNOS and transfected it into HEK293 cells. One day after transfection, cells were treated with CaM inhibitors and fractionated into soluble and insoluble fractions with lysis buffer containing 0.2% SDS. As shown in Figure 3.3, iNOS expressed in HEK293 cells mainly existed in the soluble fractions. Insoluble iNOS was barely observed in cell pellets. In the presence of either W-7 (60 μM) or trifluoperazine (40 μM), iNOS levels in the soluble fractions gradually decreased, and the aggregated

iNOS increased in the insoluble fractions as a function of time. Consistent with the finding obtained from endogenous iNOS induced in macrophages, the aggregation of exogenous iNOS expressed in HEK293 cells upon CaM inhibition further substantiated the role of CaM in stabilizing iNOS protein.

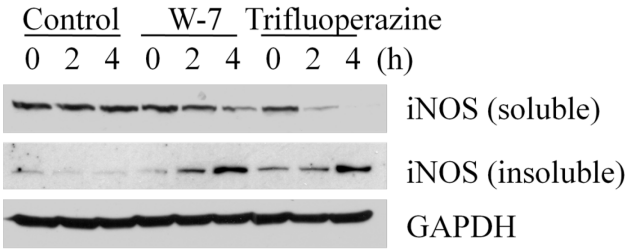

Figure 3.3 CaM inhibition caused the aggregates formation of iNOS expressed in HEK293 cells.

3.3.4 CaM inhibition triggers dissociation of CaM from iNOS

After the identification of CaM as an iNOS protein stabilizer, we then sought to obtain more information underlying the process of iNOS aggregation in the presence of CaM inhibitor trifluoperazine. Trifluoperazine is known to occupy the hydrophobic binding pockets of CaM, which are essential for client protein binding (83). Thus trifluoperazine may inhibit CaM function by disrupting the interaction between CaM and iNOS, leading to the dissociation of CaM from iNOS. To validate this hypothesis, we exposed previously purified iNOS-CaM complexes from *E. coli* to trifluoperazine (80 μM). After incubation with trifluoperazine, iNOS and its coupled CaM were harvested by 2', 5'-ADP-Sepharose 4B beads. The levels of both iNOS-associated CaM collected by

beads and CaM released from iNOS into the supernatants were monitored. As shown in Figure 3.4, trifluoperazine treatment led to a decrease in the levels of iNOS-coupled CaM in a time dependent manner. Corresponding to the loss of iNOS-bound CaM, the levels of free CaM released from iNOS into the supernatants were gradually increased. This result confirmed that CaM inhibition by trifluoperazine led to the dissociation of CaM from iNOS. The dissociation of iNOS-CaM occured prior to iNOS aggregation suggested that CaM dissociation from iNOS and consequent exposure of hydrophobic CaM-binding site on iNOS triggered iNOS aggregation.

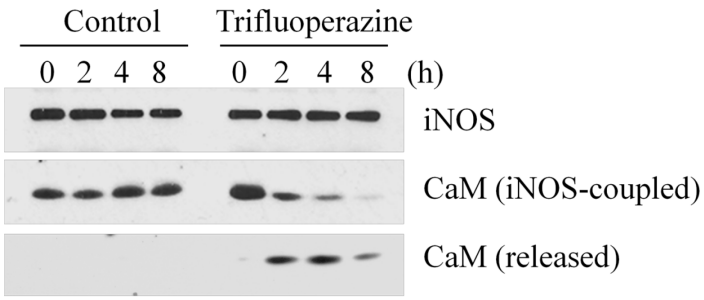

Figure 3.4 CaM inhibition rendered CaM dissociation from iNOS.
Trifluoperazine (80 μM) decreased the levels of CaM coupled with iNOS and increased the levels of free CaM released from CaM-iNOS complexes in a time dependent manner. Representative data were shown from three independent experiments.

3.3.5 CaM fails to bind with ΔCaM-iNOS lacking CaM-interacting domain

CaM is known to interact with iNOS through the CaM-binding site (AA 503-523 of iNOS) between the reductase and oxygenase domains of iNOS. The CaM-binding domain (RRREIRFRVLVKVVFFASMLM) on iNOS consists of around 50% hydrophobic amino acid residues (88), thus we proposed that iNOS aggregation was

mediated by the hydrophobic CaM-interacting domain, which was exposed when CaM dissociated from iNOS upon CaM inhibition. To examine our hypothesis, we constructed CaM-binding domain deletion iNOS (ΔCaM-iNOS) and expressed it in HEK293 cells. Cells were harvested and the cell lysates containing ΔCaM-iNOS were treated with trifluoperazine, followed by 2', 5'-ADP-Sepharose 4B beads incubation. As shown in Figure 3.5, deleting CaM-binding domain on iNOS disrupted CaM-iNOS interaction. iNOS-coupled CaM was undetectable regardless of the absence or presence of trifluoperazine. Therefore CaM-binding domain deficient mutant ΔCaM-iNOS lost the ability to interact with CaM.

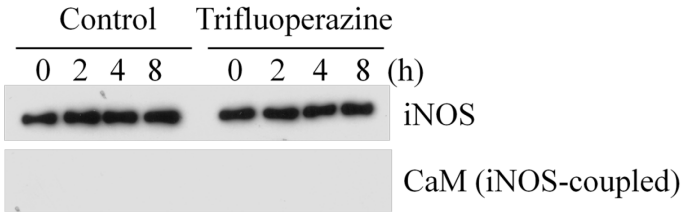

Figure 3.5 Deletion of CaM-binding domain on iNOS disrupted the interaction of CaM and iNOS.

3.3.6 CaM antagonists have no effect on the stability of ΔCaM-iNOS

To demonstrate the necessity of the CaM-interacting domain in iNOS aggregation under CaM inhibition, ΔCaM-iNOS was expressed in HEK293 cells. Cells were harvested and fractionated in lysis buffer containing 0.2% SDS at designated time points. The levels of iNOS in both soluble and insoluble fractions were monitored. Similar to wild-type iNOS expressed in HEK293 cells, ΔCaM-iNOS existed as soluble proteins in

the absence of CaM inhibitors. While CaM inhibition caused wild-type iNOS to form aggregates in HEK293 cells, ΔCaM-iNOS remained soluble when exposed to either W-7 (60 μM) or trifluoperazine (40 μM) (Figure 3.6). Consistent with the steady levels of soluble ΔCaM-iNOS, increased levels of aggregated ΔCaM-iNOS was not observed in the insoluble fractions. Thus deletion of CaM-binding domain from iNOS made it a stable protein insensitive to CaM inhibition. These findings indicated that the CaM-binding domain on iNOS mediated iNOS aggregation upon CaM inhibition.

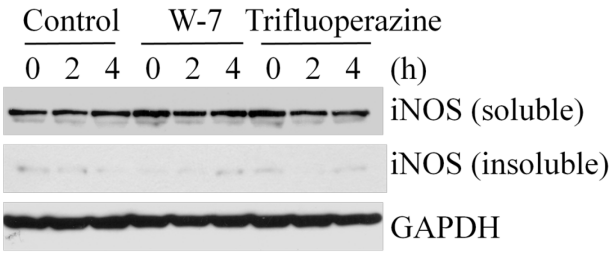

Figure 3.6 CaM inhibition failed to cause the aggregation of CaM-binding domain deficient mutant ΔCaM-iNOS.

3.3.7 Fluorescence imaging of GFP-iNOS and GFP-ΔCaM-iNOS expressed in HEK293 cells in the absence and presence of CaM inhibitor.

To validate the intracellular effect of CaM inhibitor on iNOS protein stability, we constructed a pEGFP-C3/iNOS vector encoding GFP-iNOS fusion proteins and expressed it in HEK293 cells. Expressed iNOS distributed evenly in the cytosol of HEK293 cells (Figure 3.7A). In the presence of W-7 (60 μM), the aggregation of GFP-iNOS was indicated by fluorescent particles inside cells (Figure 3.7B). This finding was

consistent with the results obtained from the cell fractionation studies. Thus these data further demonstrated that functional CaM is crucial for the maintenance of iNOS as a soluble protein in cytosol.

To further ascertain the role of CaM-binding domain on iNOS in aggresome formation, we also subcloned ΔCaM-iNOS into the GFP-tagged vector and transfected it into HEK293 cells. As shown in Figure 3.7C, similar to wild-type iNOS, GFP-ΔCaM-iNOS fusion proteins lacking the CaM-binding domain were evenly distributed in the cytosol of HEK293 cells. Inhibition of CaM with W-7 (60 μM) failed to cause ΔCaM-iNOS aggregation, which was indicated by even distribution of fluorescence in cells (Figure 3.7D). These imaging data strongly substantiated that CaM-interacting domain was essential for the aggresome formation of iNOS in CaM-inhibited cells.

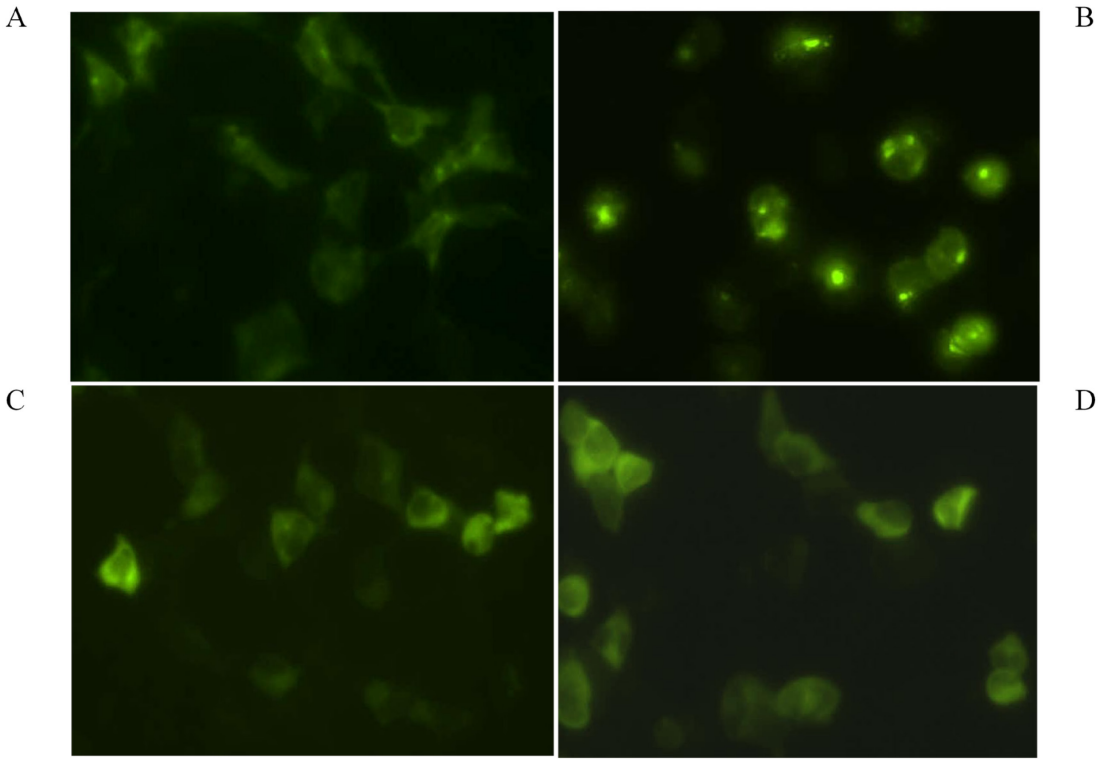

Figure 3.7 Demonstration of CaM-interacting domain-mediated GFP-iNOS aggregation in HEK293 cells.
(A) Wild-type iNOS was evenly distributed in cytosol of HEK293 cells. (B) CaM inhibition with W-7 (60 μM) led to the aggregation of wild-type iNOS expressed in HEK293 cells. (C) A uniform distribution of ΔCaM-iNOS was observed in HEK293 cells in the absence of W-7. (D) ΔCaM-iNOS without CaM-interacting domain remained stable in CaM-inhibited cells.

3.4 Discussion

One important finding of this study is that iNOS function is mediated by aggresome formation under CaM inhibition. Different from constitutively expressed eNOS and nNOS whose activities are initiated by elevation of intracellular Ca^{2+}, iNOS is constantly active once expressed by inflammatory mediator stimulation. Thus robust NO generation from iNOS was believed to be largely controlled by iNOS protein expression

levels. Based on the finding that iNOS was a soluble protein in cytosol, very few studies examined the potential role of protein stability in regulating iNOS function. Such perception has been changed by recent studies in which iNOS aggregation and the effect of aggregated iNOS on enzyme activity were reported. In our study, iNOS aggregation was also observed. CaM inhibition caused iNOS aggregation and aggregated iNOS was found to lose its NO-generating activity. Hence NO production from iNOS in macrophages stimulated by inflammatory mediators requires CaM to maintain the soluble and active status of iNOS protein. Our studies demonstrated that in addition to iNOS protein expression, iNOS activity can also be regulated by protein stability alteration via iNOS aggregation.

The key finding of this study is that CaM is essential for maintaining iNOS as a soluble protein in cells. Characterized as Ca^{2+}-dependent proteins, activation of eNOS and nNOS requires increased intracellular Ca^{2+} and subsequent CaM binding. Although iNOS activity does not require Ca^{2+} flux inside cells, CaM coupling is indispensable for NO generation from iNOS. CaM interaction with NOS enzymes is known to facilitate electron transfer from the reductase domain to the oxygenase domain and is essential for NOS activity. So far CaM is regarded as an enzyme cofactor of all three NOS isoforms. However, our prior study revealed an essential role of CaM in iNOS gene transactivation. Furthermore, our present study identified CaM as a crucial mediator of iNOS protein stability. iNOS-CaM complexes exist as soluble proteins evenly distributed in cytosol. Upon CaM inhibition, soluble iNOS protein is no longer stable and iNOS aggregates were directly observed in cells. Therefore in addition to its long recognized role in

assisting enzyme catalytic activity and recently discovered function in iNOS gene transactivation, CaM has been further identified as an iNOS protein stabilizer.

The mechanism underlying CaM-mediated iNOS aggregation was also deciphered in this study. According to the time course of CaM-iNOS dissociation and that of iNOS aggregation, our data suggested that iNOS aggregation under CaM inhibition started from the dissociation of dysfunctional CaM from iNOS. Based on such observation, we speculated that release of CaM from iNOS led to the exposure of hydrophobic CaM-binding domain, which was on longer stable in cytosol. As a result, CaM-uncoupled iNOS formed aggregates as an energy preferred form via its vacant CaM-interacting domain. Our further studies confirmed the essential role of CaM-interacting site in iNOS aggregation triggered by CaM inhibition. Our data showed that deletion of CaM-binding domain on iNOS made it a soluble protein regardless of the absence or presence of CaM inhibitor. CaM is known to tightly bind with iNOS after its expression, and our present study revealed that such association is essential for iNOS protein stability. Unlike iNOS, deactivated eNOS and nNOS are not coupled with CaM, but they remained as soluble proteins inside cells. Sequence alignment of the CaM-binding site amid all three NOS isoforms identified several iNOS specific hydrophobic residues likely involved in the aggregation of iNOS. This might provide a plausible explanation to why iNOS forms aggregates when uncoupled with CaM whereas the other two NOS isoforms do not. Thus it will be interesting to investigate the essential residues for iNOS aggregation among these candidates in the future.

In summary, this study revealed the essential role of CaM in regulating iNOS protein stability. Besides its recently identified role in modulating iNOS gene transactivation, CaM is also indispensable for maintaining iNOS as soluble proteins. These findings further enhance the understanding of CaM as an enzyme catalytic assistant in iNOS biochemistry. The facts that CaM inhibition caused iNOS aggregation and subsequent loss of function suggest CaM as a potential target to intervene NO generation from iNOS inside cells.

CHAPTER 4

4 iNOS aggregation mediated by self-derived NO

4.1 Introduction

Nitric oxide (NO) is dubbed as a double-edged sword as it can cause opposite biological effects depending on its concentrations (7, 8, 127, 129). Physiological levels of NO function as a signaling molecule in regulating neuronal and cardiovascular activities. However, as a free radical, excessive amount of NO can damage cells. Thus, NO has been implicated in inflammatory injury in various diseases. On the other hand, the destructive feature of NO is also utilized in host defense against microbe invaders. In mammals, NO is produced by a family of NO synthase (NOS) including neuronal NOS (nNOS), inducible NOS (iNOS), and endothelial NOS (eNOS) (18, 130, 131). Among the three isoforms, iNOS primarily involves in cell injury and host defense (87, 132). All NOS isoforms use L-arginine, oxygen, and NADPH as co-substrates to synthesize NO. Compared to the other two isoforms, iNOS possesses the highest NO-generating potency and this feature is thought to be ideal for its function in host defense.

nNOS and eNOS constitutively exist in cells, whereas little iNOS can be detected in normal cells and tissues. iNOS expression is induced by inflammatory mediators. Bacterial product lipopolysaccharide (LPS) and cytokines, such as interferon-γ (IFN-γ), are potent inducers of iNOS expression. Once expressed, iNOS has high binding affinity

with its catalytic cofactor calmodulin and exhibits constant activity (86, 133). Thus, NO production from iNOS is largely determined by the levels of iNOS proteins. It has been thought that iNOS stays as a soluble and stable protein in the cytosol. However, a recent study reported that iNOS forms aggresomes inside cells (54, 55). Aggresome formation deactivates iNOS and this is proposed as a possible mechanism to down-regulate NO production in inflammation. Indeed, iNOS aggregation was observed in our prior study upon CaM inhibition. But an important question remains regarding what causes iNOS aggresome formation under physiological conditions. In this study, we provided evidence demonstrating that NO per se causes iNOS aggresome formation. Blocking NO production prevents iNOS aggresome formation. This finding may shed new light on the long-sought mechanism of the feedback inhibition of iNOS by NO.

4.2 Materials and methods

4.2.1 Materials

Cell culture materials were purchased from Invitrogen (Carlsbad, CA). Anti-iNOS antibody was obtained from BD Transduction Laboratories (Franklin Lakes, NJ). LPS, recombinant mouse IFN-γ, N-nitro-L-arginine methyl ester (L-NAME), anti-GAPDH antibody were products of Sigma (St. Louis, MO). 1400W and S-nitroso-N-acetyl-DL-penicillamine (SNAP) were purchased from Biomol (Plymouth Meeting, PA). Unless otherwise indicated, all other chemicals used in this study were purchased from Sigma.

4.2.2 Cell culture

Mouse macrophages (RAW264.7, ATCC), human embryonic kidney 293 (HEK293) cells and African green monkey SV40-transfected kidney fibroblast (COS-7) cells were grown in Dulbecco's modified Eagle's medium with 10% fetal calf serum in a 37°C humidified atmosphere of 95% air and 5% CO_2. Expression of iNOS in RAW264.7 cells was induced by LPS (2 μg/ml, serotype 026:B6) and IFN-γ (100 U/ml).

4.2.3 Western blot analysis

Cells were harvested and lysed in lysis buffer (50 mM Tris-HCl, pH 7.4, 150 mM NaCl, 1% Nonidet P-40, 0.25% sodium deoxycholate, 50 mM NaF, 1 mM Na_3VO_4, 5 mM sodium pyrophosphate, 1 mM EDTA and protease inhibitor tablet). After 30 min incubation on ice, lysates were centrifuged at 14,000 × g for 15 min at 4°C. The supernatants and pellets were recovered as soluble and insoluble fractions, respectively. Protein concentrations of soluble fractions were determined by using the detergent-compatible protein assay kit (Bio-Rad). The insoluble pellets were washed by PBS. After 5 min boiling in 1×SDS/PAGE sample buffer (62.5 mM Tris-HCl, pH 6.8, 2% SDS, 40 mM dithiothreitol, 10% glycerol, and 0.01% bromophenol blue), the proteins were separated by SDS-PAGE, transferred to nitrocellulose membranes, and probed with the appropriate primary antibodies. Membrane-bound primary antibodies were detected with secondary antibodies conjugated with horseradish peroxidase. Immunoblots were developed on films using the enhanced chemiluminescence technique (SuperSignal West Pico, Pierce).

4.2.4 iNOS activity assay

iNOS activity was measured by the L-[^{14}C]arginine to L-[^{14}C]citrulline conversion assay. iNOS expression was induced in RAW264.7 by LPS/IFN-γ. After 12-hour induction, cells were homogenized in homogenate buffer (50 mM Tris-HCl, pH 7.4, 50 mM NaF, 1 mM Na_3VO_4, and protease inhibitor mixture). The homogenate was then centrifuged (14,000 × g for 30 min at 4°C), and the supernatants were recovered and used for measuring soluble iNOS activity. To obtain aggregated iNOS generated by NO accumulation, cells were incubated with iNOS inducers (LPS/IFN-γ) for 30 hours, and then homogenized in homogenate buffer. After centrifugation and stringent wash, the pellets were resuspended in the homogenate buffer and used for activity measurements of aggregated iNOS. The cell lysates were added to the reaction mixture containing 50 mM Tris-HCl, pH 7.4, 0.5 mM NADPH, 10 nM $CaCl_2$, 10 μg/ml calmodulin, 10 μM BH_4, 0.1 μM L-[^{14}C]arginine, and 18 μM L-arginine. After 15 min incubation at 37°C, the reactions were terminated by ice-cold stop buffer. L-[^{14}C]Citrulline was separated by passing the reaction mixture through Dowex AG 50W-X8 (Na^+ form; Sigma) cation exchange columns and quantitated by liquid scintillation counting.

4.2.5 Nitrite assay

Total nitrite released in cell culture medium was measured with a Griess reagent kit (Invitrogen). The reaction consisted of 20 μl of Griess Reagent, 150 μl of medium, and 130 μl of deionized water. After incubation of the mixture for 30 min at room temperature, nitrite levels were measured at 548 nm using a M2 spectrophotometric microplate reader (Molecular Devices).

4.2.6 Plasmid and transient transfection

The cDNA encoding murine iNOS was subcloned into the pEGFP-C3 vector and then transfected into HEK293 cells by using Lipofectamine 2000 (Invitrogen) according to the manufacturer's instructions. Briefly, pEGFP-C3/iNOS plasmid and lipofectamine were mixed in Opti-MEM media (Invitrogen) and added to 50% confluent cells. After 4-hour incubation, serum was added back to allow cell recovery.

4.2.7 Fluorescence imaging

HEK293 cells were transfected with pEGFP-C3/iNOS plasmid in the presence and absence of L-NAME (2 mM) for 26 hours at 37°C. Images were then acquired with a Zeiss Axioskop 40 Microscope equipped with a Nikon DS-Qi1 Monochrome Digital Camera.

4.2.8 Site-directed mutagenesis

Cysteine to alanine substitutions in iNOS is conducted by using the QuikChange multi site-directed mutagenesis kit (Stratagene) according to the manufacturer's protocol. The mutation of certain amino acid residues was confirmed by DNA sequencing.

4.2.9 Statistical analysis

Data are expressed as Mean ± SE. Comparisons are made using a two-tailed Student's unpaired *t* test. Differences are considered statistically significant at $P < 0.05$.

4.3 Results

4.3.1 iNOS aggregation in mouse macrophages

To determine the mechanism of iNOS aggresome formation, we first characterized iNOS aggregation process in mouse macrophages (RAW264.7) exposed to LPS/IFN-γ. After LPS/IFN-γ induction, cells were fractioned into supernatant (soluble) and pellet (insoluble) fractions. We monitored the levels of iNOS in both soluble and pellet fractions. As shown in Figure 4.1A, at the early phase of induction, iNOS was seen only in the soluble fractions of cells. However, after 22 hours of LPS/IFN-γ induction, soluble iNOS was gradually diminished. Corresponding to the loss of iNOS in the soluble fractions, progressive iNOS accumulation was seen in the pellet fractions (Figure 4.1A, B). After 28 h induction, iNOS was mostly seen in the pellet fractions. These observations were consistent with those reported in the prior literature and indicated that iNOS formed aggresomes. Aggregation often causes proteins to lose their functions. To determine the effect of aggregation on iNOS function, we compared the activity of soluble and aggregated iNOS with the L-[^{14}C]arginine to L-[^{14}C]citrulline conversation assay. As expected, aggregated iNOS exhibited little catalytic activity (Figure 4.2). These data demonstrated that iNOS formed aggregates as a function of time in macrophages and this aggregation led to enzyme deactivation.

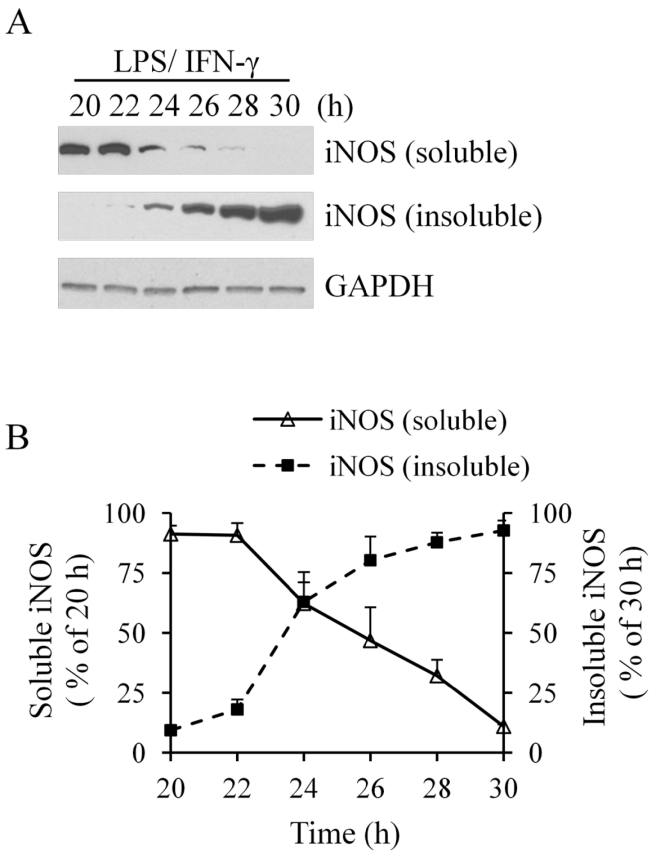

Figure 4.1 iNOS aggregation in mouse macrophages after LPS/IFN-γ stimulation. (A) iNOS expression was induced in RAW264.7 cells by LPS (2 μg/ml)/IFN-γ (100 U/ml). As shown, progressive iNOS aggregation was seen in cells after 22-hour induction. (B) Quantitative analyses of iNOS distribution in the soluble and insoluble fractions. Data are means ± SE, n = 4.

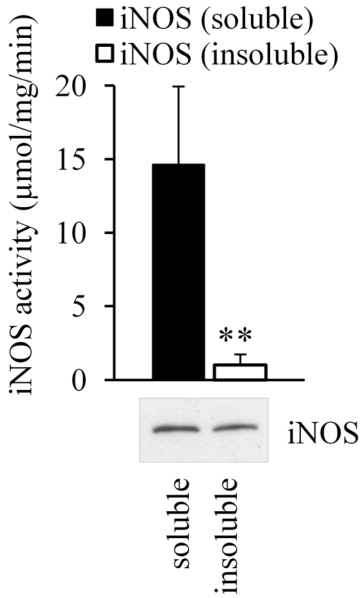

Figure 4.2 The catalytic activity of iNOS was lost after aggregation.
$^{**}P < 0.05$, n = 4.

4.3.2 Inhibition of NO production prevents iNOS aggregation

iNOS is a high-output NO-generating enzyme. We hypothesized that NO might play a role in iNOS aggresome formation. To validate such a hypothesis, iNOS expression was induced in the absence and presence of L-NAME, an L-arginine derivative that selectively blocks NOS function. As shown in Figure 4.3A, L-NAME treatment had no effect on iNOS expression in LPS/IFN-γ-stimulated cells. Remarkably, blocking NO production with L-NAME prevented iNOS aggregation in cells. To validate the results obtained by L-NAME, we also examined the effect of 1400W (10 μM), a specific inhibitor of iNOS, on iNOS aggregation. Similar to the action of L-NAME, inhibiting NO generation from iNOS with 1400W also halted iNOS aggregates formation. The relationship between NO production and iNOS aggregation was clearly

demonstrated in Figure 4.3B. These data suggested that NO played an essential role in iNOS aggresome formation.

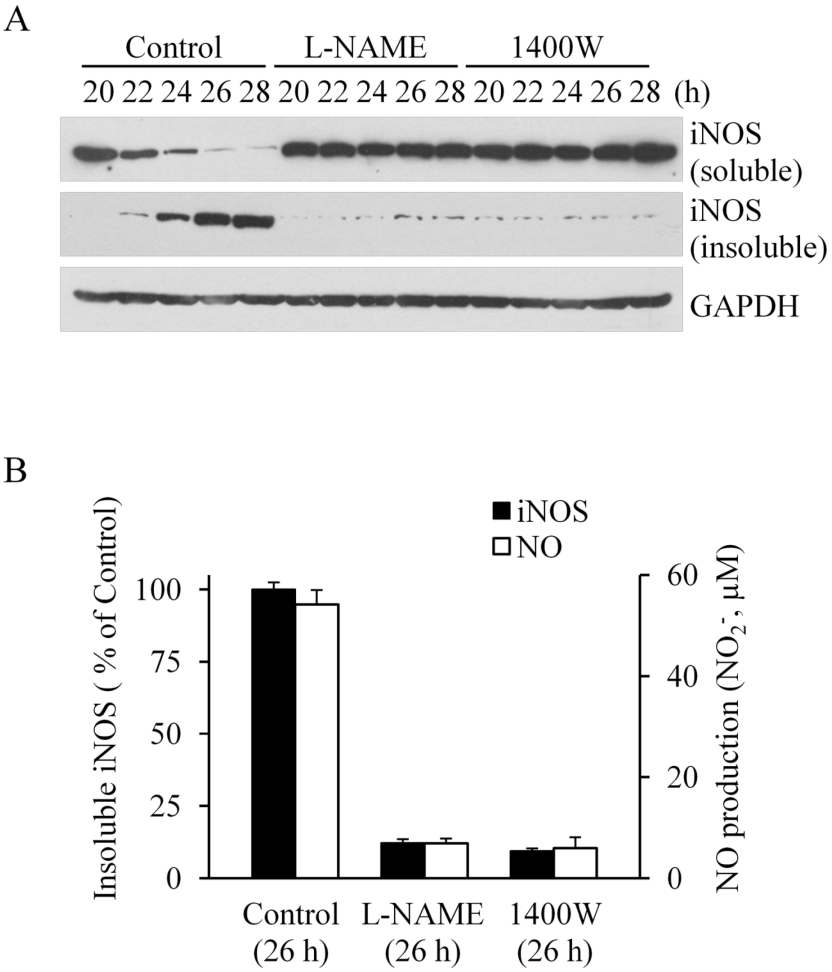

Figure 4.3 Blocking NO production prevented iNOS from aggregation.
(A) iNOS aggregation was prevented by blocking iNOS function with L-NAME (2 mM) or 1400W (10 μM). (B) Quantitative analyses of the effects of iNOS inhibitors on iNOS aggregation and NO production in cells after LPS/IFN-γ induction for 26 hours. Data are means ± SE, n = 4.

4.3.3 Removal of L-NAME from LPS/IFN-γ-stimulated cells triggers iNOS aggregation

To further corroborate the role of NO in iNOS aggregation, we induced iNOS expressions in macrophages by LPS/IFN-γ stimuli in the presence of L-NAME. After 12-hour iNOS induction, L-NAME was removed and the iNOS protein levels in both soluble and insoluble fractions were monitored. As shown in Figure 4.4, the removal of L-NAME resulted in abrupt increase of NO level (Figure 4.4B) and a time-dependent iNOS aggregation (Figure 4.4A), which was evidenced by decreased levels of soluble iNOS and increased levels of aggregated iNOS. This result further indicated that iNOS aggregation was mediated by self-derived NO.

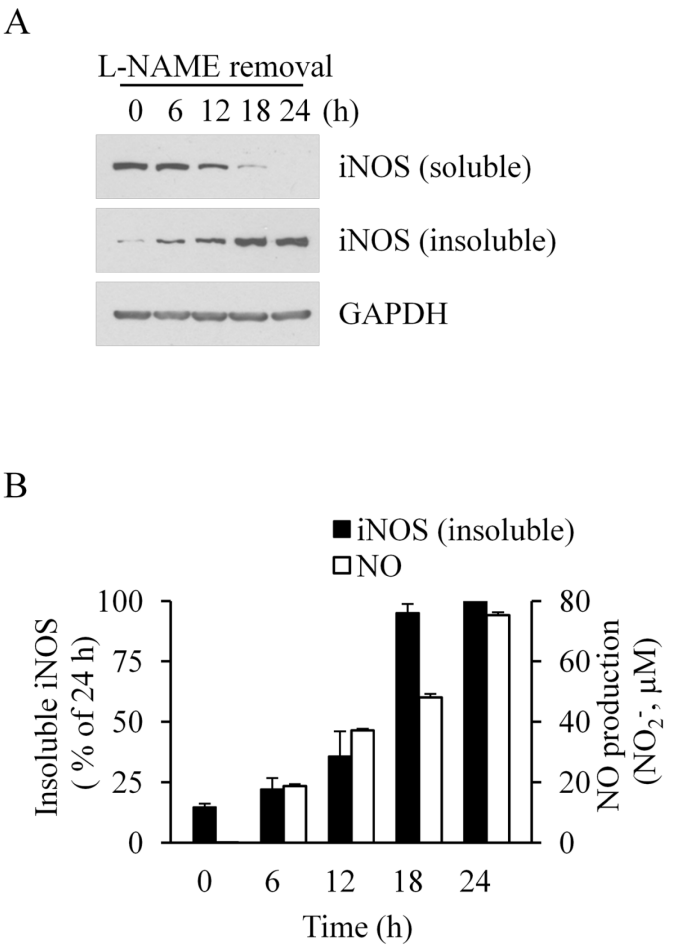

Figure 4.4 Removal of L-NAME rendered aggregates formation of iNOS induced in LPS/IFN-γ-stimulated cells.
(A) Soluble iNOS induced in macrophages in the presence of L-NAME (2 mM) aggregated as a function of time after L-NAME removal. (B) Quantitative analyses of iNOS aggregation and NO production in cells after L-NAME removal. Data are means ± SE, n = 4.

4.3.4 Demonstration of NO-mediated GFP-iNOS aggresome formation in cells

To visualize the role of NO in iNOS aggresome formation, we constructed a GFP-tagged iNOS expression vector and transfected it into HEK293 cells. Consistent with the cell fractionation studies, GFP-iNOS formed aggresomes in cells after 26-hour

transfection (Figure 4.5, left panel). In the presence of L-NAME, iNOS was evenly distributed in the cytosol and no aggresome formation was detected (Figure 4.5, right panel). To ensure this finding was not restricted to one particular type of cells, we performed similar experiment in COS-7 cells. The aggregated iNOS particles were clearly observed in COS-7 cells without L-NAME treatment (Figure 4.6, left panel). The presence of L-NAME prevented iNOS aggresome formation as evidenced by evenly distributed fluorescence inside cells (Figure 4.6, right panel). The result gained from COS-7 cells validated the finding in HEK293 cells, indicating that NO caused iNOS aggresome formation.

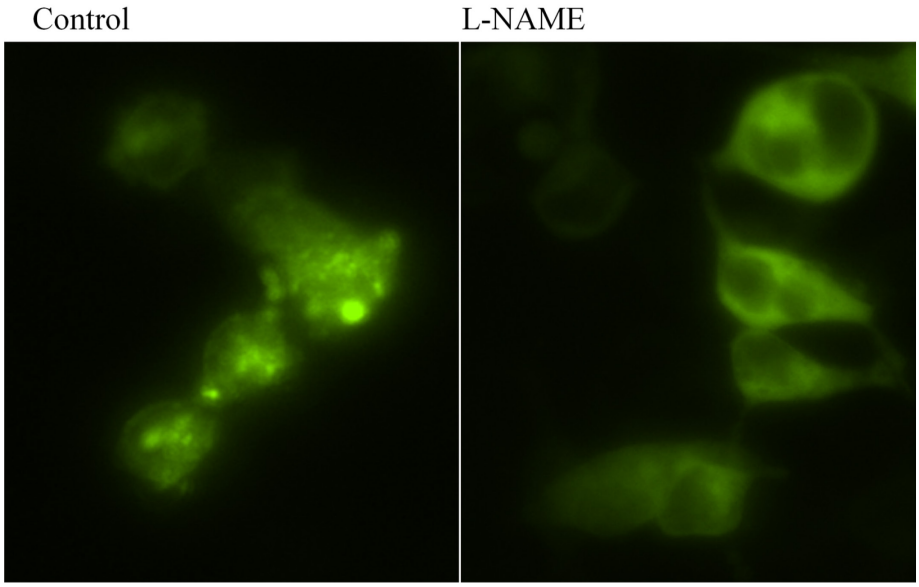

Figure 4.5 Fluorescence imaging of GFP-iNOS aggresome formation in HEK293 cells in the absence and presence of NOS inhibitor L-NAME.
GFP-iNOS fusion proteins were expressed in HEK293 cells. As shown, GFP-iNOS formed aggresomes in control cells in the absence of L-NAME. In the presence of L-NAME, a uniform distribution of GFP-iNOS was seen in the cytosol. Representative images are shown from triplicate experiments.

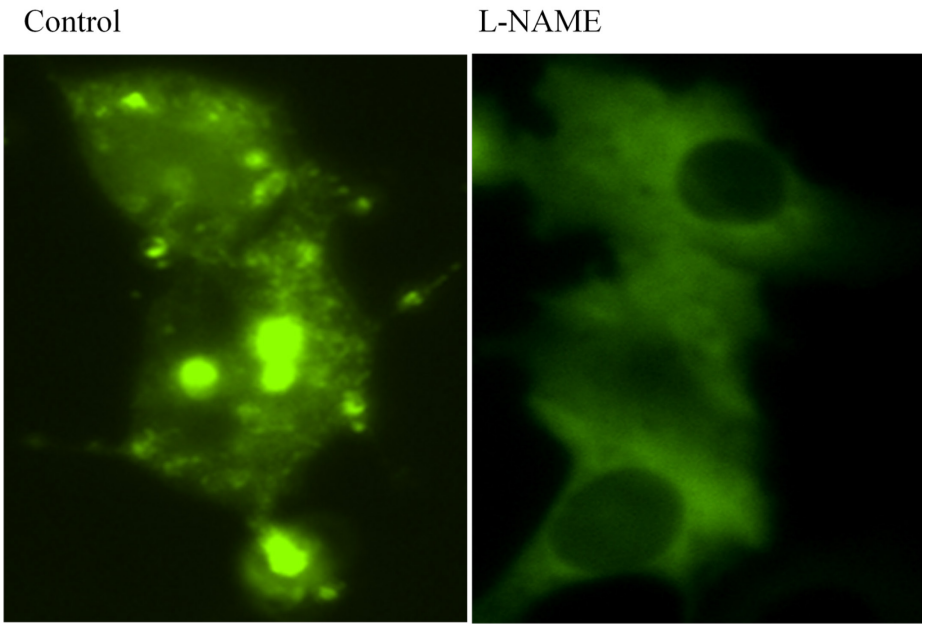

Figure 4.6 Fluorescence imaging of iNOS-derived NO-mediated GFP-iNOS aggregation in COS-7 cells.
GFP-iNOS fusion proteins were expressed in COS-7 cells. As shown, iNOS inhibition with L-NAME prevented iNOS aggregation. In the absence of L-NAME, iNOS aggregates were observed in cells. Representative images are shown from triplicate experiments.

4.3.5 Exogenous NO induces iNOS aggregation in L-NAME-treated cells

We then examined whether iNOS aggregation could be recaptured by exposing L-NAME-treated cells to exogenous NO. As shown in Figure 4.7A, iNOS stayed as a soluble protein in L-NAME-treated RAW264.7 cells. However, exposing the L-NAME-treated macrophages to NO donor SNAP (134-136) induced iNOS aggregation in a time-dependent manner. The effects of exogenous NO on iNOS aggregation in L-NAME-treated macrophages were summarized in Figure 4.7B and C. The effect of SNAP on iNOS expressed in HEK293 cells was also investigated. In the presence of L-NAME (2

mM), iNOS existed as soluble proteins inside HEK293 cells. SNAP treatment triggered iNOS aggregation as a function of time in L-NAME-treated HEK293 cells (Figure 4.8). These data further confirmed the crucial role of NO in iNOS aggresome formation.

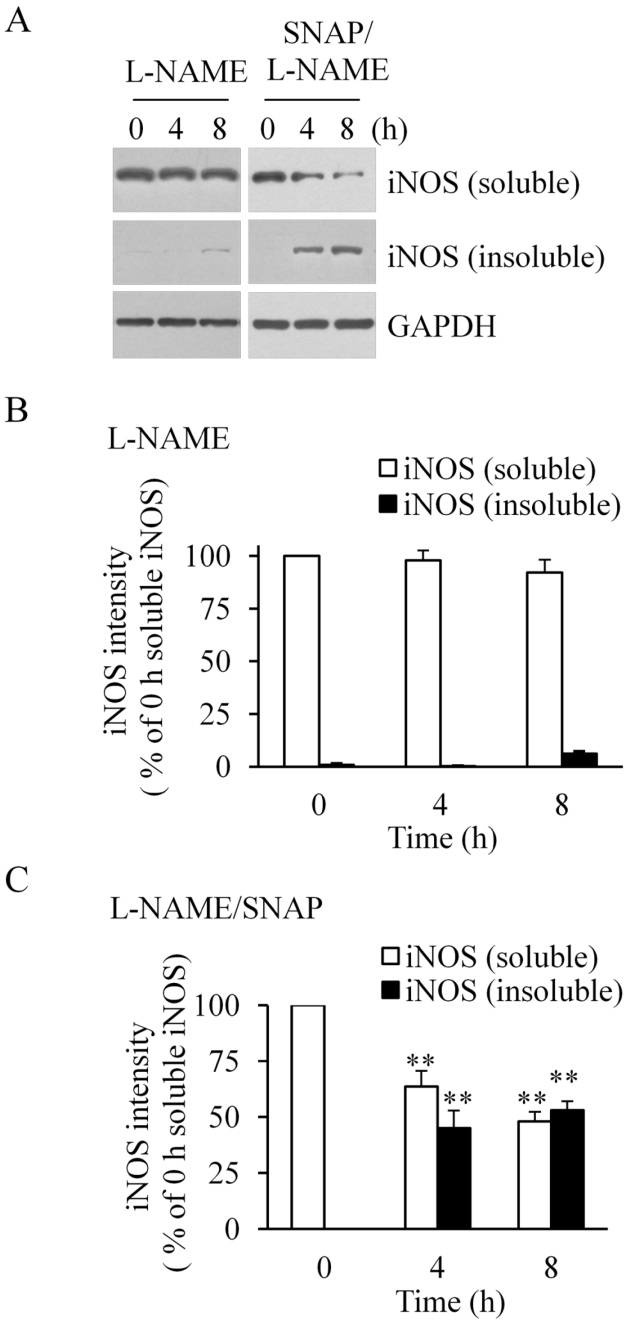

Figure 4.7 Exogenous NO caused iNOS aggregation in L-NAME-treated RAW264.7 cells.

(A) Under iNOS inhibition (L-NAME, 2 mM), iNOS stayed as a soluble protein inside cells. Exposing these L-NAME-treated cells to exogenous NO (generated by NO donor SNAP, 2 mM) triggered iNOS aggregation. (B, C) Quantitative analyses of soluble and insoluble iNOS in L-NAME-treated cells in the absence and presence of NO donor. Data

are means ± SE, ** $P < 0.05$ vs. L-NAME, n = 3-5.

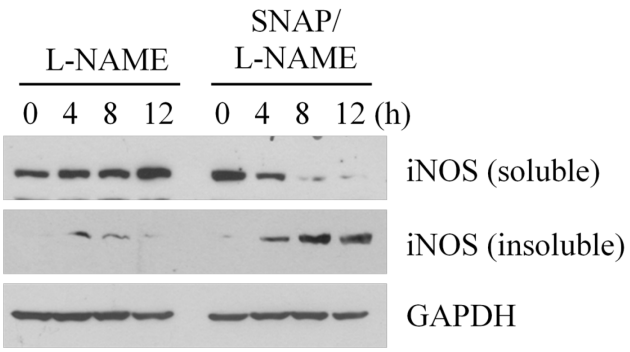

Figure 4.8 Exogenous NO triggered iNOS aggregation in HEK293 cells.
As shown, iNOS expressed as soluble proteins in L-NAME-treated HEK293 cells. Treating cells with SNAP (2 mM) caused iNOS aggregation inside HEK293 cells in the presence of L-NAME. Representative images are shown from triplicate experiments.

4.3.6 Exogenous NO has no effect on the protein stability of eNOS and nNOS

Since iNOS possesses higher NO-gerenating potency as compared with eNOS and nNOS, we then examined whether the NO-mediated aggregation also occurred on the other two NOS isoforms. Previously constructed HEK293 cells expressing eNOS or nNOS were exposed to SNAP (2 mM) in the presence of L-NAME (2 mM), respectively. As shown in Figure 4.9A, eNOS remained soluble when exposed to exogenous NO. Interestingly, SNAP treatment also failed to cause the aggregation of nNOS (Figure 4.9B). These results suggested that iNOS, but not eNOS or nNOS, underwent aggregation in the presence of high amounts of NO, indicating a feedback regulation specific for iNOS.

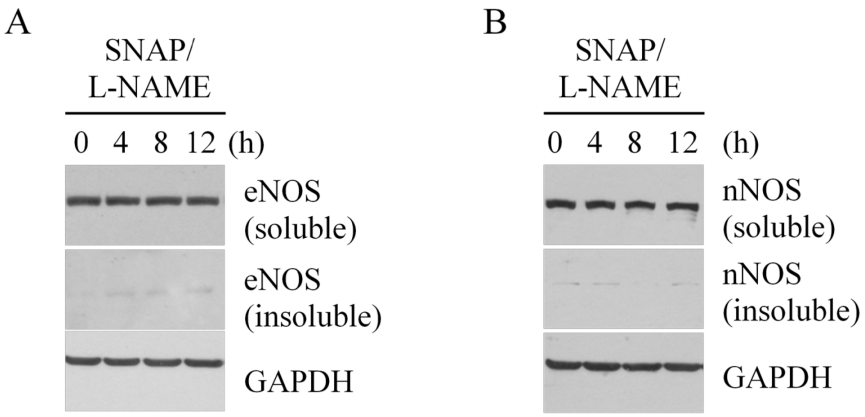

Figure 4.9 Exogenous NO had no effect on the protein stability of eNOS and nNOS. As shown, (A) eNOS or (B) nNOS stayed as soluble proteins inside L-NAME-treated HEK293 cells upon SNAP treatment (2 mM), respectively. Representative images are shown from triplicate experiments.

4.3.7 Mutation of iNOS-specific cysteines to alanines fails to prevent iNOS aggregation in SNAP-treated cells.

One of the major actions of NO on proteins is cysteine nitrosylation, during which the NO moiety was covalently attached to the thiol group of cysteine residue to form S-nitrosothiol (137). Hence we proposed that the specific effect of NO on iNOS aggregation was mediated by cysteine nitrosylation of iNOS. 24 cysteine residues are found in iNOS protein. Considering the aggregates formation is specific to iNOS rather than eNOS or nNOS, we highlighted 5 specific cysteines on iNOS through sequence alignments of all three NOS proteins. Substitutions of these cysteines with alanines were conducted to identify the residues responsible for NO-mediated iNOS aggregation. Unfortunately, Cysteine-to-alanine mutations of these iNOS-specific residues failed to prevent aggregates formation of the resulting iNOS mutant (Figure 4.10). The pivotal

residues involved in iNOS aggregation remained to be elucidated among the rest 19 candidate cysteines on iNOS.

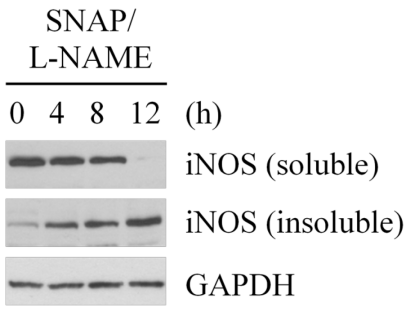

Figure 4.10 Mutation of iNOS-specific cysteines to alanines failed to prevent NO-mediated iNOS aggregation in HEK293 cells.

4.4 Discussion

The key finding of this study is that NO triggers iNOS aggregates formation and functions as an important feedback regulator of iNOS. Among the NOS isoforms, nNOS and eNOS have been shown to be anchored to the plasma membrane through the interactions with various adaptor proteins (18, 130). iNOS, however, was believed to exist as a soluble protein in the cytosol until a recent report from the Eissa group, in which they show that iNOS forms aggresomes (54, 55). They transfected GFP-iNOS into HEK293 cells and found that iNOS formed aggresomes. iNOS aggresome formation was also reported in cytokine-stimulated bronchial epithelial cells by the same group as well as mouse macrophages in the present study. However, the key question is what causes iNOS aggresome formation. The present study shows that, for the first time, it is the NO per se that causes iNOS aggregation. Blocking NO production has no effect on iNOS

expression but prevents iNOS aggresome formation in both native and transfected cells. Removal of iNOS inhibitor converts soluble iNOS into aggregates as a function of time. Soluble iNOS is a constantly active enzyme. iNOS in aggresomes, on the other hand, is inactive. It is known that NO can cause feedback inhibition to iNOS, but the mechanism has been elusive. The current discovery that NO induces iNOS aggregation and subsequent deactivation may be the long-sought mechanism underlying the feedback inhibition of iNOS by NO. Our further studies indicated that such feedback inhibition is specific to iNOS, which might be evolved to suit the robust NO-producing potency of iNOS. Nitrosylation, resulted from massive NO generation, is an important posttranslational modification specifically targeting cysteine residues. NO induces iNOS aggregation possibly via cysteine nitrosylation. However, the replacement of 5 iNOS-specific cysteines to alanines has little effect on NO-mediated iNOS aggregation. Thus the essential cysteine residues for iNOS aggregation triggered by NO remain to be identified in future studies.

CHAPTER 5

5 iNOS aggregation mediated by Hsp90 and the clearance of aggregated iNOS in the presence of Hsp90 inhibitor

5.1 Introduction

NO is a gaseous free radical playing multifaceted roles in various biological processes. Although physiological concentrations of NO serve as a signaling molecule in neuronal transmission and cardiovascular regulation, high levels of NO cause harm to cells (7, 13, 126, 127). The immune system employs the unique feature of NO to fight against microbe invaders as well as tumor cells (8, 129, 130). In mammals, NO is derived from L-arginine via a reaction catalyzed by a family of NO synthase (NOS) including neuronal NOS (nNOS), inducible NOS (iNOS), and endothelial NOS (eNOS) (18, 131). Among them, iNOS participates in cell injury and host defense (87, 132). In contrast to the constitutively existing nNOS and eNOS, little iNOS can be detected in normal cells and tissues. Inflammatory mediators, such as bacterial product lipopolysaccharide (LPS) and cytokines including interferon-γ (IFN-γ), are potent inducers of iNOS gene expression. All NOS isoforms are activated by the binding with the cofactor calmodulin (CaM) (18, 138). For nNOS and eNOS, the binding to CaM is facilitated by the rise of intracellular Ca^{2+}. iNOS, however, contains an intrinsically bound CaM and stays constantly active once expressed (18, 86, 133). The continuous activity along with the

high NO-generating efficacy is thought to suit iNOS for its functions in host defense and cell injury.

Because iNOS is constantly active, the regulation of NO production from iNOS was thought to primarily occur at enzyme transcriptional level. This notion evolves as recent studies show that iNOS function can be affected by protein-protein interactions and posttranslational modifications (115). In an early study, we showed that iNOS associates with heat shock protein 90 (Hsp90) in cells and this association enhances iNOS activity. The interaction with Hsp90 is found to be important in the cytotoxic effect of iNOS on cells. Recently, we reported that Hsp90 is necessary for the transcriptional activation of iNOS gene in cells stimulated by both LPS and IFN-γ (116). Hsp90 appeared to be essential for transcriptional factor NF-κB and STAT1 to bind with the iNOS promoter during gene transactivation. The necessary role of Hsp90 in iNOS induction was confirmed *in vivo* in myocardium infarction (116). Together, these studies demonstrate the importance of Hsp90 in regulating iNOS function and gene expression.

In addition to gene expression, the levels of active iNOS in cells are also determined by its protein stability and turnover (54, 61, 139). Whether or not Hsp90 affects iNOS protein stability, and if it does, how changed iNOS stability is coped with inside cells are the remaining questions in the study of Hsp90 regulation of iNOS. In the present study, we address these issues in mouse macrophages which are stimulated to express iNOS. Our studies find Hsp90 vital for iNOS protein stability. Loss of the interaction with Hsp90 leads to iNOS aggregation and deactivation. Cells employ the ubiquitin-proteasome system (UPS) to eliminate aggregated iNOS proteins. We further

reveal that the SPRY domain-containing SOCS box protein 2 (SPSB2), an E3 ligase-recruiting protein, is essential for the proteasomal clearance of iNOS aggregates in cells.

5.2 Materials and methods

5.2.1 Materials

Cell culture materials were purchased from Invitrogen (Carlsbad, CA). The antibody against iNOS was from BD Transduction Laboratories. Antibody against Hsp90 was a product of Cell Signaling Technology (Beverly, MA). The antibody against SPSB2 was from Santa Cruz Biotechnology (Santa Cruz, CA). LPS, recombinant mouse IFN-γ, geldanamycin (GA), radicicol, anti-GAPDH and anti-flag antibodies were products of Sigma (St. Louis, MO). Unless otherwise indicated, all other chemicals used in this study were purchased from Sigma.

5.2.2 Cell culture

Mouse macrophage (RAW264.7, ATCC), human embryonic kidney 293 (HEK293), and African green monkey SV40-transfected kidney fibroblast (COS-7) cells were grown in Dulbecco's modified Eagle's medium with 10% fetal calf serum in a 37°C humidified atmosphere of 95% air and 5% CO_2. Expression of iNOS in RAW264.7 cells was induced by LPS (2 μg/ml, serotype 026:B6) and IFN-γ (100 U/ml).

5.2.3 Cell fractionation

Cells were rinsed with phosphate-buffered saline (PBS) and lysed on ice for 30 min in a lysis buffer containing moderate detergents (50 mM Tris-HCl, pH 7.4, 150 mM NaCl, 1% Nonidet P-40, 0.25% sodium deoxycholate, 50 mM NaF, 1 mM Na_3VO_4, 5

mM sodium pyrophosphate, 1 mM EDTA and protease inhibitor tablet). After a centrifugation at 14,000 × g for 15 min at 4°C, the supernatants and pellets were recovered as soluble and insoluble fractions, respectively. The insoluble pellets were washed by PBS, and boiled in 1.5×SDS/PAGE sample buffer (90 mM Tris-HCl, pH 6.8, 3% SDS, 15% glycerol, 0.015% bromophenol blue and 62.5 mM dithiothreitol) for 7 min. Total cell samples were obtained by passing the lysates through 30G needles after 30 min incubation in high-detergent lysis buffer (50 mM Tris-HCl, pH 7.4, 150 mM NaCl, 1% Nonidet P-40, 0.25% sodium deoxycholate, 1% SDS, 1 mM EDTA and protease inhibitor tablet).

5.2.4 Western blot analysis

Cells were harvested and lysed on ice for 30 min in lysis buffer, followed by 15 min centrifugation at 14,000 × g. Protein concentrations were determined by using the detergent-compatible protein assay kit (Bio-Rad). After 5 min boiling in 1×SDS/PAGE sample buffer, the proteins were separated by SDS-PAGE, transferred to nitrocellulose membranes, and probed with the appropriate primary antibodies. Membrane-bound primary antibodies were detected with secondary antibodies conjugated with horseradish peroxidase. Immunoblots were developed on films using the enhanced chemiluminescence technique (SuperSignal West Pico, Pierce).

5.2.5 shRNA

HuSH 29mer shRNA constructs against CHIP gene (Origene Technologies) were transfected into HEK293 cells by using Lipofectamine 2000 reagents (Invitrogen). The

CHIP knockdown efficiency was confirmed by Western blotting and the CHIP-depleted cells were subjected to further treatments and analyses.

5.2.6 siRNA

Small interfering RNA (siRNA) oligonucleotides targeting SPSB2 and control nonspecific siRNA were purchased from Santa Cruz Biotechnology. In twelve-well plates, cells were seeded the day before transfection and grown to 30% confluence. siRNA oligonucleotides (100 nM) were transfected into cells by using Lipofectamine 2000 reagents. After 48 h of transfection, cells were subjected to further experiments.

5.2.7 Plasmid construction

To construct the plasmid encoding 50-1144 truncated iNOS, the fragment of iNOS encoding 50-1144 AA was PCR-amplified from previously constructed pCMV-iNOS plasmid using primers 5'-CCCAAGCTTGGGATGGGCTCCCCGCAGC and 5'-CCGCTCGAGCGGGCCAGAAGCTGGAAC. After overnight incubation with HindIII and XhoI, 50-1144 iNOS cDNA was cloned into the mammalian expression vector pCMV-Flag-Tag2B using standard molecular biology procedures. To construct pEGFP-C3/iNOS plasmid encoding GFP-iNOS fusion protein, the HindIII-XhoI fragment of pCMV-iNOS plasmid containing iNOS cDNA was cloned into HindIII-SalI site of pEGFP-C3 vector.

5.2.8 Fluorescence imaging

Plasmids encoding GFP-iNOS fusion proteins were transfected into HEK293 or COS-7 cells with Lipofectamine 2000 reagents. After 20 h of plasmid transfection, the

cells were treated with MG-132 (20 μM) for 30 min prior to 8 h incubation with geldanamycin (GA, 5 μM) or radicicol (20 μM). Imaging was performed on a fluorescence microscope (Nikon Eclipse 80i) with the Qimaging Retiga-2000R digital camera (Qimaging).

5.2.9 Nitrite assay

Total nitrite released in cell culture medium was measured with a Griess reagent kit (Invitrogen). The reaction consisted of 20 μl of Griess Reagent, 150 μl of medium, and 130 μl of deionized water. After incubation of the mixture for 30 min at room temperature, nitrite levels were measured at 548 nm using a M2 spectrophotometric microplate reader (Molecular Devices).

5.2.10 iNOS activity assay

iNOS activity was measured by the L-[^{14}C]arginine to L-[^{14}C]citrulline conversion assay (140). iNOS expression was induced in RAW264.7 by LPS/IFN-γ for 12 h. Cells were then homogenized in homogenate buffer (50 mM Tris-HCl, pH7.4, 50 mM NaF, 1 mM Na_3VO_4, and protease inhibitor mixture). After centrifugation (14,000 × g for 30 min at 4 °C), the supernatants were harvested and used for measuring soluble iNOS activity. To obtain aggregated iNOS, LPS/IFN-γ-stimulated cells were incubated with GA (5 μM) or radicicol (20 μM) in the presence of MG-132 (20 μM) for 18 h. The cells were then harvested and homogenized in homogenate buffer. After centrifugation and stringent wash, the pellets were resuspended in the homogenate buffer and used for activity measurements of aggregated iNOS. The cell lysates were added to the reaction mixture containing 50 mM Tris-HCl, pH 7.4, 0.5 mM NADPH, 10 nM $CaCl_2$, 10 μg/ml

CaM, 10 μM BH_4, 2 μM L-[^{14}C]arginine, and 36 μM L-arginine. After 15 min incubation at 37 °C, the reactions were terminated by ice-cold stop buffer. L-[^{14}C]Citrulline was separated by passing the reaction mixture through Dowex AG 50W-X8 (Na^+ form; Sigma) cation exchange columns and quantitated by liquid scintillation counting.

5.2.11 Hsp90-iNOS dissociation assay

Expression of iNOS was induced in RAW264.7 cells by LPS/IFN-γ for 12 h. Cells were harvested and lysed for 30 min in the following lysis buffer: 50 mM Tris-HCl, pH 7.4, 100 mM NaCl, 0.5% Nonidet P-40, 1 mM EDTA, 50 mM NaF, 1 mM Na_3VO_4, and protease inhibitor tablet. The cell lysates were then centrifuged at 14,000 × g for 15 min, and the supernatants were incubated with 2′, 5′-ADP-Sepharose affinity resins for 2 hours at 4 °C. The beads were washed three times with high salt buffer (50 mM Tris-HCl, 500 mM NaCl, 1 mM EDTA and 0.5% Nonidet P-40), followed by one time wash with regular washing buffer (50 mM Tris-HCl, 100 mM NaCl, 1 mM EDTA and 0.5% Nonidet P-40). Afterwards, the beads were resuspended in 50 μl washing buffer containing GA (10 μM) or radicicol (20 μM) and then harvested at designated time point. After 1 min centrifugation at 14,000 × g, the supernatants were recovered and the proteins bound to beads were eluted by 5 min boiling of the beads in 1.5×SDS/PAGE sample buffer. Both supernatant and eluted samples were characterized by Western blotting with appropriate antibodies.

5.2.12 Statistical analysis

Data are expressed as Mean ± SE. Comparisons are made using a two-tailed Student's paired or unpaired *t* test. Differences are considered statistically significant at $P < 0.05$.

5.3 Results

5.3.1 Hsp90 inhibition causes iNOS aggregation and iNOS aggregates are cleared by proteasomes

To determine the effects of Hsp90 on iNOS protein stability and turnover, mouse macrophage RAW264.7 cells were stimulated by LPS/IFN-γ. Cells were then fractioned into supernatant (soluble) and pellet (insoluble) fractions in a buffer containing moderate detergent (1% NP-40). As shown in Figure 5.1A, normal iNOS was a soluble protein. Little iNOS was detected in the pellet fractions. Radicicol, a specific inhibitor of Hsp90, reduced soluble iNOS levels in a time-dependent manner (Figure 5.1A). Interestingly, pretreatment of cells with the proteasome blocker MG-132 failed to prevent the loss of iNOS in the soluble fractions of Hsp90-inhibted cells; instead, progressive iNOS accumulation was observed in the insoluble fractions upon proteasomal blockade. With high levels of strong detergent (1% SDS), the insoluble iNOS proteins could be extracted into soluble fractions (Figure 5.1B). Under this condition, Hsp90 inhibition-induced iNOS depletion was seen to be prevented by MG-132 treatment, a characteristic feature expected to the proteins that are degraded by the proteasome. These data suggested that Hsp90 inhibition caused iNOS to form aggregates and these iNOS aggregates were subsequently cleared by proteasomes.

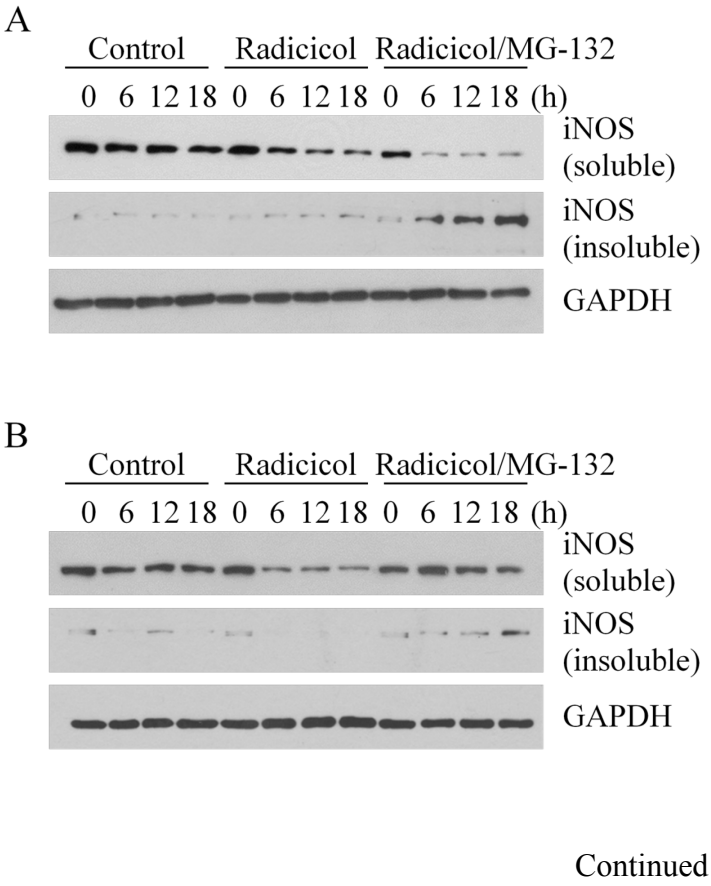

Continued

Figure 5.1 Hsp90 control of iNOS protein stability and turnover in mouse macrophage.
(A) iNOS expression was induced in RAW264.7 cells by LPS/IFN-γ. Hsp90 inhibition with radicicol (20 μM) caused iNOS aggregation and the iNOS aggregates were cleared by the proteasome (B) Insoluble iNOS aggregates in radicicol-treated cells were dissolved in strong detergent containing buffer (1% SDS) and the characteristic MG-132-sensitive feature of the proteins degraded by the proteasome was shown. (C, D) Geldanamycin (GA, 5 μM), another Hsp90 inhibitor that structurally differed from radicicol, also caused iNOS aggregation and the clearance of iNOS aggregates was prevented by proteasomal inhibition. Representative blots shown from 3-5 experiments.

Figure 5.1 continued

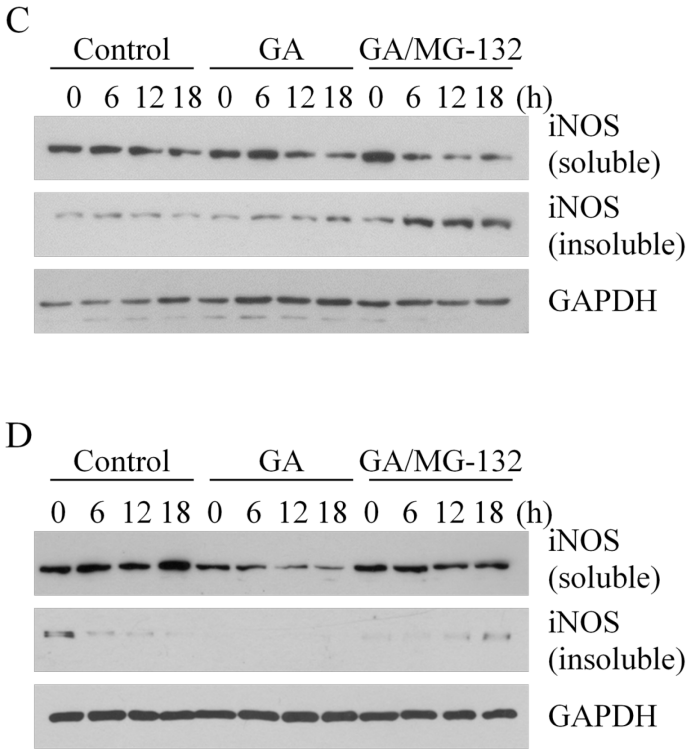

Radicicol is a specific Hsp90 inhibitor (115, 141). To further eliminate the concern on the potential off-target effects of pharmacological inhibitors, we repeated the above experiments with geldanamycin (GA), another Hsp90 selective inhibitor whose structure is different from that of radicicol. In accordance with the findings obtained with radicicol, Hsp90 inhibition with GA also rendered iNOS aggregation and the aggregated iNOS was degraded by proteasomes (Figure 5.1C and D).

The autophagy-lysosome pathway has been reported to be involved in bulk degradation of macromolecules such as aggregated proteins (73). To identify whether

autophagy-lysosome pathway is involved in the clearance of aggregated iNOS in the presence of Hsp90 inhibitors, we monitored the change of iNOS protein levels in both soluble and insoluble fractions in cells exposed to lysosomal inhibitor NH_4Cl (20 mM). Blockade of lysosome failed to protect iNOS turnover under Hsp90-inhibited conditions (Figure 5.2A and B). These data indicated that lysosomal function was not required in the degradation of aggregated iNOS in Hsp90-inhibited cells. The comparisons of the iNOS decay curves in the absence and presence of Hsp90 inhibitor, MG-132 and NH_4Cl suggested proteasome as the major machinary responsible for the clearance of iNOS aggregates upon Hsp90 inhibition (Figure 5.3A and B).

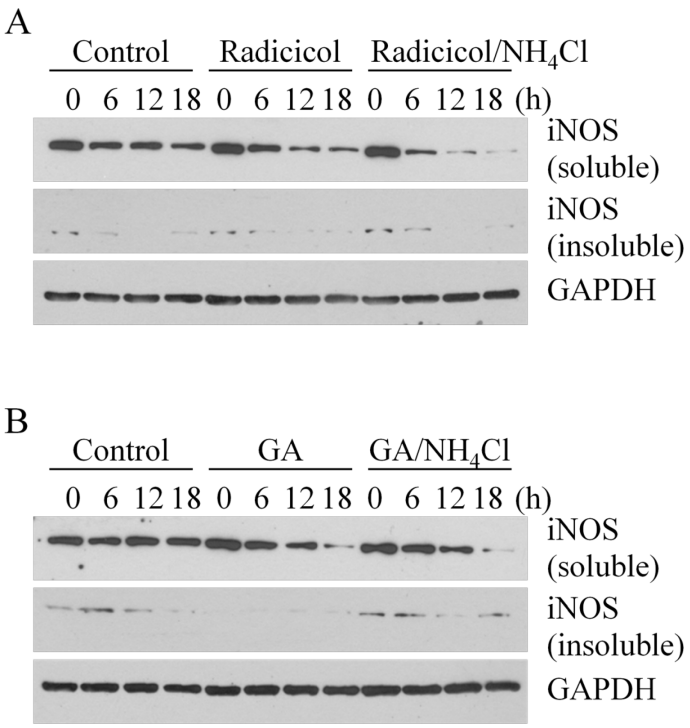

Figure 5.2 Inhibition of lysosome had no effect on the degradation of iNOS in Hsp90-inhibited cells.
Lysosome inhibition with NH_4Cl (20 mM) failed to prevent the degradation of iNOS upon Hsp90 inhibition with (A) radicicol (20 μM) or (B) GA (5 μM), respectively. Representative blots shown from 3-5 experiments.

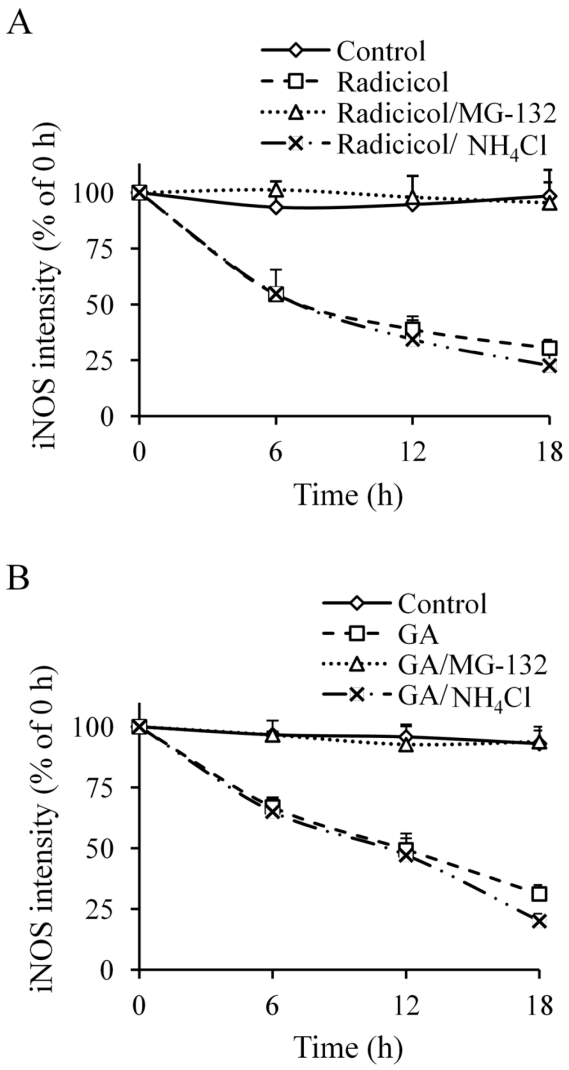

Figure 5.3 Quantitative analyses of iNOS degradation in the absence and presence of Hsp90, proteasome and lysosome inhibitors.
Data are means ± SE, n = 4.

5.3.2 GFP-iNOS aggregation and degradation in transfected cells

To visualize iNOS aggregation and degradation under Hsp90 inhibition, we constructed a GFP-tagged iNOS plasmid and transfected it into HEK293 cells. Expressed

iNOS was evenly distributed in cytosol (Figure 5.4, left panels). Hsp90 inhibition with radicicol or GA decreased intracellular iNOS as evidenced by reduced fluorescence in cells (Figure 5.4, middle panels). Blocking proteasome resulted in intense fluorescence cluster formation in cells (Figure 5.4, right panels).

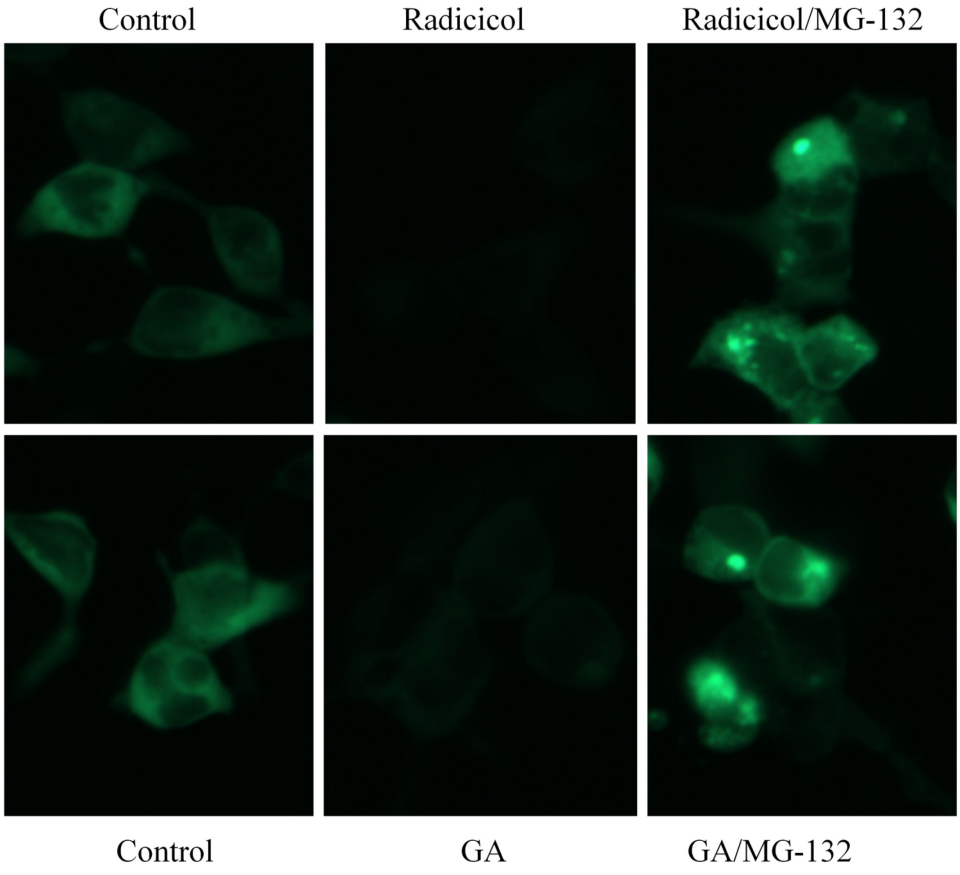

Figure 5.4 Fluorescence imaging of Hsp90 inhibition-induced GFP-iNOS aggregation and clearance in HEK293 cells.
As shown, Hsp90 inhibition (Radicicol, 20 μM; GA, 5 μM) depleted GFP-iNOS. In the presence of proteasome inhibitor (MG-132, 20 μM), iNOS aggregates were seen in cells. Representative images are shown from triplicate experiments.

With COS-7 cells whose size is bigger than that of HEK293 cells, Hsp90 inhibition-induced iNOS aggregation was clearly demonstrated after blocking proteasomes (Figure 5.5, right panels). These aggregates displayed as fluorescent particles with different sizes and shapes. In the absence of proteasome inhibitor, no iNOS aggregates but only reduced GFP-iNOS levels were observed (Figure 5.5, middle panels). These imaging data were consistent with the findings from the cell fractionation experiments. These two lines of evidence together demonstrated that Hsp90 was essential for the stability of iNOS as a soluble protein in cytosol.

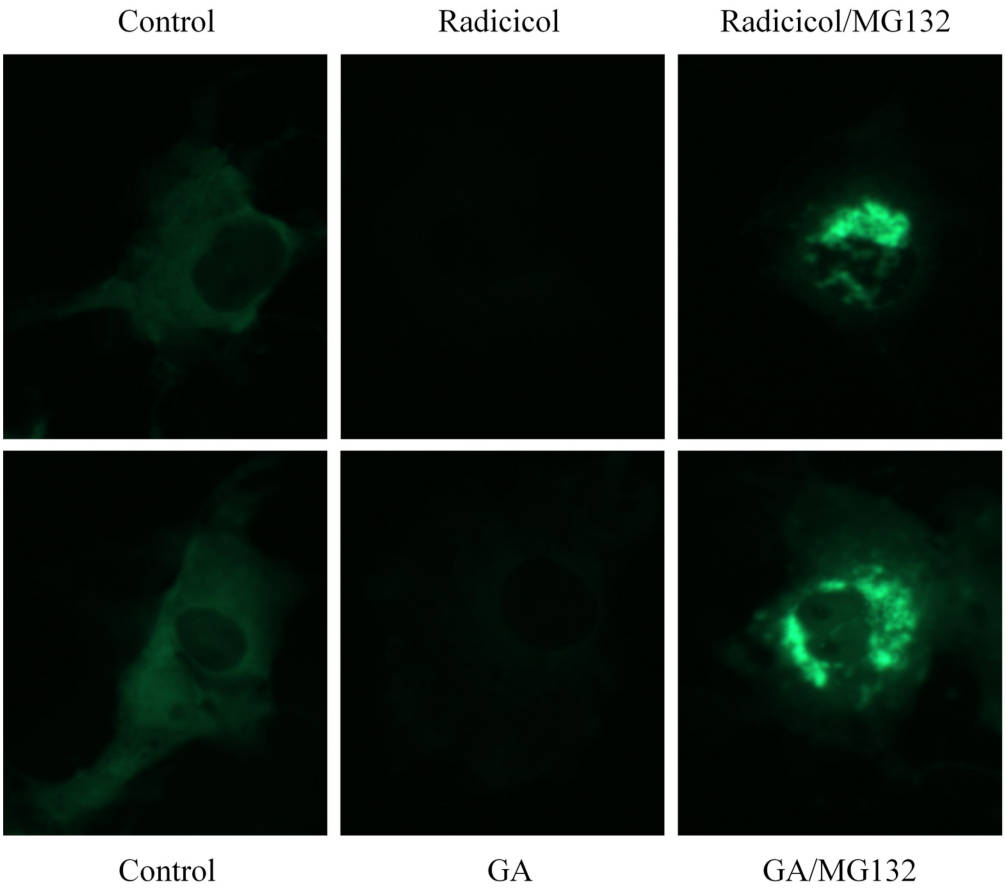

Figure 5.5 Fluorescence imaging of GFP-iNOS expressed in COS-7 cells in the absence and presence of Hsp90 antagonists and proteasomal inhibitor.

5.3.3 Aggregation deactivates iNOS

Aggregation usually leads to the loss of protein function (55, 142, 143). To determine the effect of protein aggregation on iNOS function inside cells, we measured NO productions from iNOS-induced cells in the absence and presence of Hsp90 inhibitors. Compared to that in the control groups, markedly decreased NO productions were seen in Hsp90-inhibited cells in which aggregated iNOS was preserved by MG-132 (Figure 5.6), suggesting that aggregation deactivated iNOS. To further demonstrate the

functional consequence of iNOS aggregation, we measured the catalytic activity of soluble and aggregated iNOS *in vitro*. As shown in Figure 5.7A and B, soluble iNOS exhibited robust NO-generating activity. In contrast, aggregated iNOS from either radicicol or GA-treated cells largely lost its catalytic function. Thus, these *in vitro* and cell culture studies collectively showed that aggregation resulted in iNOS inactivation.

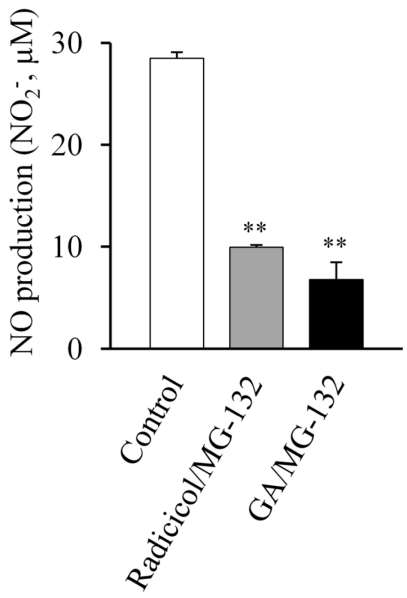

Figure 5.6 NO production from iNOS expressed in RAW264.7 cells in the absence and presence of Hsp90 and proteasome inhibitors.
Data are means ± SE. ** $P < 0.01$ vs. control, n=3.

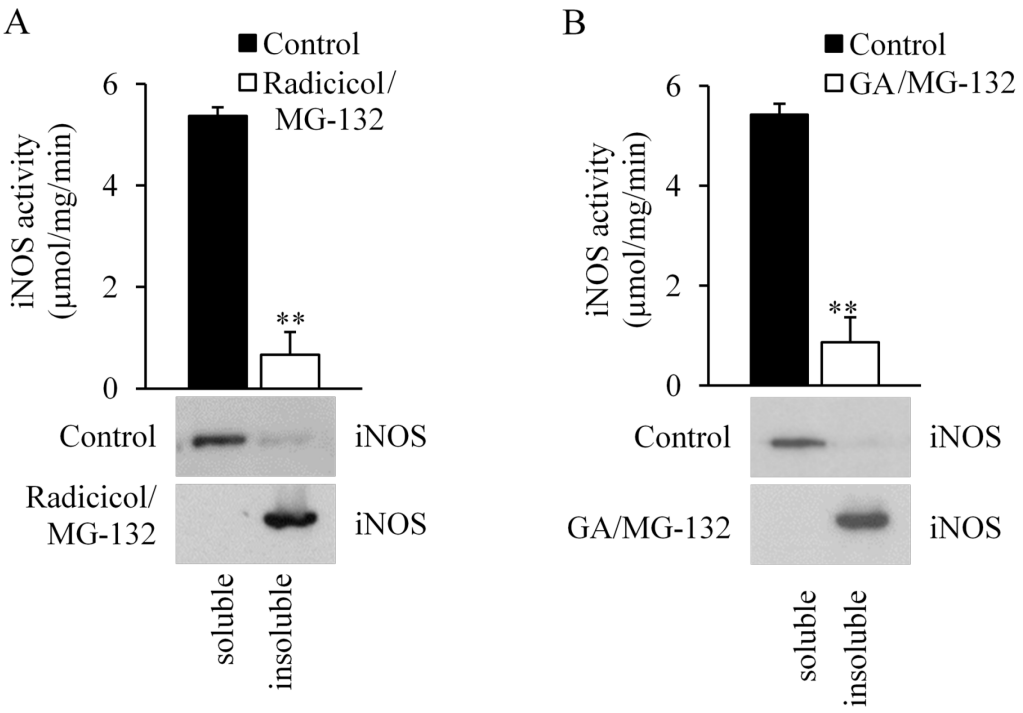

Figure 5.7 Aggregation caused iNOS to lose catalytic function.
(A) Hsp90 inhibition with radicicol (20 μM) rendered iNOS aggregation and deactivation. (B) Under Hsp90 inhibition with GA (5 μM), the catalytic activity of iNOS was largely lost after aggregation. ** $P < 0.01$ vs. control, n = 4.

5.3.4 Hsp90 inhibition induces Hsp90-iNOS dissociation

We then sought to gain some further understandings on the process of iNOS aggregation after Hsp90 inhibition. Both radicicol and GA target the ATPase pocket of Hsp90 (144-146). It is unclear whether or not radicicol or GA disrupted Hsp90-iNOS association in the process of iNOS aggregation. To address this question, we isolated iNOS-Hsp90 complexes from cells, exposed them to Hsp90 inhibitors, and monitored the alterations of the Hsp90 bound with iNOS as well as those released in the supernatants. As shown in Figure 5.8A and B, both radicicol and GA treatment caused a time-

dependent decrease in the Hsp90 bound with iNOS. Inversely proportional to the decreases in the Hsp90 bound to iNOS, the levels of free Hsp90 released into the supernatants were increased. These data demonstrated that Hsp90 inhibition caused iNOS-Hsp90 dissociation. It was noted that the Hsp90-iNOS dissociation occurred ahead of iNOS aggregation, suggesting that these two processes were interrelated.

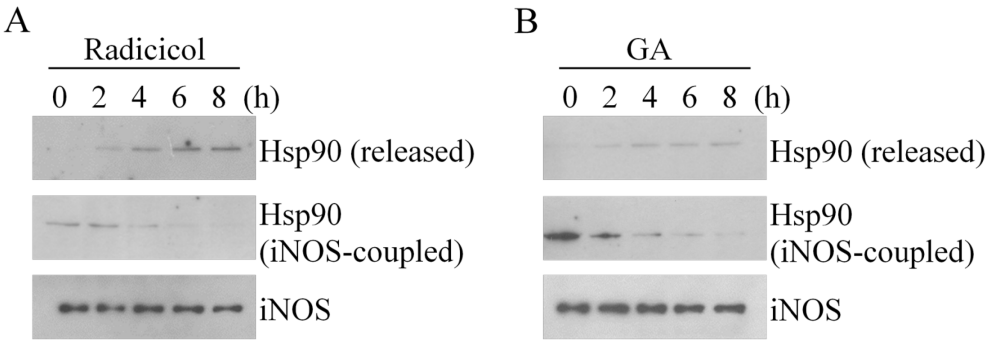

Figure 5.8 Hsp90 inhibition caused Hsp90 dissociation from iNOS.
(A) Radicicol decreased the levels of Hsp90 that bound with iNOS. Meanwhile, the amounts of free Hsp90 released from Hsp90-iNOS complexes were increased following radicicol treatment. (B) Hsp90 inhibition with GA also rendered Hsp90 dissociation from iNOS. Representative data were shown from three independent experiments.

5.3.5 CHIP is dispensable for the clearance of iNOS aggregates

Previous studies reported that iNOS can be degraded by the UPS and the carboxyl terminus of Hsp70 interacting protein (CHIP) has been implicated in iNOS protein turnover (30, 61-63). CHIP is an Hsp70/Hsp90-dependent E3 ligase. Both radicicol and GA have been used to block Hsp90, a protein required for CHIP function (147, 148). The fact that Hsp90 inhibition promoted iNOS degradation via UPS suggested that other E3

ligases likely existed for the proteasomal clearance of iNOS aggregates under Hsp90 inhibition condition. To further rule out the involvement of CHIP in the clearance of iNOS aggregates in Hsp90-inhibited cells, we expressed iNOS into control and CHIP knockdown HEK293 cells and exposed them to Hsp90 inhibitor. To focus on the degradation process of iNOS aggregates, we extracted intracellular iNOS with strong detergent-containing buffer (1% SDS) and monitored the changes of total iNOS levels in this experiment and hereafter. As shown in Figure 5.9A, Hsp90 inhibition caused iNOS degradation in both control and CHIP knockdown cells. The time courses of iNOS decline in control and CHIP knockdown cells were indistinguishable (Figure 5.9B). These data unambiguously demonstrated that CHIP was not required in the degradation of iNOS aggregates in Hsp90-inhibited cells.

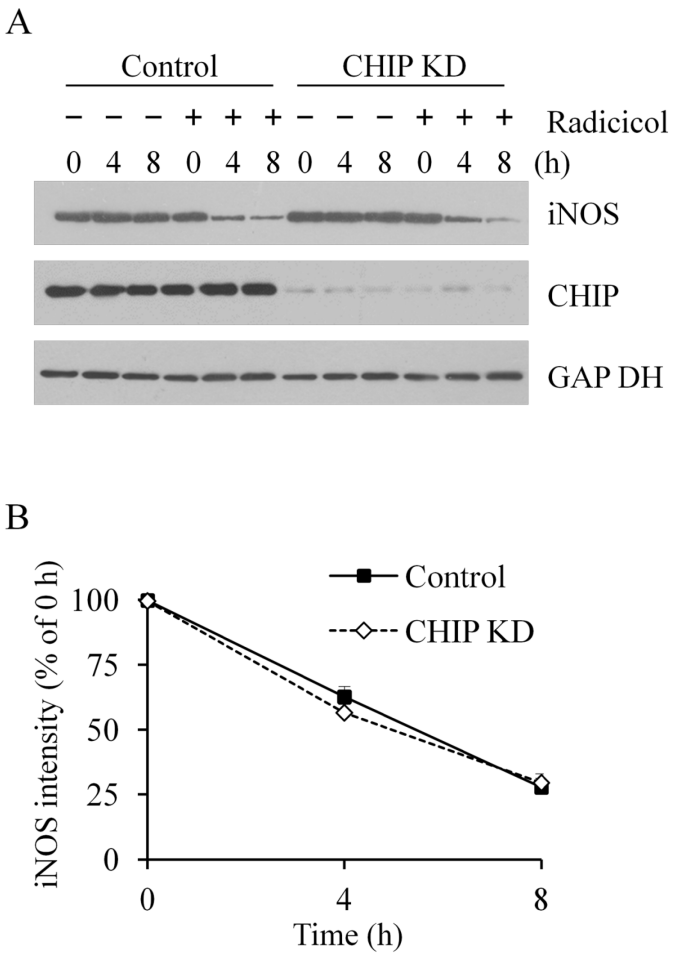

Figure 5.9 CHIP depletion had no effect on iNOS degradation in Hsp90-inhibited cells.
(A) Knockdown of CHIP in HEK293 cells failed to prevent the iNOS depletion in radicicol-treated cells. (B) Quantitative analyses of the effects of CHIP knockdown on iNOS degradation in Hsp90-inhibited cells. Data are means ± SE, n = 4.

5.3.6 SPSB2 is essential for UPS clearance of iNOS aggregates

A recent study reported that the SPRY domain-containing SOCS box protein 2 (SPSB2), an E3 ligase-recruiting protein, participates in iNOS ubiquitination and turnover in normal conditions (64, 65). We thus explored if SPSB2 played roles in the proteasomal clearance of iNOS aggregates in Hsp90-inhibited cells. As shown in Figure

5.10A and B, SPSB2 knockdown largely prevented the degradation of iNOS aggregates, indicating that SPSB2 mediated the ubiquitination and degradation of aggregated iNOS. Indeed, we isolated iNOS aggregates from Hsp90-inhibited cells and found their ubiquitination levels were markedly reduced in SPSB2 knockdown cells (Figure 5.10C). These results revealed that the SPSB2 was required for ubiquitination and degradation of iNOS aggregates.

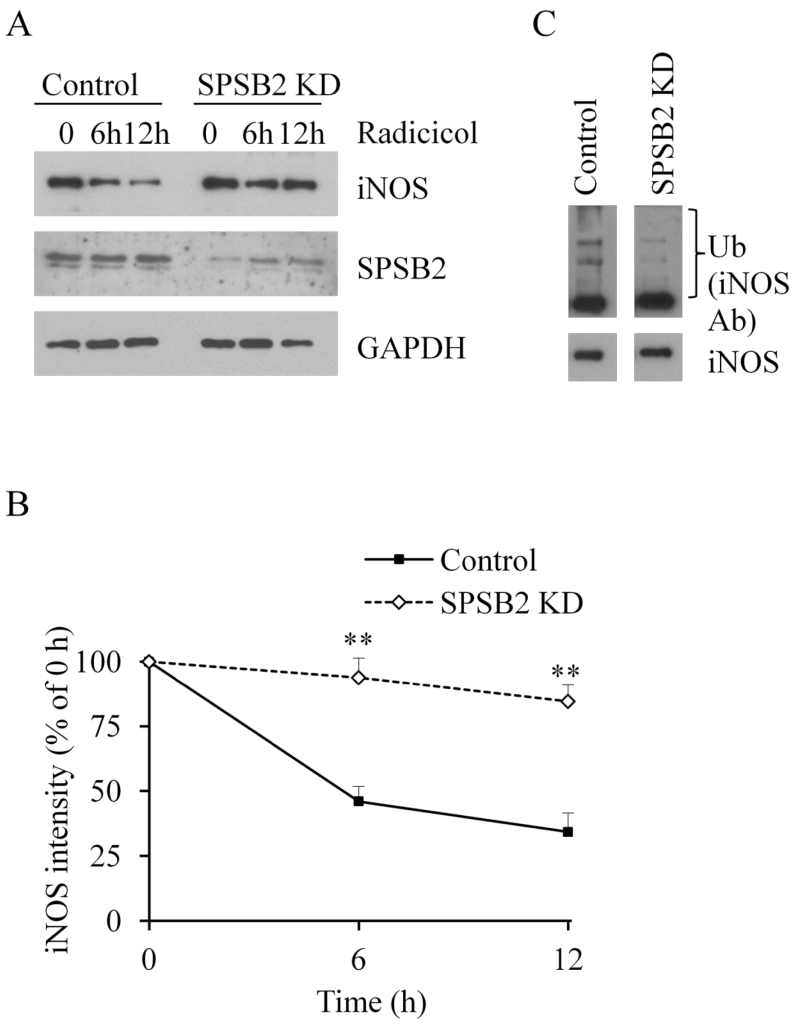

Figure 5.10 SPSB2 was essential for the ubiquitination and degradation of iNOS aggregates upon Hsp90 inhibition.
(A) SPSB2 konckdown prevented the loss of iNOS in radicicol-treated cells. (B) Quantitative analyses of the effects of SPSB2 knockdown on iNOS degradation after Hsp90 inhibition. Data are means ± SE. ** $P < 0.01$ vs. control, n = 4. (C) Ubiquitination levels of iNOS aggregates were markedly reduced by SPSB2 knockdown in RAW264.7 cells. Representative images are shown from triplicate experiments.

5.3.7 Eradicating the SPSB2-binding domain on iNOS prevents the clearance of iNOS aggregates

iNOS is known to interact with SPSB2 through a DINNN containing domain (amino acids 23-27) in its N-terminal region (64, 65). To demonstrate the necessity of the interaction with SPSB2 in the clearance of iNOS aggregates, we constructed a SPSB2-binding domain deletion iNOS ($iNOS_{50-1144}$, Figure 5.11A) and expressed it into HEK293 cells. As shown in Figure 5.11B, the removal of the SPSB2-binding domain had no effect on the catalytic function of iNOS as evidenced by the similar NO productions in the cells expressing iNOS or $iNOS_{50-1144}$. This data suggested that there was no major change in iNOS folding or conformation after removing the SPSB2 binding domain. However, deleting the SPSB2-binding domain largely prevented the clearance of iNOS aggregates (Figure 5.12A and B). This indicated that the interaction with SPSB2 was requested for proteasomal clearance of iNOS aggregates. To ensure these findings were not restricted to one particular type of cells, we conducted similar experiments in COS-7 cells. Again, deleting the SPSB2-binding domain abrogated the clearance of iNOS aggregates after Hsp90 inhibition (Figure 5.12C and D). These results demonstrated the essentiality of SPSB2-iNOS interaction in the UPS clearance of iNOS aggregates in Hsp90-inhibited cells.

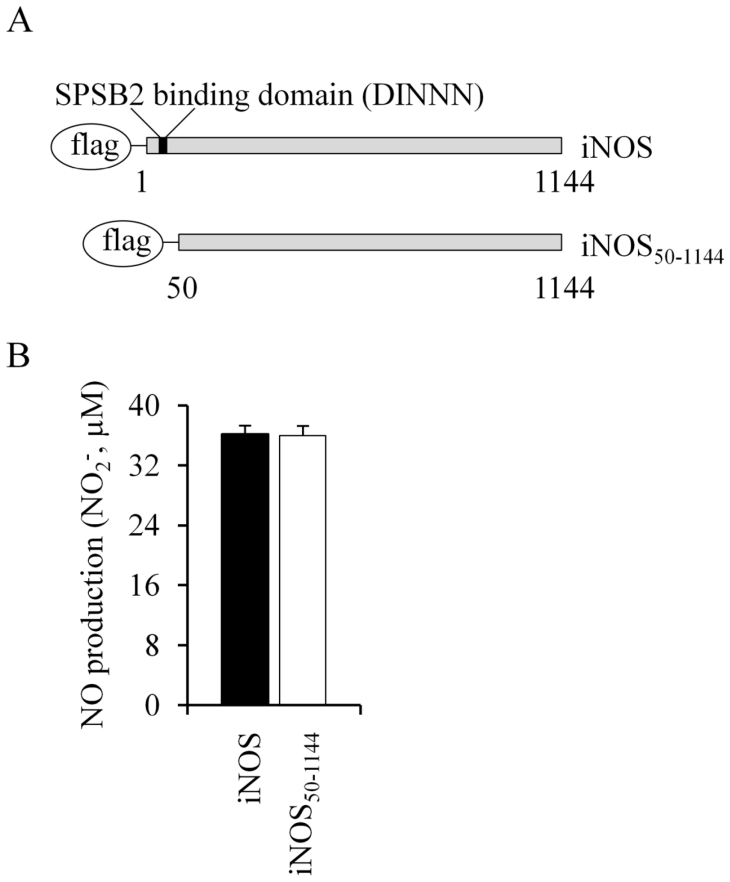

Figure 5.11 A schematic representation of wild-type iNOS and SPSB2-binding domain deficient mutant $iNOS_{50-1144}$.
(A) Schematic representation of wild-type iNOS and $iNOS_{50-1144}$ mutant. (B) Wild-type and truncated $iNOS_{50-1144}$ exhibited the same NO-generating activity. Data are means ± SE, n = 4.

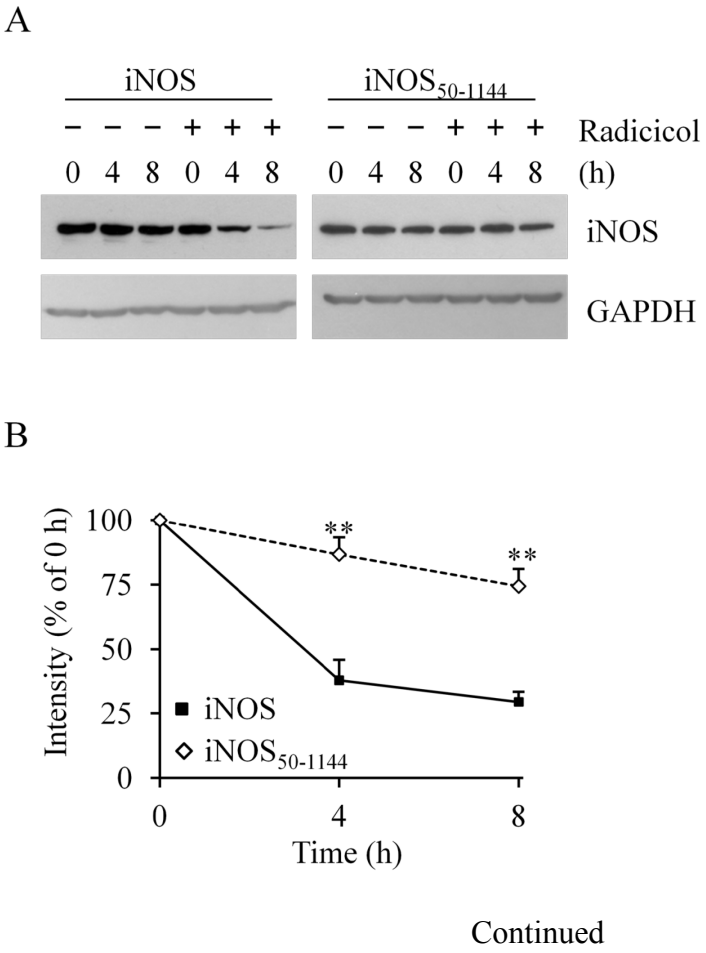

Continued

Figure 5.12 Deletion of SPSB2-interacting domain on iNOS prevented iNOS degradation in Hsp90-inhibited cells.
(A) Hsp90 inhibition-induced iNOS degradation in HEK293 cells was significantly decelerated by deleting the SPSB2-binding domain on iNOS. (B) Quantitative analyses of the effects of deleting SPSB2-interacting domain from iNOS on its degradation in Hsp90-inhibited HEK293 cells. $^{**}P < 0.01$ vs. control, n = 3. (C) Deletion of the SPSB2-binding domain also prevented the degradation of iNOS in COS-7 cells after Hsp90 inhibition. (D) Quantitative analyses of the turnover rate of wild-type and $iNOS_{50\text{-}1144}$ in Hsp90-inhibited COS-7 cells. $^{**}P < 0.01$ vs. control, n = 3.

Figure 5.12 continued

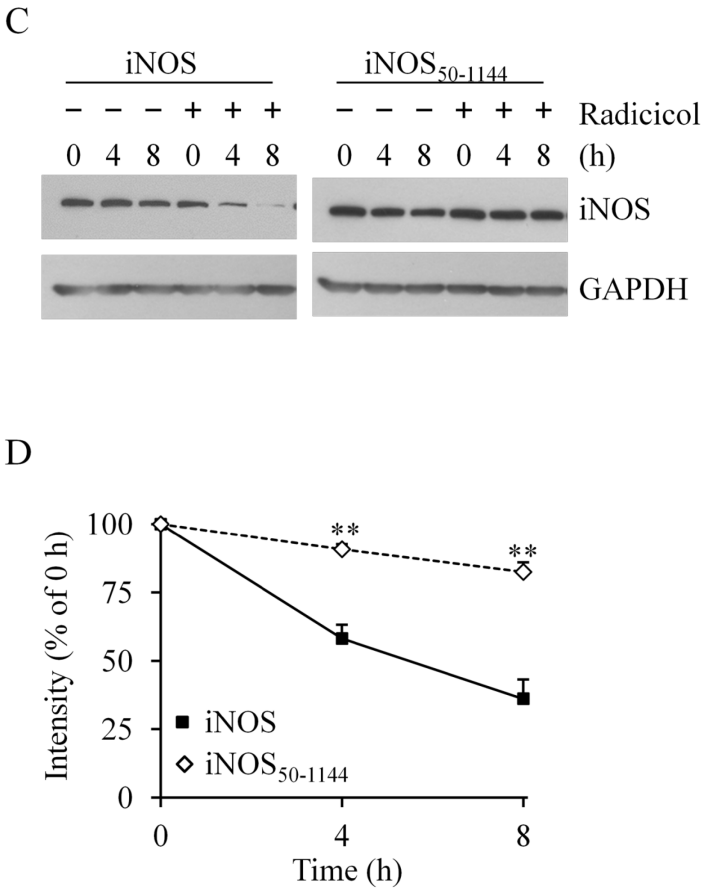

5.4 Discussion

The key finding of this study is that Hsp90 is essential for maintaining the protein stability of iNOS. Unlike eNOS or nNOS whose activation is largely driven by transient intracellular Ca^{2+} increases, NO production from iNOS is dependent on the levels of iNOS proteins. Historically, intracellular iNOS levels have been thought to be determined by the magnitude of its gene transcription. Thus, most studies in this field focused on

deciphering the mechanisms of iNOS gene transactivation (128, 149, 150). Little attention was paid to the potential roles of changed protein stability or turnover in iNOS biology. Recently, studies on the changes in iNOS protein stability and the impacts of these changes on iNOS function began to emerge (54, 55, 61, 139). The findings in current study underscore the importance of protein aggregation in affecting iNOS function, and identify Hsp90 as a critical component in controlling iNOS protein stability. Hsp90 inhibition causes iNOS aggregation and deactivation. NO production in macrophages exposed to inflammatory stimuli is dependent on Hsp90. Under Hsp90 inhibition, NO production is largely diminished because of iNOS aggregation. Hence in addition to the previously reported roles in regulating iNOS function and expression (115, 116), Hsp90 is also essential in keeping iNOS proteins stable inside cells.

The details of iNOS aggregation following Hsp90 inhibition remain to be determined. Nevertheless, our data suggest that the aggregation process may begin with Hsp90 dissociation from iNOS. A comparison of the time-courses of Hsp90 dissociation and iNOS aggregation showed that Hsp90-iNOS dissociation occurred prior to iNOS aggregation. This suggests a model that Hsp90 inhibition cause Hsp90-iNOS dissociation and the latter subsequently forms aggregates (Figure 5.13). Further studies are needed to verify such a model and decipher why Hsp90-uncoupled iNOS is prone to aggregation. As a chaperon protein, Hsp90 is known to play crucial roles in maintaining the conformation of its client proteins. It is conceivable that lacking the chaperon of Hsp90 may render iNOS into an unstable conformation that favors protein aggregation.

Another finding in this study is the elucidation on how iNOS aggregates are coped with in cells. Different from previously discovered NO-triggered iNOS aggregates, Hsp90 inhibition generated transient iNOS aggregates which are quickly eliminated by cells. Our data show that iNOS aggregates are cleared via the UPS. Aggregation not only causes proteins to lose their functionalities, aggregated proteins often inflame additional harm to cells. In fact, abnormal accumulations of protein aggregates are a mechanism of many diseases. Whether or not iNOS aggregates further cause detrimental consequences remains to be seen. Nonetheless, cells appear to take prompt actions to eliminate iNOS aggregates under Hsp90-inhibited conditions. Thus, when UPS function is normal, iNOS aggregation can be effectively coped with except for the cells to lose NO-generating capability. However, when UPS function is hampered, as occurred in various diseases, iNOS aggregates will retain in cells. These aggregated iNOS not only stops producing NO, but also may pose a new burden to cells. It will be interesting to investigate whether or not iNOS aggregates induce detrimental effects in disease conditions in the future.

Prior to proteasomal degradation, target proteins must be ubiquitinated and this is mainly accomplished by a cascade of reactions catalyzed by a group of enzymes including E1, E2, and E3 (151). Among them, the E3 ligase is responsible for target specificity and thus plays determining role in directing proteins to the proteasome for degradation. The E3 ligase CHIP was previously reported to facilitate iNOS ubiquitination and proteasomal degradation in transfected cells (30, 63). A recent study, however, shows that CHIP was not responsible for iNOS ubiquitination and lifetime in macrophages (152). Interestingly, CHIP is an Hsp90 dependent enzyme. In fact, GA and

radicicol are shown to affect CHIP function in many studies (68, 148, 153). Our findings that Hsp90 inhibition promotes iNOS degradation indicate that CHIP is dispensable for proteasomal clearance of iNOS. Indeed, CHIP knockdown has no effect on iNOS degradation in Hsp90-inhibited cells. These results do not exclude the possible role of CHIP in iNOS turnover under certain circumstances. But they demonstrate that when CHIP is inhibited or absent, there are other E3 ligases that account for iNOS ubiquitination and degradation.

Our studies show that SPSB2-associated E3 ligase is responsible for iNOS ubiquitination and degradation in Hsp90-inhibited cells. SPSB2 belongs to a group of SOCS box-containing proteins that regulate other proteins via a SOCS box associated E3 ligase (69, 154). Nicholson and colleagues reported that SPSB2 interacts with iNOS via an iNOS N-terminal DINNN motif. SPSB2 couples with the elongin B/C-cullin5-SPRY protein complex to form an E3 ligase to ubiquitinate iNOS (64, 65). This report addressed the role of SPSB2 in controlling the lifetime of normal iNOS. Important question remains regarding the role of SPSB2 in the turnover of other forms of iNOS proteins. We now show that SPSB2 is also essential for proteasomal clearance of aggregated iNOS. Knockdown of SPSB2 markedly reduced the ubiquitination of iNOS aggregates in Hsp90-inhibted cells. SPSB2 knockdown or deleting the SPSB2-interating domain in iNOS prevented the degradation of iNOS aggregates. Together with previous reports (64, 65, 152), our findings highlighted the crucial role of SPSB2 in controlling iNOS ubiquitination and turnover in both physiological and pathphysiological settings (Figure 5.13).

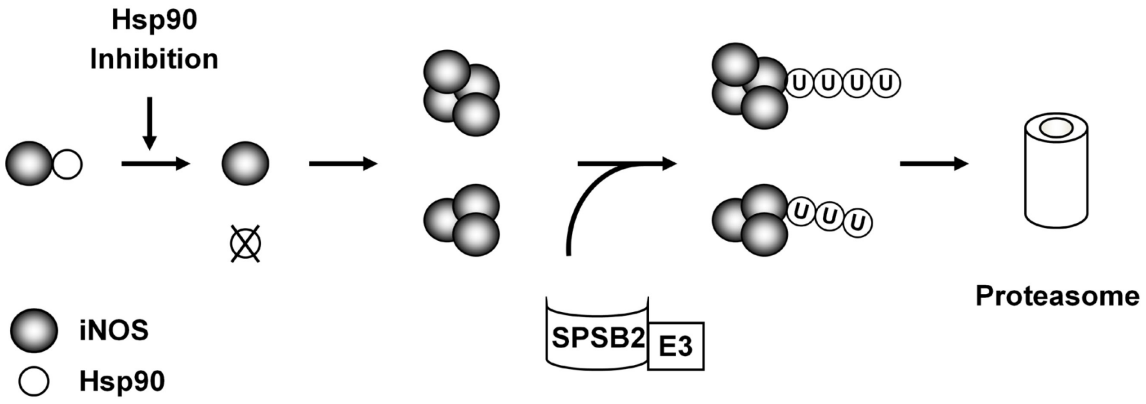

Figure 5.13 Model for iNOS aggregation and degradation in Hsp90-inhibited cells. Hsp90 inhibition triggers the dissociation of Hsp90 from iNOS and subsequent iNOS aggregation. SPSB2 interacts with iNOS and recruits E3 ligase to ubiquitinate aggregated iNOS. Ubiquitinated iNOS aggregates are finally degraded by the proteasome.

Aggregation and proteasomal clearance are efficient means to remove active iNOS in cells. As iNOS levels determine the NO formation quantity; in principle, NO production can be modulated through Hsp90 control of iNOS stability and turnover. Known as a molecular chaperon, Hsp90 is often thought to function as a supporter rather than an initiator in cell signaling. For example, Hsp90 is known to serve as a structural scaffold to bring kinases and their substrates together. This process may not need a change of Hsp90 function. However, recent progresses demonstrate that Hsp90 is able to actively participate in molecular regulation. Hsp90 function can be modulated by protein phosphorylation and protein-protein interactions (155-157). Therefore, down-regulation of Hsp90 function would be expected to lead to iNOS aggregation and removal. This could serve as a counter mechanism to gene induction so that the homeostasis of iNOS proteins can be precisely balanced according to the need. Thus, it will be interesting to

study if intrinsic pathways exist to modulate NO production in host defense via Hsp90 control of iNOS protein stability. Exploring this issue may give rise to novel mechanisms in iNOS regulation.

In summary, in the third part of studies about iNOS regulation via protein stability, we show that the interaction with Hsp90 is crucial for iNOS protein stability. Together with previous reports, we have demonstrated a comprehensive role of Hsp90 in modulating iNOS gene transcription, catalytic function, and protein stability. Lack of Hsp90 interaction results in iNOS aggregation and loss of catalytic function. iNOS aggregates are cleared by the UPS and this is mediated by SPSB2. The identified Hsp90 control of iNOS protein stability and turnover suggests a novel approach to modulate NO production from iNOS in cells.

CHAPTER 6

6 Degradation of normal iNOS under physiological conditions through ubiquitin-proteasome system

6.1 Introduction

NO plays an important role in various biological processes such as host defense, vasodilatation, neuronal signal transmission and memory (5, 8, 12, 127). It is known that a family of NOS enzymes including eNOS, iNOS and nNOS were involved in NO syntheses. Although eNOS and nNOS are constitutively expressed, they normally produce low levels of NO and their activities are Ca^{2+}-dependent. In contrast, iNOS is constantly active once expressed, generating relatively large amounts of NO as compared with the other two isoforms (8, 87). Unlike eNOS and nNOS, little iNOS exists inside resting cells. The expression of iNOS is mainly induced by a variety of cytokines and inflammatory substances such as LPS and IFN-γ. Although NO produced by iNOS was initially recognized to be beneficial to immune system, excessive NO production may cause cell injury and lead to various diseases (4, 33, 34). High level of NO generated by iNOS has been proved to be associated with inflammation, neurodegenerative disease, cardiovascular disease and cancer. Therefore, NO production from iNOS must be precisely controlled in biological systems.

iNOS-derived NO can be regulated by intracellular iNOS protein levels through iNOS expression, NOS protein stability and turnover. Studies on iNOS regulation mainly focused on the iNOS induction stage. Little is known about the roles of protein stability and degradation in iNOS regulation. However, a recent report from Eissa group, indicating that iNOS aggresome formation deactivated iNOS and proposed this as a possible mechanism to down-regulate NO production from iNOS (54, 55). Our previous studies identified CaM, Hsp90 as well as iNOS self-derived NO as essential modulators of iNOS protein stability. These updates provided important information for the understanding of iNOS regulation in terms of protein stability.

Besides aggresome formation, protein turnover also decreases the active iNOS levels inside cells. In eukaryotic cells, the two major pathways responsible for protein turnover are ubiquitin-proteasome system (UPS) and autophagy-lysosome pathway (60, 73, 151). The UPS pathway eliminates ubiquitin-tagged proteins that are destined for degradation. The autophagy-lysosome pathway mainly involves in bulk degradation of macromolecules such as aggregated proteins. Several recent studies showed that UPS collaborated with autophagy-lysosome pathway by labeling target proteins via ubiquitination. Previous studies suggested that iNOS elimination was mainly mediated by the 26S proteasome (61). Further studies indicated that iNOS ubiquitination is required for its degradation (62). In addition, our prior study demonstrated that aggregated iNOS was degraded via UPS in Hsp90-inhibited cells. However, the ubiquitination site on iNOS involved in proteasome-dependent degradation remains to be identified. Furthermore, whether autophagy-lysosome pathway also plays a role in iNOS turnover

remains to be explored. In this study we showed that the N-terminal region (1-100 amino acids) of iNOS is crucial for its degradation. Interestingly, substitution of all lysines inside this region with arginines failed to prevent iNOS degradation. Alanine replacements of 2 cysteine residues appeared to retard iNOS degradation, but failed to down-regulate the ubiquitination levels of this iNOS mutant. Further mutations of serine and threonine residues among 25-50 amino acids of iNOS to alanines not only remarkably prevented iNOS turnover, but also attenuated the magnitude of iNOS ubiquitination levels, indicating their roles in the proteasomal degradation of iNOS.

6.2 Materials and methods

6.2.1 Materials

Cell culture materials were purchased from Invitrogen (Carlsbad, CA). The antibody against iNOS was obtained from BD Transduction Laboratories. LPS, recombinant mouse IFN-γ, geldanamycin, radicicol, ANTI-FLAG® M2 Affinity Gel, 3× FLAG® Peptide, anti-GAPDH, anti-HA and anti-flag antibodies were products of Sigma (St. Louis, MO). Cycloheximide and MG-132 were from Biomol (Plymouth Meeting, PA). HA-Ubiquitin plasmid was purchased from Addgene (Cambridge, MA). Unless otherwise indicated, all other chemicals used in this study were purchased from Sigma.

6.2.2 Cell culture

Mouse macrophage (RAW264.7, ATCC) and African green monkey SV40-transfected kidney fibroblast (COS-7) cells were grown in Dulbecco's modified Eagle's medium with 10% fetal calf serum in a 37°C humidified atmosphere of 95% air and 5%

CO_2. Expression of iNOS in RAW264.7 cells was induced by LPS (4 ng/ml, serotype 026:B6) and IFN-γ (5 U/ml).

6.2.3 Western blot analysis

Cells were harvested and lysed on ice for 30 min in lysis buffer, followed by 15 min centrifugation at 14,000 × g. Protein concentrations were determined by using the detergent-compatible protein assay kit (Bio-Rad). After 5 min boiling in 1×SDS/PAGE sample buffer (62.5 mM Tris-HCl, pH 6.8, 2% SDS, 40 mM dithiothreitol, 10% glycerol, and 0.01% bromophenol blue), the proteins were separated by SDS-PAGE, transferred to nitrocellulose membranes, and probed with the appropriate primary antibodies. Membrane-bound primary antibodies were detected with secondary antibodies conjugated with horseradish peroxidase. Immunoblots were developed on films using the enhanced chemiluminescence technique (SuperSignal West Pico, Pierce).

6.2.4 Plasmid construction

A series of cDNAs encoding full length iNOS and truncated iNOS mutants ($iNOS_{1-600}$, $iNOS_{1-500}$, $iNOS_{1-400}$, $iNOS_{1-300}$, $iNOS_{1-200}$, $iNOS_{1-100}$, $iNOS_{98-1144}$, $iNOS_{25-1144}$, $iNOS_{50-1144}$ and $iNOS_{75-1144}$) were cloned into the pCMV-Tag2B vector (Stratagene). Plasmids were then transfected into COS-7 cells with Lipofectamine 2000 reagent (Invitrogen) according to the manufacturer's instructions.

6.2.5 Site-directed mutagenesis

Amino acid substitution (Lysine to Arginine, Cysteine to Alanine, and Serine/Threonine to Alanine) among the N-terminal region (1-100 AAs) of iNOS was

performed by using the QuikChange Site-directed Mutagenesis Kit (Stratagene) according to the manufacturer's protocol. The mutation of certain amino acid residues was confirmed by DNA sequencing.

6.2.6 Immunoprecipitation

Cells were lysed on ice for 30 min in lysis buffer (50 mM Tris-HCl, pH 7.4, 150 mM NaCl, 1% Nonidet P-40, 0.25% sodium deoxycholate, 50 mM NaF, 1 mM Na_3VO_4, 5 mM sodium pyrophosphate, 1 mM EDTA and protease inhibitor tablet). After centrifugation, the supernatants were incubated with anti-flag® M2 affinity gel for 2 h at 4°C. After stringent wash, immunoprecipitates were eluted by 4 h incubation with 3× FLAG® Peptide at room temperature and then characterized by Western blotting.

6.2.7 Statistical analysis

Data are expressed as Mean ± SE. Comparisons are made using a two-tailed Student's paired or unpaired *t* test. Differences are considered statistically significant at $P < 0.05$.

6.3 Results

6.3.1 iNOS turnover is mediated by UPS

To confirm the role of ubiquitin-proteasome system (UPS) in iNOS degradation, mouse macrophage RAW264.7 cells were stimulated by LPS/IFN-γ. After 12 h induction of iNOS, protein expressions were halted by protein biosynthesis inhibitor cycloheximide (CHX, 100 μg/ml). CHX treatment led to a time-dependent degradation of iNOS.

Pretreatment of cells with proteasome inhibitor MG-132 (50 μM) prevented the loss of iNOS upon CHX treatment (Figure 6.1A). Since LPS or IFN-γ alone can induce iNOS expression via different signaling cascades, the degradation of iNOS in cells stimulated by single inducer was also examined. Again, the presence of MG-132 blocked iNOS turnover in either LPS- or IFN-γ-stimulated macrophages upon CHX treatment (Figure 6.1B, C). These results confirmed that proteasome was involved in iNOS degradation. To validate the role of proteasome in exogenous iNOS turnover, we constructed a plasmid encoding murine iNOS and transfected it into COS-7 cells. Similar to the result obtained from RAW264.7 cells, the presence of CHX caused the degradation of exogenous iNOS expressed in COS-7 cells, and again such elimination process was blocked by MG-132 (Figure 6.2A). To determine whether lysosome also plays a role in iNOS turnover, we performed a similar experiment with lysosomal inhibitor NH_4Cl (20 mM) in COS-7 cells. Different from the effect of MG-132, pretreating cells with NH_4Cl failed to prevent iNOS degradation in CHX-treated cells (Figure 6.2B). Taken together, these findings confirmed that proteasome rather than lysosome was responsible for the elimination of iNOS.

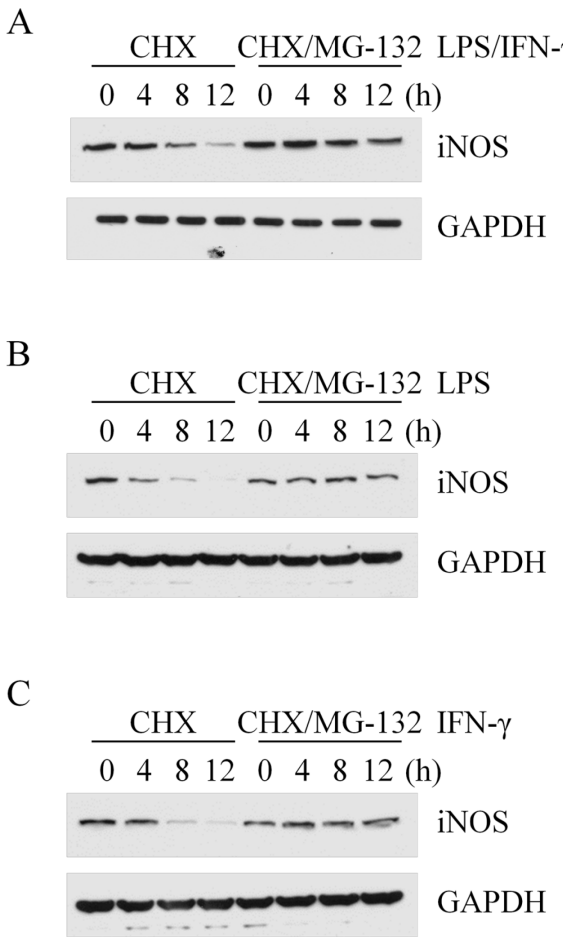

Figure 6.1 Proteasome was responsible for the degradation of iNOS induced in RAW264.7 cells.
iNOS was induced in RAW264.7 cells by (A) a combination of LPS and IFN-γ, (B) LPS, or (C) IFN-γ. Inhibition of iNOS synthesis with CHX (100 μg/ml) resulted in iNOS degradation inside cells. The clearance of iNOS was blocked by proteasomal inhibitior MG-132 (50 μM). Representative blots shown from 3-5 experiments.

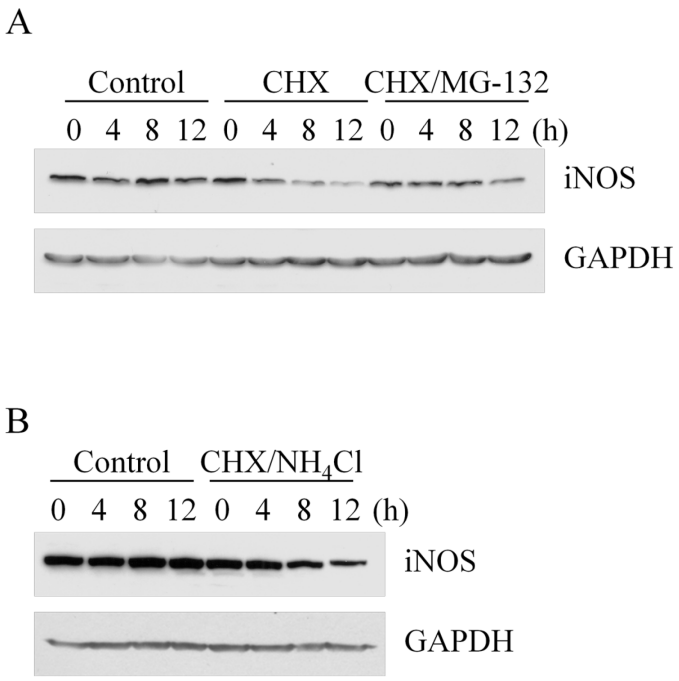

Figure 6.2 Proteasome but not lysosome played an essential role in iNOS turnover in COS-7 cells.
(A) iNOS was expressed in COS-7 cells. iNOS turnover in the presence of CHX was prevented by proteasome inhibitior MG-132 (50 μM). (B) Lysosomal inhibition with NH_4Cl (20 mM) failed to prevent iNOS degradation upon CHX treatment. Representative blots shown from 3-5 experiments.

6.3.2 N-terminal 1-100 amino acids are essential for iNOS degradation

To identify the possible region in iNOS where ubiquitination occurs, we generated a series of plasmids encoding truncated iNOS proteins ($iNOS_{1-600}$, $iNOS_{1-500}$, $iNOS_{1-400}$, $iNOS_{1-300}$, $iNOS_{1-200}$, and $iNOS_{1-100}$) and expressed them in COS-7 cells. The degradation processes of all these truncated iNOS mutants were monitored in the presence of CHX. As shown in Figure 6.3A-F, all truncated iNOS proteins with different lengths from $iNOS_{1-600}$ to $iNOS_{1-100}$ degraded upon CHX treatment, and such degradations were prevented by MG-132 of no exception. These findings indicated that

iNOS turnover was mediated by the N-terminal 100 amino acids (AAs). To further validate our finding, we constructed a truncated iNOS mutant lacking the N-terminal 97 AAs ($iNOS_{98-1144}$) and expressed it in COS-7 cells. The deletion of N-terminal 97 AAs prevented the degradation of $iNOS_{98-1144}$ in the presence of CHX (Figure 6.4A, B). Consistent with the observation that protein levels of $iNOS_{98-1144}$ remained stable upon CHX treatment, the ubiquitination level of $iNOS_{98-1144}$ was also dramatically decreased as compared with that of wild-type iNOS (Figure 6.4C). These data suggested that the N-terminal 100 AA segment of iNOS was the likely region where ubiquitination occured.

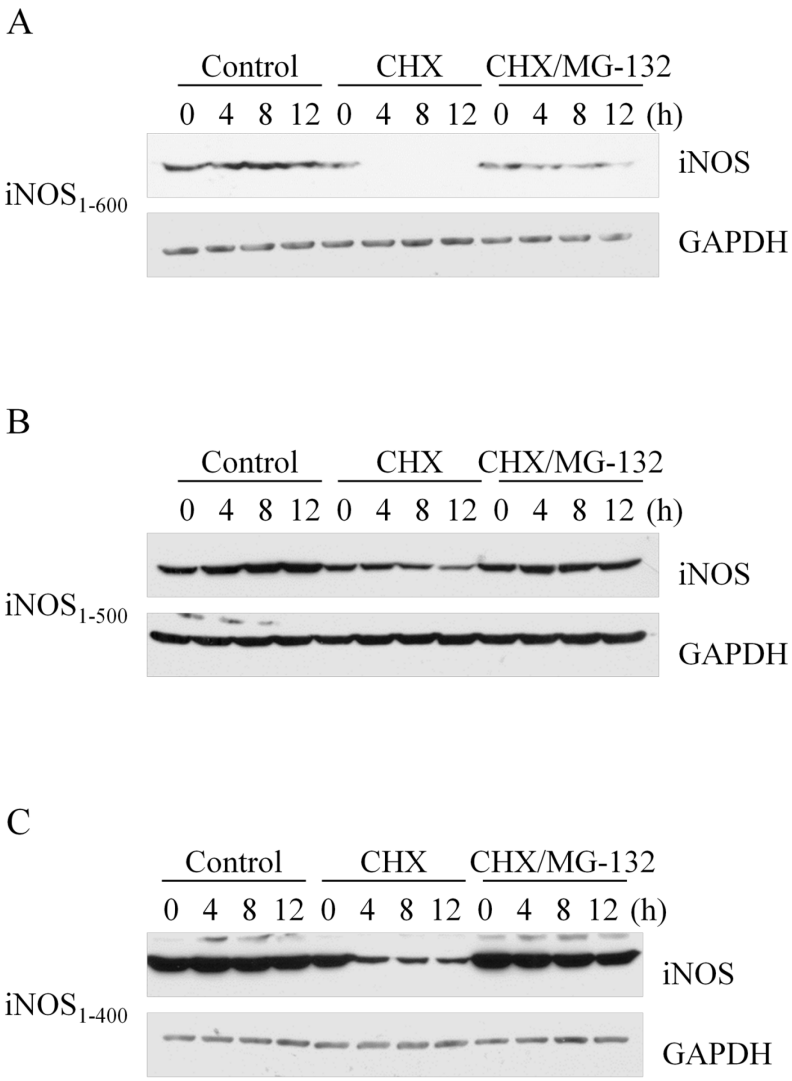

Continued

Figure 6.3 The N-terminal 100 amino acids of iNOS were crucial for iNOS degradation mediated by proteasome.

A series of plasmids encoding truncated iNOS proteins of different lengths including (A) $iNOS_{1-600}$, (B) $iNOS_{1-500}$, (C) $iNOS_{1-400}$, (D) $iNOS_{1-300}$, (E) $iNOS_{1-200}$ and (F) $iNOS_{1-100}$, were expressed in COS-7 cells, respectively. All of these iNOS mutants underwent proteasomal degradation upon CHX treatment. Representative blots shown from 3-5 experiments.

Figure 6.3 continued

D

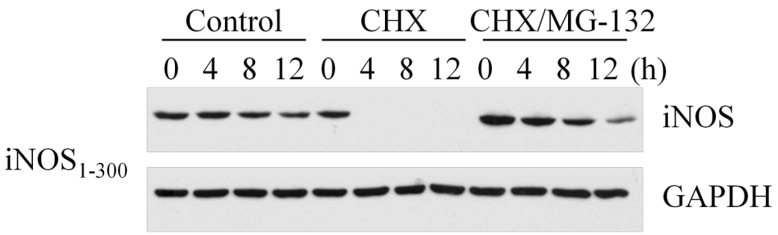

E

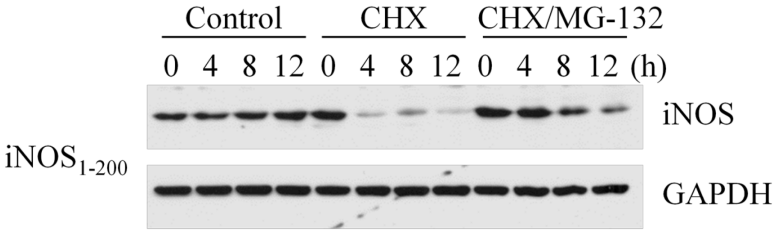

F

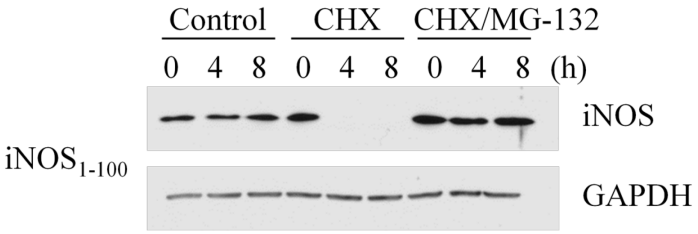

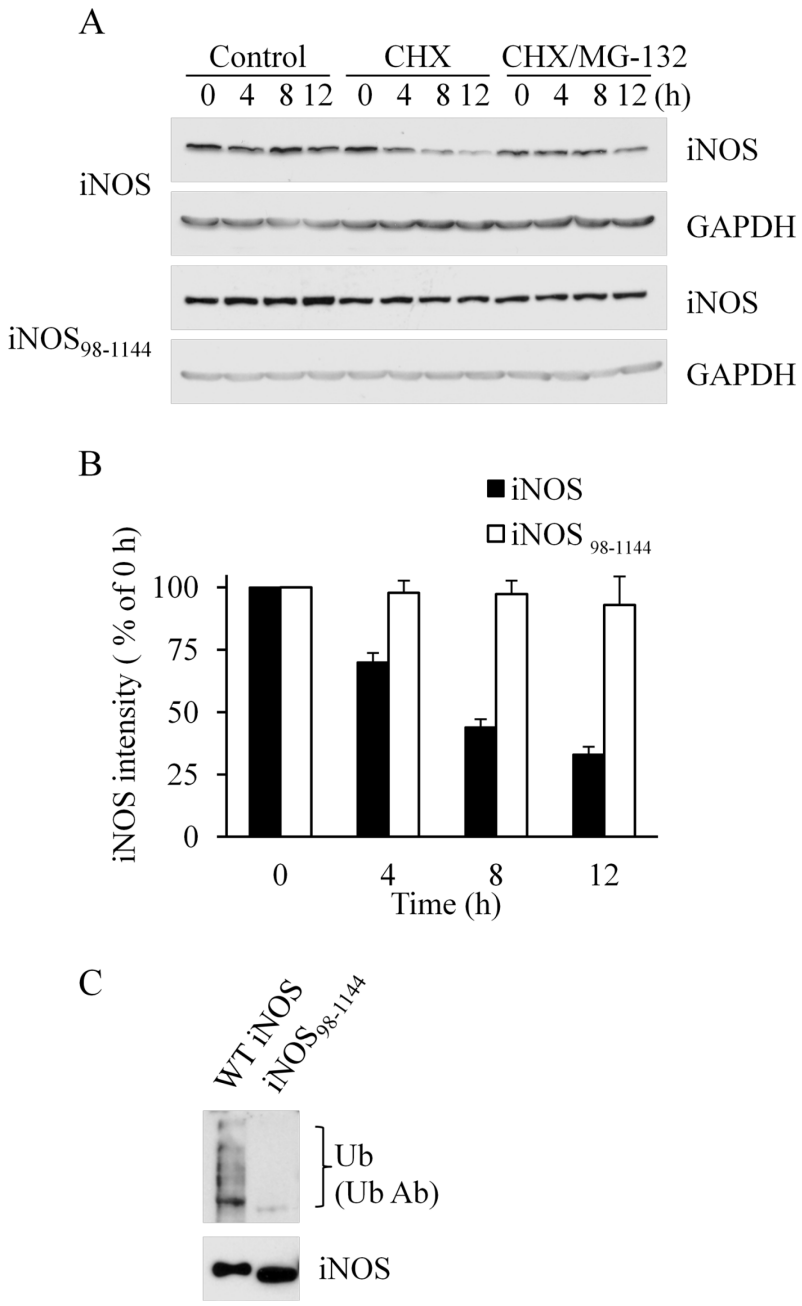

Figure 6.4 The N-terminal region (1-100 AAs) of iNOS was responsible for the ubiquitination and proteasomal degradation of iNOS.
(A) $iNOS_{98-1144}$ lacking the N-terminal 1-97 AAs was resistant to the degradation caused by CHX treatment. (B) Quantitative analyses of the degradation of wild-type iNOS and $iNOS_{98-1144}$ in the presence of CHX. Data are means ± SE, n = 5. (C) The ubiquitination levels of $iNOS_{98-1144}$ were largely reduced by deleting the N-terminal 1-97 AAs. Representative blots shown from triplicate experiments.

6.3.3 Substitution of all lysines among the N-terminal 1-100 AAs with arginines fails to prevent iNOS elimination

We then tried to identify the essential residues for covalent ubiquitin attachment. As ubiquitin is conventionally conjugated to lysine (K) residues (56, 158), the 11 lysines among the N-terminal 1-100 AA segment of iNOS are considered as potential sites for iNOS ubiquitination. Substitutions of all 11 lysines with arginines (R) were conducted and the resulting ($K0_{1\text{-}100}$) iNOS with null lysine residues among N-termial 100 AAs was subjected to proteasomal degradation. Interestingly, mutation of all K to R residues had little effect on the proteasomal degradation of ($K0_{1\text{-}100}$) iNOS (Figure 6.5 A, B). This result indicated that these lysine residues among the N-terminal region were not essential for iNOS degradation mediated by UPS.

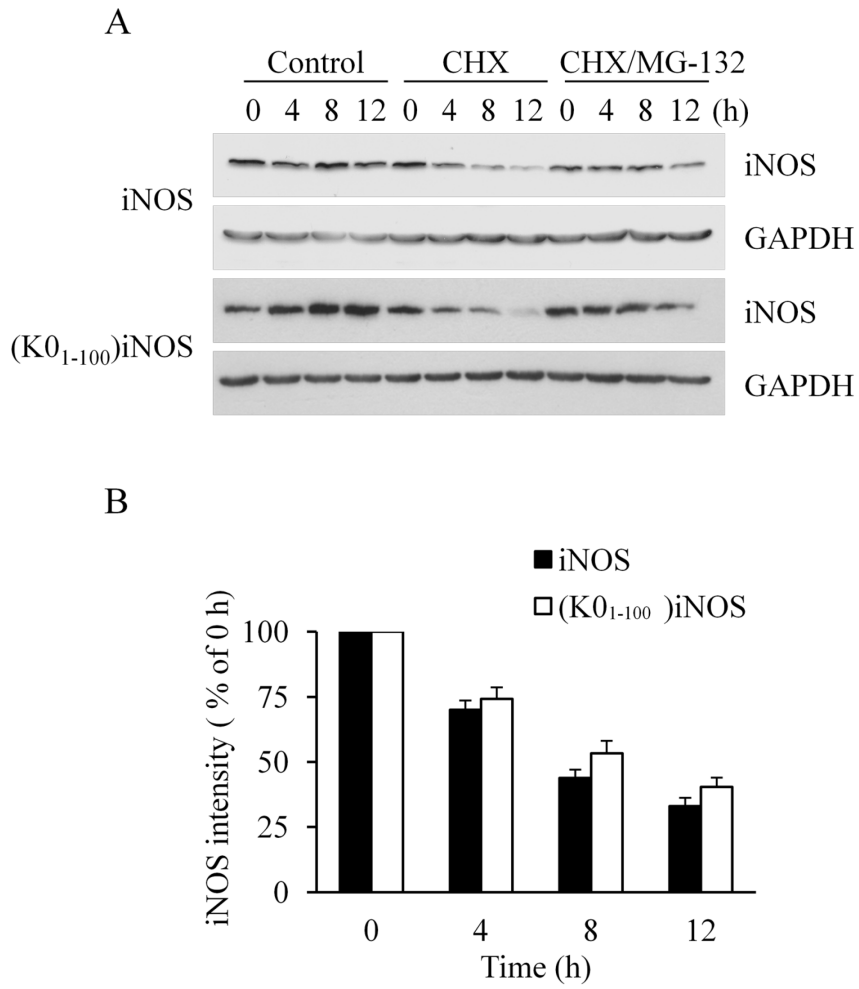

Figure 6.5 Lysine-to-arginine mutations among the N-terminal 100 AAs of iNOS failed to prevent its proteasomal degradation.
(A) (K0$_{1-100}$) iNOS containing null lysines among the N-terminal 1-100 AA region was generated via substitution of all the 11 lysines with arginines. The (K0$_{1-100}$) iNOS protein underwent proteasomal degradation upon CHX treatment. (B) Quantitative analyses of the degradation of wild-type iNOS and (K0$_{1-100}$) iNOS in the presence of CHX. Data are means ± SE, n = 5.

6.3.4 Further cysteine-to-alanine mutations decrease the degradation rate of iNOS but have little effect on its ubiquitination level

Although ubiquitin was normally thought to be conjugated to the lysine residues, recent studies reported cysteine (C) as possible site for ubiquitination (159, 160). Therefore, the 2 C residues among the N-terminal 1-100 AA region of iNOS were considered as possible ubiquitination sites. Cysteine-to-alanine (A) mutation was performed and the ($C0K0_{1\text{-}100}$) iNOS mutant was generated. As shown in Figure 6.6A and B, substitution of 2 C with A residues retarded the turnover of ($C0K0_{1\text{-}100}$) iNOS. However, ($C0K0_{1\text{-}100}$) iNOS exhibited a similar ubiquitination level as that of wild-type iNOS or previously constructed ($K0_{1\text{-}100}$) iNOS (Figure 6.6C). These data suggested that the two cysteine residues were involved in iNOS degradation but not responsible for ubiquitin attachment.

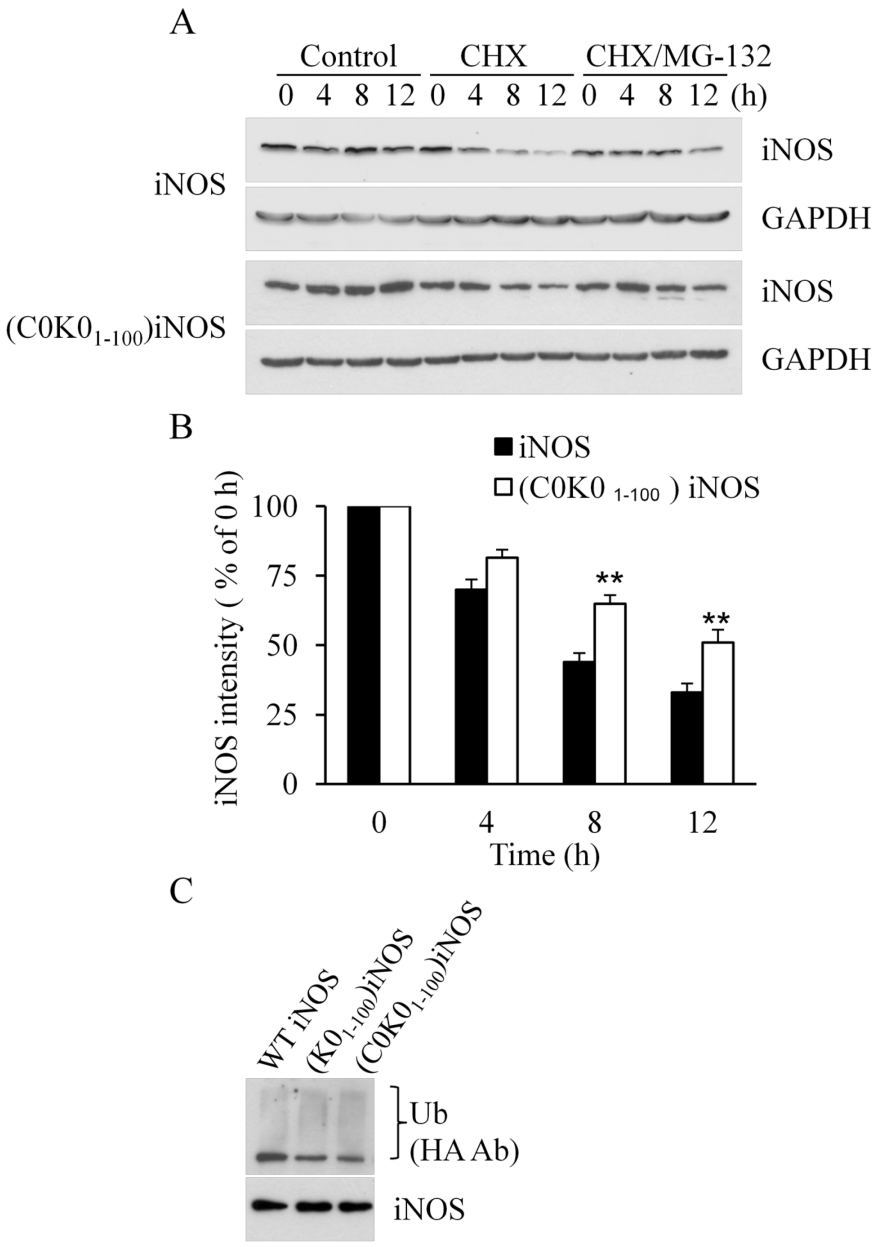

Figure 6.6 The essential role of 2 cysteines in the proteasomal degradation of iNOS. (A) The 2 cysteines in the N-terminal 1-100 AA region of iNOS were substituted with alanines, generating the (C0K0$_{1-100}$) iNOS. Cysteine-to-alanine mutations markedly prevented iNOS turnover in CHX-treated cells. (B) Quantitative analyses of wild-type and (C0K0$_{1-100}$) iNOS turnover in the presence of CHX. Data are means ± SE, ** $P <$ 0.05 vs. iNOS, n = 4-5. (C) The ubiquitination levels of wild-type, (K0$_{1-100}$) and (C0K0$_{1-100}$) iNOS appeared to be indistinguishable. Representative blots shown from triplicate experiments.

6.3.5 Residues among 25-49 AA of iNOS are essential for iNOS degradation

To determine the key residues among the N-terminal 1-100 AAs for iNOS ubiquitination, we constructed plasmids encoding $iNOS_{25\text{-}1144}$, $iNOS_{50\text{-}1144}$, and $iNOS_{75\text{-}1144}$ to further narrow down the essential region mediating iNOS turnover. As shown in Figure 6.7A, deleting 1-24 AAs exhibited certain protective effect on the degradation of $iNOS_{25\text{-}1144}$. Removal of additional 25 AAs (25-49 AAs) remarkably retarded $iNOS_{50\text{-}1144}$ turnover (Figure 6.7B). Deletion of another 25 AAs (50-74 AAs) had no further protective effect on the clearance of $iNOS_{75\text{-}1144}$ as compared with that of $iNOS_{50\text{-}1144}$ (Figure 6.7C). The comparisons of the degradation curves of these truncated iNOS mutants in Figure 6.7D strongly indicated that the region containing 25-49 AAs on iNOS was essential for its degradation.

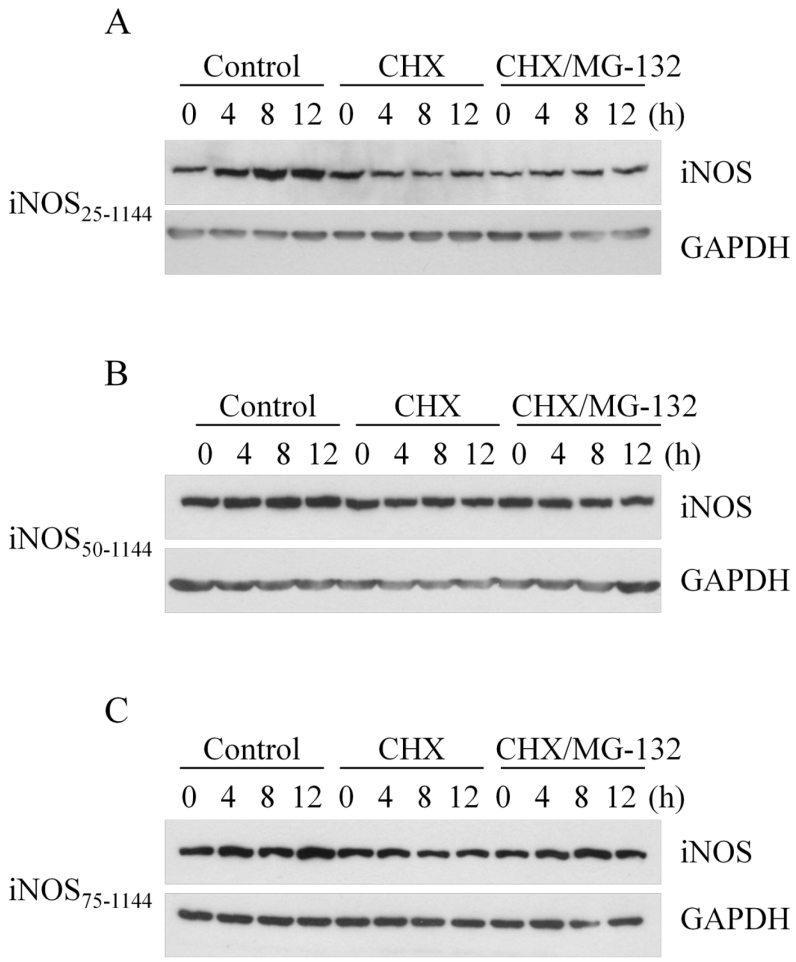

Continued

Figure 6.7 The 25-49 AAs on iNOS were crucial for iNOS proteasomal turnover. The protein levels of (A) $iNOS_{25-1144}$, (B) $iNOS_{50-1144}$ and (C) $iNOS_{75-1144}$ were monitored inside COS-7 cells in the presence of CHX, respectively. Deleting 25-49 AAs from iNOS significantly prevented its degradation. (D) Quantitative analyses of $iNOS_{25-1144}$, $iNOS_{50-1144}$ and $iNOS_{75-1144}$ turnover in the presence of CHX. Data are means ± SE, n = 4-5.

Figure 6.7 continued

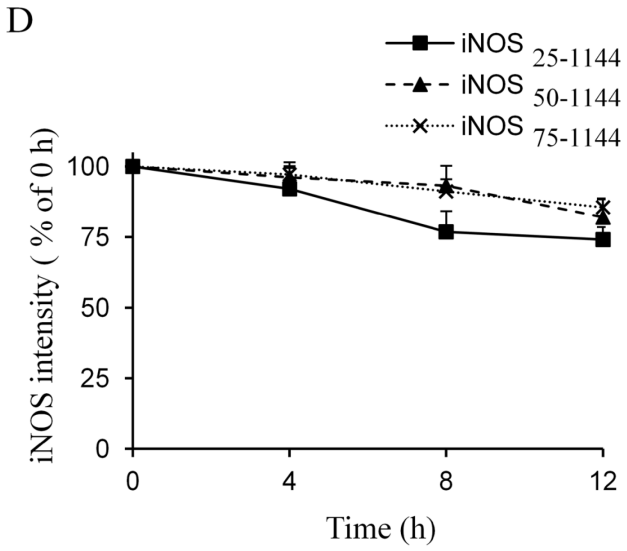

6.3.6 Mutations of serine/threonine (T31, S37, T39 and S46) to alanine significantly prevent iNOS degradation and reduce its ubiquitination level

Besides cysteine, serine (S) and threonine (T) residues were also reported to be alternative sites for ubiquitination in recent studies (161). After replacing all the K and C residues among iNOS 1-100 AA region, further mutations of serine/threonine to alanine were conducted to identify the ubiquitination site on iNOS. Degradations of truncated iNOS, including $iNOS_{25\text{-}1144}$, $iNOS_{50\text{-}1144}$, and $iNOS_{75\text{-}1144}$, suggested the 25-49 AA segment on iNOS a possible region responsible for iNOS proteasomal turnover. Thus we replaced all serine/threonine (T31, S37, T39 and S46) with alanine residues within this region and subjected the resulting ($C0K0_{1\text{-}100}S0T0_{25\text{-}50}$) iNOS mutant to proteasomal

degradation in COS-7 cells. Alanine replacement of these S/T residues remarkably prevented iNOS turnover in CHX-treated cells (Figure 6.8A, B). Corresponding to its reduced degradation rate, the ubiquitination levels of ($C0K0_{1\text{-}100}S0T0_{25\text{-}50}$) iNOS were also largely reduced as compared with that of wild-type (WT) or ($K0_{1\text{-}100}$) iNOS (Figure 6.8C). In fact, the ubiquitination level of ($C0K0_{1\text{-}100}S0T0_{25\text{-}50}$) iNOS was observed to be similar to that of $iNOS_{98\text{-}1144}$, whose protein level remained stable in the presence of CHX. These data strongly indicated that these four residues (T31, S37, T39 and S46) on iNOS were essential for the proteasomal degradation of iNOS. The contribution of individual residue in iNOS degradation remains to be explored in future studies.

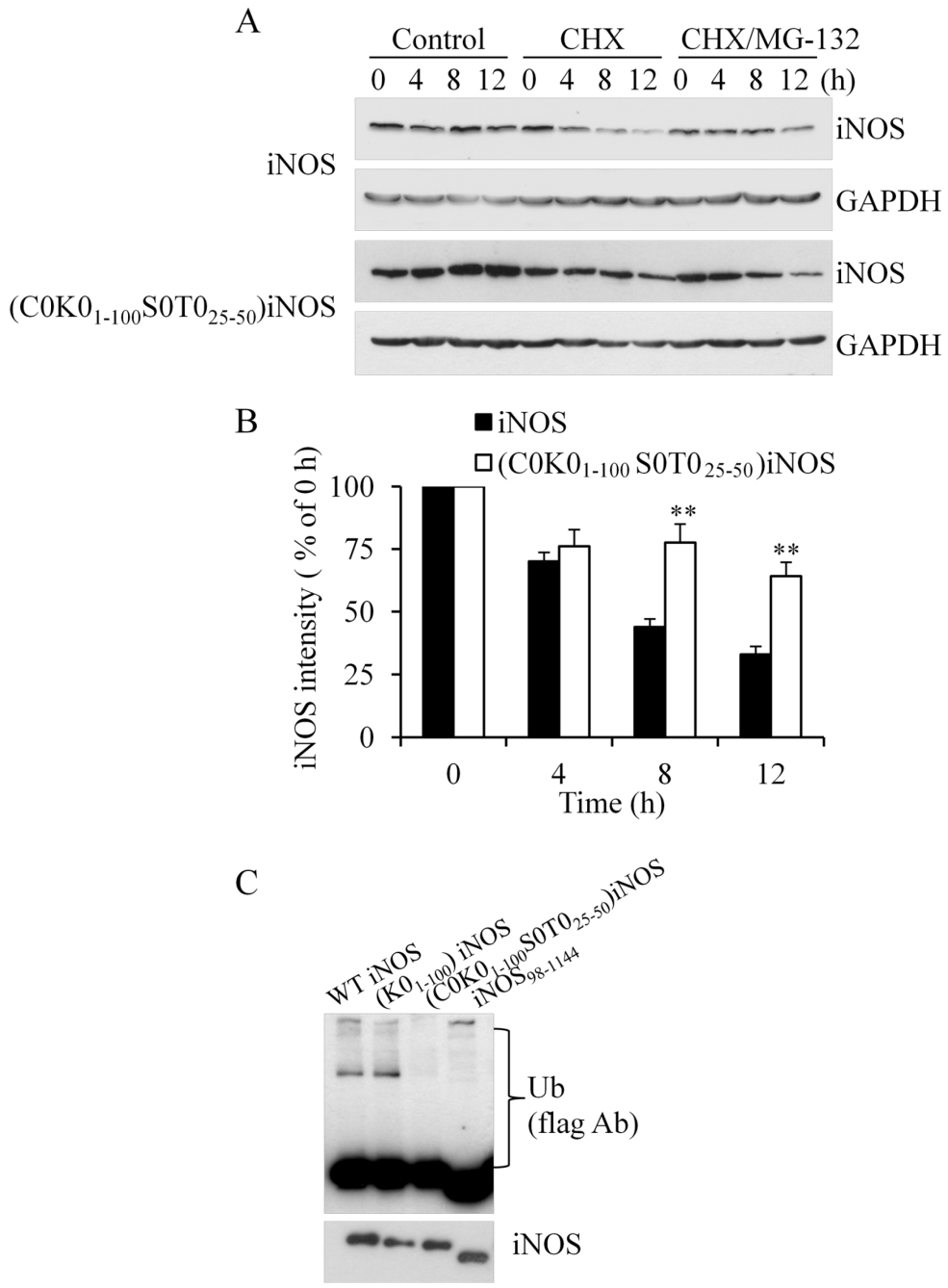

Figure 6.8 T31, S37, T39 and S46 residues on iNOS were essential for its proteasomal degradation.

(A) Alanine replacement of T31, S37, T39 and S46 on iNOS markedly prevented its degradation. (B) Quantitative analyses of wild-type and (C0K0$_{1-100}$S0T0$_{25-50}$) iNOS elimination in the presence of CHX. Data are means ± SE, ** P <0.05 vs. iNOS, n = 4-5. (C) The ubiquitination level of iNOS was remarkably reduced via substitution of T31, S37, T39 and S46 with alanines.

6.4 Discussion

The key finding of this study is that unlike the conventional lysine residues, four serine/threonine residues, including T31, S37, T39 and S46, play a crucial role in the ubiquitination and proteasomal degradation of iNOS. Previous studies reported that iNOS degradation is mediated by proteasome (61). However, whether autophagy-lysosome also plays a role in the degradation process of iNOS is unknown. Here we confirmed that proteasome but not lysosome is responsible for iNOS turnover. Although it has been long recognized that ubiquitination of iNOS is required for subsequent proteasomal degradation, the ubiquitination sites on iNOS remain to be identified. Our present study revealed that the N-terminal 1-100 AA region of iNOS is essential for its ubiquitination and proteasomal degradation. Although ubiquitin is usually linked to the lysine residues, our results showed that none of the lysine residues among the N-terminal 1-100 AAs of iNOS was responsible for ubiquitin chain attachment. Further mutations of cysteine to alanine residues lightly protected the degradation of resulting ($C0K0_{1\text{-}100}$) iNOS, but failed to reduce the ubiquitination level of the same iNOS mutant. Further studies narrowed the region essential for proteasomal degradation of iNOS down to 25-50 AAs on iNOS. Moreover, alanine replacements of all the serine/threonine residues among this region led to significantly decreased degradation rate of ($C0K0_{1\text{-}100}S0T0_{25\text{-}50}$) iNOS. The ubiquitination level of ($C0K0_{1\text{-}100}S0T0_{25\text{-}50}$) iNOS was also markedly reduced as compared with that of wild-type iNOS or ($K0_{1\text{-}100}$) iNOS. However, these serine/threonine-to-alanine mutations were conducted based on the previously constructed ($C0K0_{1\text{-}100}$) iNOS mutant. It remained unknown whether or not those mutated

K and C residues also contributed to the protection of iNOS against proteasomal degradation. Furthermore, whether the four AAs (T31, S37, T39 and S46) act in combination to mediate iNOS turnover remains to be explored. Moreover, the pivotal residues among these AAs responsible for ubiquitin conjugation have not yet been identified. Nevertheless, the discovery of the four essential AAs (T31, S37, T39 and S46) involved in iNOS ubiquitination and subsequent proteasomal degradation partially revealed the long-sought iNOS ubiquitination sites responsible for its degradation via UPS.

CHAPTER 7

7 Summary and future work

NO synthesized by iNOS plays multifaceted roles in various physiological and pathological processes. On one hand, NO is essential for immune system. On the other hand, overproduced NO is associated with cell injury in various diseases, such as Alzheimer's disease, asthma, stroke, arthritis and septic shock. Thus understanding the molecular mechanism of iNOS expression and turnover is crucial for developing novel therapeutic strategies for the diseases associated with iNOS activity. This study supplements the understanding of this important enzyme at three logically interrelated levels: protein expression, stability control and degradation.

In Chapter 2, we revealed the novel role of CaM in iNOS expression. CaM has always been thought as an enzyme cofactor of iNOS. Our studies, however, changed this doctrine by demonstrating CaM as an essential component in iNOS gene transcription in cell culture and sepsis. Further studies uncovered a master control mechanism that governs both NF-κB and STAT1 pathways during iNOS induction. CaMKII has been identified as the downstream target of CaM, and an upstream kinase of both NF-κB and STAT1 signaling cascades. We also unexpectedly discovered that intracellular Ca^{2+} flux, although not required for iNOS function, was indispensable for the activation of upstream

CaMKII and subsequent signaling transduction via NF-κB and STAT1 pathways leading to iNOS induction. Finally, our studies showed that CaM inhibition led to blockage of iNOS expression in endotoxemic mice. As a consequence of attenuated iNOS levels, the survival rates of endotoxemic mice were significantly enhanced upon CaM inhibition. One CaM inhibitor trifluoperazine applied in this study is a clinically used medicine and thus the trial on its effectiveness in treating septic patients is immediately pursuable. However, disappointing results were obtained from cecal ligation and puncture model. Contrary to the protective effects on endotoxemia model, trifluoperazine failed to decrease the mortality rates of mice in either moderate or severe grade CLP models. We attempted to administrate trifluoperazine via different routes such as oral and intraperitoneal to enhance its effect, but the mortality rates of mice remained unimproved. Some studies reported improved therapeutic effect of CLP-treated mice when certain treatment was applied in combination with antibiotics. Thus future studies will reexamine the effect of trifluoperazine on CLP-treated mice with combined antibiotic administration.

Once expressed, iNOS function depends on the status of its protein stability, which is studied in detail in Chapter 3-5. In Chapter 3, we elucidated the key role of CaM in maintaining iNOS protein stability. CaM inhibition led to the dissociation of CaM from iNOS and subsequent iNOS aggregation. Further studies demonstrated that the aggregates formation of iNOS was mediated via its hydrophobic CaM-binding domain. In future work the CaM-binding domain will be further characterized. The essential residues as well as the minimal residue requirement for iNOS aggregation will be identified. In

addition, the molecular property of iNOS aggregates and the kinetics of iNOS aggregation upon CaM inhibition will also be investigated in future studies. Taken together, Chapter 2 and 3 discovered the essential role of CaM to serve as iNOS induction modulator as well as iNOS protein stabilizer, in addition to its previously known function as catalytic assistant.

In Chapter 4, we demonstrated the role of gaseous NO molecule in regulating iNOS protein stability under physiological conditions. Our data suggested that long term exposure to massive NO led to iNOS aggregation and deactivation. Inhibition of NO production from iNOS remarkably prevented iNOS aggregates formation. Further studies indicated that such NO-mediated aggregation is specific to iNOS but not eNOS or nNOS, suggesting an iNOS-specific feedback regulation by self-derived NO. Future work will focus on elucidating the mechanism underlying such feedback regulation, especially on revealing the cysteine residues responsible for nitrosylation as a result of NO exposure.

After investigation on physiological iNOS aggregation mediated by NO, we then explored iNOS stability under pathological conditions upon Hsp90 inhibition. In Chapter 5, we identified Hsp90 as a crucial modulator of iNOS protein stability. Our data clearly indicated that inhibition of Hsp90 rendered iNOS aggregation and subsequent degradation. Proteasome rather than lysosome is responsible for the turnover process. Previous studies reported the involvement of CHIP as an essential E3 ligase in iNOS degradation under physiological circumstance. However, our study showed that depleting CHIP had no effect on aggregated iNOS elimination in Hsp90-inhibited cells, suggesting the possibility of another E3 ligase responsible for the turnover process of iNOS in

abnormal condition. Further studies identified SPSB2 as the E3 ligase adapter protein for iNOS ubiquitination through the UPS pathway. Hence besides our previously discovered roles of Hsp90 in modulating iNOS gene transcription and protein activity, our studies further extended the function of Hsp90 to iNOS protein stabilizer. Taken together, our studies provided a comprehensive understanding of the function of Hsp90 in iNOS biochemistry. In conclusion, Chapter 3-5 identified the roles of CaM, iNOS-synthesized NO and Hsp90 in regulating iNOS protein stability. The discovery of these iNOS protein stability modulators offered possible targets for intervening iNOS protein activity.

Finally, to gain a complete understanding on iNOS regulation, we characterized the degradation process of iNOS proteins under physiological conditions in Chapter 6. The role of ubiquitin-proteasome system but not lysosome in iNOS turnover was confirmed. Our data also identified four pivotal non-lysine residues (T31, S37, T39 and S46) responsible for covalent ubiquitin attachment. Corresponding to their roles in ubiquitination, these residues were also demonstrated to be essential for proteasomal degradation of iNOS. Thus our studies identified iNOS as an example for atypical ubiquitination occurring on non-lysine residues. However, the key residues among these four AAs responsible for proteasomal degradation of iNOS remain to be further investigated in future work.

In summary, our investigations in this study revealed ample new information on the life cycle of iNOS, as well as its implications in diseases. The identification of CaM as an essential regulator in iNOS induction and protein stability will fundamentally change the view on the role of CaM in iNOS biochemistry. iNOS-derived NO has been

showed to mediate iNOS aggregation and deactivation, revealing the long-sought mechanism underlying the feedback inhibition of iNOS. Furthermore, the discovery of Hsp90 as iNOS protein stabilizer renewed our understanding of Hsp90 as a modulator of iNOS gene transactivation and protein activity. Moreover, studies characterizing normal iNOS degradation process, together with those on iNOS aggregates turnover, provided comprehensive understanding of iNOS protein clearance under both physiological and pathological circumstances. Taken together, imformation gained from these studies suggest new approaches to modulate NO production from iNOS by regulating iNOS levels via protein induction, stability and degradation.

References

1. Naseem, K.M., and Roberts, W. (2011) Nitric oxide at a glance. *Platelets.* **22,** 148-152

2. Rosselli, M., Keller, P.J., and Dubey, R.K. (1998) Role of nitric oxide in the biology, physiology and pathophysiology of reproduction. *Hum.Reprod.Update.* **4,** 3-24

3. Pellegrino, D., and Parisella, M.L. (2010) Nitrite as a physiological source of nitric oxide and a signalling molecule in the regulation of the cardiovascular system in both mammalian and non-mammalian vertebrates. *Recent Pat Cardiovasc Drug Discov.* **5,** 91-96

4. Naseem, K.M. (2005) The role of nitric oxide in cardiovascular diseases. *Mol.Aspects Med.* **26,** 33-65

5. Vincent, S.R. (2010) Nitric oxide neurons and neurotransmission. *Prog.Neurobiol.* **90,** 246-255

6. Yun, H.Y., Dawson, V.L., and Dawson, T.M. (1997) Nitric oxide in health and disease of the nervous system. *Mol.Psychiatry.* **2,** 300-310

7. Lowenstein, C.J., and Snyder, S.H. (1992) Nitric oxide, a novel biologic messenger. *Cell.* **70,** 705-707

8. MacMicking, J., Xie, Q.W., and Nathan, C. (1997) Nitric oxide and macrophage function. *Annu.Rev.Immunol.* **15,** 323-350

9. Laskin, J.D., Heck, D.E., and Laskin, D.L. (1994) Multifunctional role of nitric oxide in inflammation. *Trends Endocrinol.Metab.* **5,** 377-382

10. Kirkeboen, K.A., and Strand, O.A. (1999) The role of nitric oxide in sepsis--an overview. *Acta Anaesthesiol.Scand.* **43,** 275-288

11. Szabo, C. (1998) Role of nitric oxide in endotoxic shock. An overview of recent advances. *Ann.N.Y.Acad.Sci.* **851,** 422-425

12. Champion, H.C., Skaf, M.W., and Hare, J.M. (2003) Role of nitric oxide in the pathophysiology of heart failure. *Heart Fail.Rev.* **8,** 35-46

13. Kojda, G., and Kottenberg, K. (1999) Regulation of basal myocardial function by NO. *Cardiovasc.Res.* **41,** 514-523

14. Nathan, C. (1992) Nitric oxide as a secretory product of mammalian cells. *FASEB J.* **6,** 3051-3064

15. Alderton, W.K., Cooper, C.E., and Knowles, R.G. (2001) Nitric oxide synthases: structure, function and inhibition. *Biochem.J.* **357,** 593-615

16. Xie, Q.W., Cho, H., Kashiwabara, Y., Baum, M., Weidner, J.R., Elliston, K., Mumford, R., and Nathan, C. (1994) Carboxyl terminus of inducible nitric oxide synthase. Contribution to NADPH binding and enzymatic activity. *J.Biol.Chem.* **269,** 28500-28505

17. Li, H., and Poulos, T.L. (2005) Structure-function studies on nitric oxide synthases. *J.Inorg.Biochem.* **99,** 293-305

18. Griffith, O.W., and Stuehr, D.J. (1995) Nitric oxide synthases: properties and catalytic mechanism. *Annu.Rev.Physiol.* **57,** 707-736

19. Vasquez-Vivar, J., Kalyanaraman, B., Martasek, P., Hogg, N., Masters, B.S., Karoui, H., Tordo, P., and Pritchard, K.A.,Jr (1998) Superoxide generation by endothelial nitric oxide synthase: the influence of cofactors. *Proc.Natl.Acad.Sci.U.S.A.* **95,** 9220-9225

20. Hillier, B.J., Christopherson, K.S., Prehoda, K.E., Bredt, D.S., and Lim, W.A. (1999) Unexpected modes of PDZ domain scaffolding revealed by structure of nNOS-syntrophin complex. *Science.* **284,** 812-815

21. Harris, B.Z., and Lim, W.A. (2001) Mechanism and role of PDZ domains in signaling complex assembly. *J.Cell.Sci.* **114,** 3219-3231

22. Salerno, J.C., Harris, D.E., Irizarry, K., Patel, B., Morales, A.J., Smith, S.M., Martasek, P., Roman, L.J., Masters, B.S., Jones, C.L., Weissman, B.A., Lane, P., Liu, Q., and Gross, S.S. (1997) An autoinhibitory control element defines calcium-regulated isoforms of nitric oxide synthase. *J.Biol.Chem.* **272,** 29769-29777

23. Lane, P., and Gross, S.S. (2002) Disabling a C-terminal autoinhibitory control element in endothelial nitric-oxide synthase by phosphorylation provides a molecular explanation for activation of vascular NO synthesis by diverse physiological stimuli. *J.Biol.Chem.* **277,** 19087-19094

24. Dudzinski, D.M., and Michel, T. (2007) Life history of eNOS: partners and pathways. *Cardiovasc.Res.* **75,** 247-260

25. Jaffrey, S.R., and Snyder, S.H. (1995) Nitric oxide: a neural messenger. *Annu.Rev.Cell Dev.Biol.* **11,** 417-440

26. Sase, K., and Michel, T. (1997) Expression and regulation of endothelial nitric oxide synthase. *Trends Cardiovasc.Med.* **7,** 28-37

27. Abu-Soud, H.M., and Stuehr, D.J. (1993) Nitric oxide synthases reveal a role for calmodulin in controlling electron transfer. *Proc.Natl.Acad.Sci.U.S.A.* **90,** 10769-10772

28. Gorren, A.C., and Mayer, B. (1998) The versatile and complex enzymology of nitric oxide synthase. *Biochemistry (Mosc).* **63,** 734-743

29. Hook, S.S., and Means, A.R. (2001) Ca(2+)/CaM-dependent kinases: from activation to function. *Annu.Rev.Pharmacol.Toxicol.* **41,** 471-505

30. Sha, Y., Pandit, L., Zeng, S., and Eissa, N.T. (2009) A critical role for CHIP in the aggresome pathway. *Mol.Cell.Biol.* **29,** 116-128

31. Marechal, A., Mattioli, T.A., Stuehr, D.J., and Santolini, J. (2010) NO synthase isoforms specifically modify peroxynitrite reactivity. *FEBS J.* **277,** 3963-3973

32. Togo, T., Katsuse, O., and Iseki, E. (2004) Nitric oxide pathways in Alzheimer's disease and other neurodegenerative dementias. *Neurol.Res.* **26,** 563-566

33. Ashutosh, K. (2000) Nitric oxide and asthma: a review. *Curr.Opin.Pulm.Med.* **6,** 21-25

34. Vincent, J.L., Zhang, H., Szabo, C., and Preiser, J.C. (2000) Effects of nitric oxide in septic shock. *Am.J.Respir.Crit.Care Med.* **161,** 1781-1785

35. Hotchkiss, R.S., and Karl, I.E. (2003) The pathophysiology and treatment of sepsis. *N.Engl.J.Med.* **348,** 138-150

36. Spiel, A.O., and Mayr, F.B. (2006) NO-synthase inhibition in sepsis. *Thromb.Haemost.* **95,** 591-592

37. Tunctan, B., Uludag, O., Altug, S., and Abacioglu, N. (1998) Effects of nitric oxide synthase inhibition in lipopolysaccharide-induced sepsis in mice. *Pharmacol.Res.* **38,** 405-411

38. Strunk, V., Hahnenkamp, K., Schneuing, M., Fischer, L.G., and Rich, G.F. (2001) Selective iNOS inhibition prevents hypotension in septic rats while preserving endothelium-dependent vasodilation. *Anesth.Analg.* **92,** 681-687

39. Heemskerk, S., Masereeuw, R., Russel, F.G.M., and Pickkers, P. (2009) Selective iNOS inhibition for the treatment of sepsis-induced acute kidney injury. *Nat Rev Nephrol.* **5,** 629-640

40. Cobb, J.P., Hotchkiss, R.S., Swanson, P.E., Chang, K., Qiu, Y., Laubach, V.E., Karl, I.E., and Buchman, T.G. (1999) Inducible nitric oxide synthase (iNOS) gene deficiency increases the mortality of sepsis in mice. *Surgery.* **126,** 438-442

41. Laubach, V.E., Shesely, E.G., Smithies, O., and Sherman, P.A. (1995) Mice lacking inducible nitric oxide synthase are not resistant to lipopolysaccharide-induced death. *Proc.Natl.Acad.Sci.U.S.A.* **92,** 10688-10692

42. Lopez, A., Lorente, J.A., Steingrub, J., Bakker, J., McLuckie, A., Willatts, S., Brockway, M., Anzueto, A., Holzapfel, L., Breen, D., Silverman, M.S., Takala, J., Donaldson, J., Arneson, C., Grove, G., Grossman, S., and Grover, R. (2004) Multiple-center, randomized, placebo-controlled, double-blind study of the nitric oxide synthase inhibitor 546C88: effect on survival in patients with septic shock. *Crit.Care Med.* **32,** 21-30

43. Riedemann, N.C., Guo, R., and Ward, P.A. (2003) Novel strategies for the treatment of sepsis. *Nat.Med.* **9,** 517-524

44. Ando, H., Takamura, T., Ota, T., Nagai, Y., and Kobayashi, K. (2000) Cerivastatin improves survival of mice with lipopolysaccharide-induced sepsis. *J.Pharmacol.Exp.Ther.* **294,** 1043-1046

45. Anel, R., and Kumar, A. (2005) Human endotoxemia and human sepsis: limits to the model. *Crit.Care.* **9,** 151-152

46. Rittirsch, D., Huber-Lang, M.S., Flierl, M.A., and Ward, P.A. (2009) Immunodesign of experimental sepsis by cecal ligation and puncture. *Nat Protoc.* **4,** 31-36

47. Ceponis, P.J.M., Riff, J.D., and Sherman, P.M. (2005) Epithelial cell signaling responses to enterohemorrhagic Escherichia coli infection. *Mem.Inst.Oswaldo Cruz.* **100 Suppl 1,** 199-203

48. Chan, E.D., Morris, K.R., Belisle, J.T., Hill, P., Remigio, L.K., Brennan, P.J., and Riches, D.W. (2001) Induction of inducible nitric oxide synthase-NO* by lipoarabinomannan of Mycobacterium tuberculosis is mediated by MEK1-ERK, MKK7-JNK, and NF-kappaB signaling pathways. *Infect.Immun.* **69,** 2001-2010

49. Schroder, K., Hertzog, P.J., Ravasi, T., and Hume, D.A. (2004) Interferon-gamma: an overview of signals, mechanisms and functions. *J.Leukoc.Biol.* **75,** 163-189

50. Delgado, M. (2003) Inhibition of interferon (IFN) gamma-induced Jak-STAT1 activation in microglia by vasoactive intestinal peptide: inhibitory effect on CD40, IFN-induced protein-10, and inducible nitric-oxide synthase expression. *J.Biol.Chem.* **278,** 27620-27629

51. Stempelj, M., Kedinger, M., Augenlicht, L., and Klampfer, L. (2007) Essential role of the JAK/STAT1 signaling pathway in the expression of inducible nitric-oxide synthase in intestinal epithelial cells and its regulation by butyrate. *J.Biol.Chem.* **282,** 9797-9804

52. Markossian, K.A., Zamyatnin, A.A., and Kurganov, B.I. (2004) Antibacterial proline-rich oligopeptides and their target proteins. *Biochemistry Mosc.* **69,** 1082-1091

53. Kopito, R.R. (2000) Aggresomes, inclusion bodies and protein aggregation. *Trends Cell Biol.* **10,** 524-530

54. Kolodziejska, K.E., Burns, A.R., Moore, R.H., Stenoien, D.L., and Eissa, N.T. (2005) Regulation of inducible nitric oxide synthase by aggresome formation. *Proc.Natl.Acad.Sci.U.S.A.* **102,** 4854-4859

55. Pandit, L., Kolodziejska, K.E., Zeng, S., and Eissa, N.T. (2009) The physiologic aggresome mediates cellular inactivation of iNOS. *Proc.Natl.Acad.Sci.U.S.A.* **106,** 1211-1215

56. Tai, H., and Schuman, E.M. (2008) Ubiquitin, the proteasome and protein degradation in neuronal function and dysfunction. *Nat.Rev.Neurosci.* **9,** 826-838

57. Sassa, Y., Yamasaki, T., Horiuchi, M., Inoshima, Y., and Ishiguro, N. (2010) The effects of lysosomal and proteasomal inhibitors on abnormal forms of prion protein degradation in murine macrophages. *Microbiol.Immunol.* **54,** 763-768

58. Goldberg, A.L. (2003) Protein degradation and protection against misfolded or damaged proteins. *Nature.* **426,** 895-899

59. Passmore, L.A., and Barford, D. (2004) Getting into position: the catalytic mechanisms of protein ubiquitylation. *Biochem.J.* **379,** 513-525

60. Ravid, T., and Hochstrasser, M. (2008) Diversity of degradation signals in the ubiquitin-proteasome system. *Nat.Rev.Mol.Cell Biol.* **9,** 679-690

61. Musial, A., and Eissa, N.T. (2001) Inducible nitric-oxide synthase is regulated by the proteasome degradation pathway. *J.Biol.Chem.* **276,** 24268-24273

62. Kolodziejski, P.J., Musial, A., Koo, J., and Eissa, N.T. (2002) Ubiquitination of inducible nitric oxide synthase is required for its degradation. *Proc.Natl.Acad.Sci.U.S.A.* **99,** 12315-12320

63. Chen, L., Kong, X., Fu, J., Xu, Y., Fang, S., Hua, P., Luo, L., and Yin, Z. (2009) CHIP facilitates ubiquitination of inducible nitric oxide synthase and promotes its proteasomal degradation. *Cell.Immunol.* **258,** 38-43

64. Nishiya, T., Matsumoto, K., Maekawa, S., Kajita, E., Horinouchi, T., Fujimuro, M., Ogasawara, K., Uehara, T., and Miwa, S. (2011) Regulation of inducible nitric-oxide synthase by the SPRY domain- and SOCS box-containing proteins. *J.Biol.Chem.* **286,** 9009-9019

65. Kuang, Z., Lewis, R.S., Curtis, J.M., Zhan, Y., Saunders, B.M., Babon, J.J., Kolesnik, T.B., Low, A., Masters, S.L., Willson, T.A., Kedzierski, L., Yao, S., Handman, E., Norton, R.S., and Nicholson, S.E. (2010) The SPRY domain-containing SOCS box protein SPSB2 targets iNOS for proteasomal degradation. *J.Cell Biol.* **190,** 129-141

66. Ballinger, C.A., Connell, P., Wu, Y., Hu, Z., Thompson, L.J., Yin, L.Y., and Patterson, C. (1999) Identification of CHIP, a novel tetratricopeptide repeat-containing protein that interacts with heat shock proteins and negatively regulates chaperone functions. *Mol.Cell.Biol.* **19,** 4535-4545

67. Jiang, J., Ballinger, C.A., Wu, Y., Dai, Q., Cyr, D.M., Hohfeld, J., and Patterson, C. (2001) CHIP is a U-box-dependent E3 ubiquitin ligase: identification of Hsc70 as a target for ubiquitylation. *J.Biol.Chem.* **276,** 42938-42944

68. McDonough, H., and Patterson, C. (2003) CHIP: a link between the chaperone and proteasome systems. *Cell Stress Chaperones.* **8,** 303-308

69. Kamura, T., Sato, S., Haque, D., Liu, L., Kaelin, W.G.,Jr, Conaway, R.C., and Conaway, J.W. (1998) The Elongin BC complex interacts with the conserved SOCS-box motif present in members of the SOCS, ras, WD-40 repeat, and ankyrin repeat families. *Genes Dev.* **12,** 3872-3881

70. Kamura, T., Maenaka, K., Kotoshiba, S., Matsumoto, M., Kohda, D., Conaway, R.C., Conaway, J.W., and Nakayama, K.I. (2004) VHL-box and SOCS-box domains determine binding specificity for Cul2-Rbx1 and Cul5-Rbx2 modules of ubiquitin ligases. *Genes Dev.* **18,** 3055-3065

71. Kuang, Z., Yao, S., Xu, Y., Lewis, R.S., Low, A., Masters, S.L., Willson, T.A., Kolesnik, T.B., Nicholson, S.E., Garrett, T.J., and Norton, R.S. (2009) SPRY domain-containing SOCS box protein 2: crystal structure and residues critical for protein binding. *J.Mol.Biol.* **386,** 662-674

72. Woo, J.S., Suh, H.Y., Park, S.Y., and Oh, B.H. (2006) Structural basis for protein recognition by B30.2/SPRY domains. *Mol.Cell.* **24,** 967-976

73. Rajawat, Y.S., Hilioti, Z., and Bossis, I. (2009) Aging: central role for autophagy and the lysosomal degradative system. *Ageing Res Rev.* **8,** 199-213

74. Butler, D., and Bahr, B.A. (2006) Oxidative stress and lysosomes: CNS-related consequences and implications for lysosomal enhancement strategies and induction of autophagy. *Antioxid.Redox Signal.* **8,** 185-196

75. Marques, C., Pereira, P., Taylor, A., Liang, J.N., Reddy, V.N., Szweda, L.I., and Shang, F. (2004) Ubiquitin-dependent lysosomal degradation of the HNE-modified proteins in lens epithelial cells. *FASEB J.* **18,** 1424-1426

76. Schmidt, H.H., Pollock, J.S., Nakane, M., Forstermann, U., and Murad, F. (1992) Ca2+/calmodulin-regulated nitric oxide synthases. *Cell Calcium.* **13,** 427-434

77. Lee, S.J., and Stull, J.T. (1998) Calmodulin-dependent regulation of inducible and neuronal nitric-oxide synthase. *J.Biol.Chem.* **273,** 27430-27437

78. Feng, C. (2012) Mechanism of Nitric Oxide Synthase Regulation: Electron Transfer and Interdomain Interactions. *Coord.Chem.Rev.* **256,** 393-411

79. Klee, C.B., Crouch, T.H., and Richman, P.G. (1980) Calmodulin. *Annu.Rev.Biochem.* **49,** 489-515

80. Kuboniwa, H., Tjandra, N., Grzesiek, S., Ren, H., Klee, C.B., and Bax, A. (1995) Solution structure of calcium-free calmodulin. *Nat.Struct.Biol.* **2,** 768-776

81. Babu, Y.S., Bugg, C.E., and Cook, W.J. (1988) Structure of calmodulin refined at 2.2 A resolution. *J.Mol.Biol.* **204,** 191-204

82. Hidaka, H., Sasaki, Y., Tanaka, T., Endo, T., Ohno, S., Fujii, Y., and Nagata, T. (1981) N-(6-aminohexyl)-5-chloro-1-naphthalenesulfonamide, a calmodulin antagonist, inhibits cell proliferation. *Proc.Natl.Acad.Sci.U.S.A.* **78,** 4354-4357

83. Vandonselaar, M., Hickie, R.A., Quail, J.W., and Delbaere, L.T. (1994) Trifluoperazine-induced conformational change in Ca(2+)-calmodulin. *Nat.Struct.Biol.* **1,** 795-801

84. Osawa, M., Swindells, M.B., Tanikawa, J., Tanaka, T., Mase, T., Furuya, T., and Ikura, M. (1998) Solution structure of calmodulin-W-7 complex: the basis of diversity in molecular recognition. *J.Mol.Biol.* **276,** 165-176

85. Cook, W.J., Walter, L.J., and Walter, M.R. (1994) Drug binding by calmodulin: crystal structure of a calmodulin-trifluoperazine complex. *Biochemistry.* **33,** 15259-15265

86. Cho, H.J., Xie, Q.W., Calaycay, J., Mumford, R.A., Swiderek, K.M., Lee, T.D., and Nathan, C. (1992) Calmodulin is a subunit of nitric oxide synthase from macrophages. *J.Exp.Med.* **176,** 599-604

87. Nathan, C. (1997) Inducible nitric oxide synthase: what difference does it make?. *J.Clin.Invest.* **100,** 2417-2423

88. Aoyagi, M., Arvai, A.S., Tainer, J.A., and Getzoff, E.D. (2003) Structural basis for endothelial nitric oxide synthase binding to calmodulin. *EMBO J.* **22,** 766-775

89. Colomer, J., and Means, A.R. (2007) Physiological roles of the Ca2+/CaM-dependent protein kinase cascade in health and disease. *Subcell.Biochem.* **45,** 169-214

90. Hudmon, A., and Schulman, H. (2002) Structure-function of the multifunctional Ca2+/calmodulin-dependent protein kinase II. *Biochem.J.* **364,** 593-611

91. Griffith, L.C. (2004) Regulation of calcium/calmodulin-dependent protein kinase II activation by intramolecular and intermolecular interactions. *J.Neurosci.* **24,** 8394-8398

92. Nair, J.S., DaFonseca, C.J., Tjernberg, A., Sun, W., Darnell, J.E., Chait, B.T., and Zhang, J.J. (2002) Requirement of Ca2+ and CaMKII for Stat1 Ser-727 phosphorylation in response to IFN-gamma. *Proc.Natl.Acad.Sci.U.S.A.* **99,** 5971-5976

93. Kashiwase, K., Higuchi, Y., Hirotani, S., Yamaguchi, O., Hikoso, S., Takeda, T., Watanabe, T., Taniike, M., Nakai, A., Tsujimoto, I., Matsumura, Y., Ueno, H., Nishida, K., Hori, M., and Otsu, K. (2005) CaMKII activates ASK1 and NF-kappaB to induce cardiomyocyte hypertrophy. *Biochem.Biophys.Res.Commun.* **327,** 136-142

94. Ishiguro, K., Green, T., Rapley, J., Wachtel, H., Giallourakis, C., Landry, A., Cao, Z., Lu, N., Takafumi, A., Goto, H., Daly, M.J., and Xavier, R.J. (2006) Ca2+/calmodulin-dependent protein kinase II is a modulator of CARMA1-mediated NF-kappaB activation. *Mol.Cell.Biol.* **26,** 5497-5508

95. Nathan, D.F., Vos, M.H., and Lindquist, S. (1997) In vivo functions of the Saccharomyces cerevisiae Hsp90 chaperone. *Proc.Natl.Acad.Sci.U.S.A.* **94,** 12949-12956

96. Schneider, C., Sepp-Lorenzino, L., Nimmesgern, E., Ouerfelli, O., Danishefsky, S., Rosen, N., and Hartl, F.U. (1996) Pharmacologic shifting of a balance between protein refolding and degradation mediated by Hsp90. *Proc.Natl.Acad.Sci.U.S.A.* **93,** 14536-14541

97. Pratt, W.B., and Toft, D.O. (2003) Regulation of signaling protein function and trafficking by the hsp90/hsp70-based chaperone machinery. *Exp.Biol.Med.(Maywood).* **228,** 111-133

98. Pratt, W.B. (1998) The hsp90-based chaperone system: involvement in signal transduction from a variety of hormone and growth factor receptors. *Proc.Soc.Exp.Biol.Med.* **217,** 420-434

99. Nathan, D.F., and Lindquist, S. (1995) Mutational analysis of Hsp90 function: interactions with a steroid receptor and a protein kinase. *Mol.Cell.Biol.* **15,** 3917-3925

100. Hadden, M.K., Lubbers, D.J., and Blagg, B.S. (2006) Geldanamycin, radicicol, and chimeric inhibitors of the Hsp90 N-terminal ATP binding site. *Curr.Top.Med.Chem.* **6,** 1173-1182

101. Ruckova, E., Muller, P., and Vojtesek, B. (2011) Hsp90--a target for anticancer therapy. *Klin.Onkol.* **24,** 329-337

102. Kamal, A., and Burrows, F.J. (2004) Hsp90 inhibitors as selective anticancer drugs. *Discov.Med.* **4,** 277-280

103. Garcia-Cardena, G., Fan, R., Shah, V., Sorrentino, R., Cirino, G., Papapetropoulos, A., and Sessa, W.C. (1998) Dynamic activation of endothelial nitric oxide synthase by Hsp90. *Nature.* **392,** 821-824

104. Russell, K.S., Haynes, M.P., Caulin-Glaser, T., Rosneck, J., Sessa, W.C., and Bender, J.R. (2000) Estrogen stimulates heat shock protein 90 binding to endothelial nitric oxide synthase in human vascular endothelial cells. Effects on calcium sensitivity and NO release. *J.Biol.Chem.* **275,** 5026-5030

105. Fontana, J., Fulton, D., Chen, Y., Fairchild, T.A., McCabe, T.J., Fujita, N., Tsuruo, T., and Sessa, W.C. (2002) Domain mapping studies reveal that the M domain of hsp90 serves as a molecular scaffold to regulate Akt-dependent phosphorylation of endothelial nitric oxide synthase and NO release. *Circ.Res.* **90,** 866-873

106. Takahashi, S., and Mendelsohn, M.E. (2003) Synergistic activation of endothelial nitric-oxide synthase (eNOS) by HSP90 and Akt: calcium-independent eNOS activation involves formation of an HSP90-Akt-CaM-bound eNOS complex. *J.Biol.Chem.* **278,** 30821-30827

107. Gratton, J.P., Fontana, J., O'Connor, D.S., Garcia-Cardena, G., McCabe, T.J., and Sessa, W.C. (2000) Reconstitution of an endothelial nitric-oxide synthase (eNOS), hsp90, and caveolin-1 complex in vitro. Evidence that hsp90 facilitates calmodulin stimulated displacement of eNOS from caveolin-1. *J.Biol.Chem.* **275,** 22268-22272

108. Fleming, I., and Busse, R. (2003) Molecular mechanisms involved in the regulation of the endothelial nitric oxide synthase. *Am.J.Physiol.Regul.Integr.Comp.Physiol.* **284,** R1-12

109. Papapetropoulos, A., Rudic, R.D., and Sessa, W.C. (1999) Molecular control of nitric oxide synthases in the cardiovascular system. *Cardiovasc.Res.* **43,** 509-520

110. Wei, Q., and Xia, Y. (2005) Roles of 3-phosphoinositide-dependent kinase 1 in the regulation of endothelial nitric-oxide synthase phosphorylation and function by heat shock protein 90. *J.Biol.Chem.* **280,** 18081-18086

111. Bender, A.T., Silverstein, A.M., Demady, D.R., Kanelakis, K.C., Noguchi, S., Pratt, W.B., and Osawa, Y. (1999) Neuronal nitric-oxide synthase is regulated by the Hsp90-based chaperone system in vivo. *J.Biol.Chem.* **274,** 1472-1478

112. Song, Y., Zweier, J.L., and Xia, Y. (2001) Heat-shock protein 90 augments neuronal nitric oxide synthase activity by enhancing Ca2+/calmodulin binding. *Biochem.J.* **355,** 357-360

113. Song, Y., Zweier, J.L., and Xia, Y. (2001) Determination of the enhancing action of HSP90 on neuronal nitric oxide synthase by EPR spectroscopy. *Am.J.Physiol., Cell Physiol.* **281,** 1819-1824

114. Song, Y., Cardounel, A.J., Zweier, J.L., and Xia, Y. (2002) Inhibition of superoxide generation from neuronal nitric oxide synthase by heat shock protein 90: implications in NOS regulation. *Biochemistry.* **41,** 10616-10622

115. Yoshida, M., and Xia, Y. (2003) Heat shock protein 90 as an endogenous protein enhancer of inducible nitric-oxide synthase. *J.Biol.Chem.* **278,** 36953-36958

116. Luo, S., Wang, T., Qin, H., Lei, H., and Xia, Y. (2011) Obligatory role of heat shock protein 90 in iNOS induction. *Am.J.Physiol.Cell.Physiol.* **301,** C227-33

117. Lowenstein, C.J., Glatt, C.S., Bredt, D.S., and Snyder, S.H. (1992) Cloned and expressed macrophage nitric oxide synthase contrasts with the brain enzyme. *Proc.Natl.Acad.Sci.U.S.A.* **89,** 6711-6715

118. Xie, Q.W., Cho, H.J., Calaycay, J., Mumford, R.A., Swiderek, K.M., Lee, T.D., Ding, A., Troso, T., and Nathan, C. (1992) Cloning and characterization of inducible nitric oxide synthase from mouse macrophages. *Science.* **256,** 225-228

119. Bredt, D.S., Hwang, P.M., Glatt, C.E., Lowenstein, C., Reed, R.R., and Snyder, S.H. (1991) Cloned and expressed nitric oxide synthase structurally resembles cytochrome P-450 reductase. *Nature.* **351,** 714-718

120. Xia, Y., and Zweier, J.L. (1997) Superoxide and peroxynitrite generation from inducible nitric oxide synthase in macrophages. *Proc.Natl.Acad.Sci.U.S.A.* **94,** 6954-6958

121. Wang, L., Tassiulas, I., Park-Min, K.H., Reid, A.C., Gil-Henn, H., Schlessinger, J., Baron, R., Zhang, J.J., and Ivashkiv, L.B. (2008) 'Tuning' of type I interferon-induced Jak-STAT1 signaling by calcium-dependent kinases in macrophages. *Nat.Immunol.* **9,** 186-193

122. Letari, O., Nicosia, S., Chiavaroli, C., Vacher, P., and Schlegel, W. (1991) Activation by bacterial lipopolysaccharide causes changes in the cytosolic free calcium concentration in single peritoneal macrophages. *J.Immunol.* **147,** 980-983

123. Zhu, W., Woo, A.Y., Yang, D., Cheng, H., Crow, M.T., and Xiao, R. (2007) Activation of CaMKIIdeltaC is a common intermediate of diverse death stimuli-induced heart muscle cell apoptosis. *J.Biol.Chem.* **282,** 10833-10839

124. Zhang, R., Khoo, M.S., Wu, Y., Yang, Y., Grueter, C.E., Ni, G., Price, E.E.,Jr, Thiel, W., Guatimosim, S., Song, L.S., Madu, E.C., Shah, A.N., Vishnivetskaya, T.A., Atkinson, J.B., Gurevich, V.V., Salama, G., Lederer, W.J., Colbran, R.J., and Anderson, M.E. (2005) Calmodulin kinase II inhibition protects against structural heart disease. *Nat.Med.* **11,** 409-417

125. Anderson, M.E., and Mohler, P.J. (2009) Rescuing a failing heart: think globally, treat locally. *Nat.Med.* **15,** 25-26

126. Bredt, D.S., and Snyder, S.H. (1994) Nitric oxide: a physiologic messenger molecule. *Annu.Rev.Biochem.* **63,** 175-195

127. Jones, S.P., and Bolli, R. (2006) The ubiquitous role of nitric oxide in cardioprotection. *J.Mol.Cell.Cardiol.* **40,** 16-23

128. Xie, Q., and Nathan, C. (1994) The high-output nitric oxide pathway: role and regulation. *J.Leukoc.Biol.* **56,** 576-582

129. Knowles, R.G., and Moncada, S. (1994) Nitric oxide synthases in mammals. *Biochem.J.* **298 (Pt 2),** 249-258

130. Nathan, C., and Xie, Q.W. (1994) Nitric oxide synthases: roles, tolls, and controls. *Cell.* **78,** 915-918

131. Masters, B.S., McMillan, K., Sheta, E.A., Nishimura, J.S., Roman, L.J., and Martasek, P. (1996) Neuronal nitric oxide synthase, a modular enzyme formed by convergent evolution: structure studies of a cysteine thiolate-liganded heme protein that hydroxylates L-arginine to produce NO. as a cellular signal. *FASEB J.* **10,** 552-558

132. MacMicking, J.D., Nathan, C., Hom, G., Chartrain, N., Fletcher, D.S., Trumbauer, M., Stevens, K., Xie, Q.W., Sokol, K., and Hutchinson, N. (1995) Altered responses to bacterial infection and endotoxic shock in mice lacking inducible nitric oxide synthase. *Cell.* **81,** 641-650

133. Marletta, M.A. (1994) Nitric oxide synthase: aspects concerning structure and catalysis. *Cell.* **78,** 927-930

134. Zhang, J., Dawson, V.L., Dawson, T.M., and Snyder, S.H. (1994) Nitric oxide activation of poly(ADP-ribose) synthetase in neurotoxicity. *Science.* **263,** 687-689

135. Karupiah, G., Xie, Q.W., Buller, R.M., Nathan, C., Duarte, C., and MacMicking, J.D. (1993) Inhibition of viral replication by interferon-gamma-induced nitric oxide synthase. *Science.* **261,** 1445-1448

136. Montague, P.R., Gancayco, C.D., Winn, M.J., Marchase, R.B., and Friedlander, M.J. (1994) Role of NO production in NMDA receptor-mediated neurotransmitter release in cerebral cortex. *Science.* **263,** 973-977

137. Stamler, J.S., Simon, D.I., Osborne, J.A., Mullins, M.E., Jaraki, O., Michel, T., Singel, D.J., and Loscalzo, J. (1992) S-nitrosylation of proteins with nitric oxide: synthesis and characterization of biologically active compounds. *Proc.Natl.Acad.Sci.U.S.A.* **89,** 444-448

138. Wu, C., Zhang, J., Abu-Soud, H., Ghosh, D.K., and Stuehr, D.J. (1996) High-Level Expression of Mouse Inducible Nitric Oxide Synthase inEscherichia coliRequires Coexpression with Calmodulin. *Biochem.Biophys.Res.Commun.* **222,** 439-444

139. Kolodziejski, P.J., Koo, J.S., and Eissa, N.T. (2004) Regulation of inducible nitric oxide synthase by rapid cellular turnover and cotranslational down-regulation by dimerization inhibitors. *Proc.Natl.Acad.Sci.U.S.A.* **101,** 18141-18146

140. Wei, Q., and Xia, Y. (2006) Proteasome inhibition down-regulates endothelial nitric-oxide synthase phosphorylation and function. *J.Biol.Chem.* **281,** 21652-21659

141. Blagosklonny, M.V. (2002) Hsp-90-associated oncoproteins: multiple targets of geldanamycin and its analogs. *Leukemia.* **16,** 455-462

142. Wang, C., Ko, H.S., Thomas, B., Tsang, F., Chew, K.C., Tay, S.P., Ho, M.W., Lim, T.M., Soong, T.W., Pletnikova, O., Troncoso, J., Dawson, V.L., Dawson, T.M., and Lim, K.L. (2005) Stress-induced alterations in parkin solubility promote parkin aggregation and compromise parkin's protective function. *Hum.Mol.Genet.* **14,** 3885-3897

143. Magzoub, M., and Miranker, A.D. (2011) Protein aggregation: p53 succumbs to peer pressure. *Nat.Chem.Biol.* **7,** 248-249

144. Pearl, L.H., Prodromou, C., and Workman, P. (2008) The Hsp90 molecular chaperone: an open and shut case for treatment. *Biochem.J.* **410,** 439-453

145. Roe, S.M., Prodromou, C., O'Brien, R., Ladbury, J.E., Piper, P.W., and Pearl, L.H. (1999) Structural basis for inhibition of the Hsp90 molecular chaperone by the antitumor antibiotics radicicol and geldanamycin. *J.Med.Chem.* **42,** 260-266

146. Grenert, J.P., Sullivan, W.P., Fadden, P., Haystead, T.A., Clark, J., Mimnaugh, E., Krutzsch, H., Ochel, H.J., Schulte, T.W., Sausville, E., Neckers, L.M., and Toft, D.O. (1997) The amino-terminal domain of heat shock protein 90 (hsp90) that binds geldanamycin is an ATP/ADP switch domain that regulates hsp90 conformation. *J.Biol.Chem.* **272,** 23843-23850

147. Murata, S., Chiba, T., and Tanaka, K. (2003) CHIP: a quality-control E3 ligase collaborating with molecular chaperones. *Int.J.Biochem.Cell Biol.* **35,** 572-578

148. Jiang, J., Cyr, D., Babbitt, R.W., Sessa, W.C., and Patterson, C. (2003) Chaperone-dependent regulation of endothelial nitric-oxide synthase intracellular trafficking by the co-chaperone/ubiquitin ligase CHIP. *J.Biol.Chem.* **278,** 49332-49341

149. Nathan, C., and Xie, Q.W. (1994) Regulation of biosynthesis of nitric oxide. *J.Biol.Chem.* **269,** 13725-13728

150. Kleinert, H., Pautz, A., Linker, K., and Schwarz, P.M. (2004) Regulation of the expression of inducible nitric oxide synthase. *Eur.J.Pharmacol.* **500,** 255-266

151. Hershko, A., and Ciechanover, A. (1998) The ubiquitin system. *Annu.Rev.Biochem.* **67,** 425-479

152. Matsumoto, K., Nishiya, T., Maekawa, S., Horinouchi, T., Ogasawara, K., Uehara, T., and Miwa, S. (2011) The ECS(SPSB) E3 ubiquitin ligase is the master regulator of the lifetime of inducible nitric-oxide synthase. *Biochem.Biophys.Res.Commun.* **409,** 46-51

153. Kundrat, L., and Regan, L. (2010) Balance between folding and degradation for Hsp90-dependent client proteins: a key role for CHIP. *Biochemistry.* **49,** 7428-7438

154. Zhang, J.G., Metcalf, D., Rakar, S., Asimakis, M., Greenhalgh, C.J., Willson, T.A., Starr, R., Nicholson, S.E., Carter, W., Alexander, W.S., Hilton, D.J., and Nicola, N.A. (2001) The SOCS box of suppressor of cytokine signaling-1 is important for inhibition of cytokine action in vivo. *Proc.Natl.Acad.Sci.U.S.A.* **98,** 13261-13265

155. Zhao, Y.G., Gilmore, R., Leone, G., Coffey, M.C., Weber, B., and Lee, P.W. (2001) Hsp90 phosphorylation is linked to its chaperoning function. Assembly of the reovirus cell attachment protein. *J.Biol.Chem.* **276,** 32822-32827

156. Zuehlke, A.D., and Johnson, J.L. (2012) Chaperoning the Chaperone: A Role for the Co-chaperone Cpr7 in Modulating Hsp90 Function in Saccharomyces cerevisiae. *Genetics.*

157. Mollapour, M., Tsutsumi, S., Truman, A.W., Xu, W., Vaughan, C.K., Beebe, K., Konstantinova, A., Vourganti, S., Panaretou, B., Piper, P.W., Trepel, J.B., Prodromou, C., Pearl, L.H., and Neckers, L. (2011) Threonine 22 phosphorylation attenuates Hsp90 interaction with cochaperones and affects its chaperone activity. *Mol.Cell.* **41,** 672-681

158. Schwartz, A.L., and Ciechanover, A. (2009) Targeting proteins for destruction by the ubiquitin system: implications for human pathobiology. *Annu.Rev.Pharmacol.Toxicol.* **49,** 73-96

159. Vosper, J.M., McDowell, G.S., Hindley, C.J., Fiore-Heriche, C.S., Kucerova, R., Horan, I., and Philpott, A. (2009) Ubiquitylation on canonical and non-canonical sites targets the transcription factor neurogenin for ubiquitin-mediated proteolysis. *J.Biol.Chem.* **284,** 15458-15468

160. Cadwell, K., and Coscoy, L. (2005) Ubiquitination on nonlysine residues by a viral E3 ubiquitin ligase. *Science.* **309,** 127-130

161. Wang, X., Herr, R.A., Chua, W., Lybarger, L., Wiertz, E.J.H.J., and Hansen, T.H. (2007) Ubiquitination of serine, threonine, or lysine residues on the cytoplasmic tail can induce ERAD of MHC-I by viral E3 ligase mK3. *J.Cell Biol.* **177,** 613-624